Identification of Extracellular Matrix Components Essential for a Conductive *Geobacter sulfurreducens* Biofilm

A DISSERTATION
SUBMITTED TO THE FACULTY OF THE GRADUATE SCHOOL
OF THE UNIVERSITY OF MINNESOTA
BY

Janet Beth Rollefson

IN PARTIAL FULFILLMENT OF THE REQUIREMENTS
FOR THE DEGREE OF
DOCTOR OF PHILOSOPHY

Advisor: Daniel R. Bond

November, 2011

Acknowledgements

I want to thank my advisor, Dr. Daniel Bond, for the opportunity to work in his laboratory and his support and advice throughout the years. Thank you to my committee members, Dr. Sandy Armstrong, Dr. Jeff Gralnick, Dr. Claudia Schmidt-Dannert, and Dr. Romas Kazlauskas for their direction and constructive feedback over the years. Thanks to the Imaging Center at the University of Minnesota for confocal assistance, and Aaron Barnes for sharing his SEM expertise.

I want to thank Craig Thelander for setting me up with the best parking spot on campus, and Justin Lawrence for moving me so far away that I needed that parking spot to make it through the last few years. Finally, thank you to fellow Bond Lab members, in particular Caleb Levar, Misha Mehta, and Clint Remarcik. Caleb for his hard work on the mutant library and his "impressive" persona. Misha Mehta for her long lasting friendship and constant unwanted advice, and Clint Remarcik for creating a fun ("hostile") work environment.

Abstract

Electron transfer from *Geobacter sulfurreducens* cells to electrodes or metal oxides requires proper expression and localization of redox-active proteins as well as attachment mechanisms that interface bacteria with surfaces and other cells. Type IV pili and *c*-type cytochromes have long been considered important components of this conductive network. In this work, a large-scale mutagenesis of *G. sulfurreducens* was performed and mutants were screened for extracellular electron transfer and attachment phenotypes, identifying new genes essential for a conductive *Geobacter* network. A mutant defective in polysaccharide export to the extracellular matrix (Δ1501, Δ*xapD::kan*) was identified based on its altered surface attachment. Characterization of this mutant revealed the importance of extracellular polysaccharides for proper attachment and anchoring of the external *c*-type cytochromes necessary for a conductive biofilm network. Furthermore, decreased polysaccharide content was found in commonly studied cytochrome and type IV pili mutants, with defects in cell to cell and cell to surface attachment correlating with levels of extracellular polysaccharides. The extracellular matrix of *G. sulfurreducens* is therefore a complex network of polysaccharides, type IV pili, and *c*-type cytochromes. Disruption of any one of these extracellular components alters overall matrix properties and impedes extracellular electron transfer and attachment.

Table of Contents

List of Tables

List of Figures

Chapter 1: Introduction

1.1 Dissimilatory metal reduction

Iron is the fourth most abundant element in the Earth's crust and an essential metal for most organisms. Once thought to be controlled by abiotic mechanisms, iron reduction and oxidation is mediated by microbial metabolism in most environments (140). Microbial reduction of Fe(III) is an essential part of iron cycling, having major impacts on the geochemistry of soils and sediments. Microbial Fe(III) reduction is thought to have played a significant role in the early oxidation of organic matter to carbon dioxide, a process important in aquatic environments today. Release of trace minerals and phosphate, which can be limiting in such environments, is also influenced by microbial reduction of metals (86). Evidence suggests the majority of Fe(III) reduction in iron-rich environments such as anaerobic sediments and soils is a consequence of dissimilatory metal reducing microorganisms (86). Microorganisms belonging to both the Archaea and Bacteria domains benefit from the ability to use Fe(III) as terminal electron acceptor, supporting growth. Alternatively, Fe(II) can be used by Fe(II)-oxidizing microorganisms as an electron donor (140).

Iron is an essential metal for most organisms, being a necessary component of many enzymes. While iron is an abundant element, at circumneutral pH it forms insoluble Fe(III) oxides and hydroxides with limited accessibility to microorganisms. Two distinct types of microbial metal reduction occur: assimilatory and dissimilatory. In assimilatory iron reduction, Fe(III) is reduced to a soluble form that can be easily brought into the cell where it can be incorporated into iron-containing proteins. In dissimilatory

metabolism, Fe(III) serves as the terminal electron acceptor. Electrons from internal oxidative reactions are transferred to external Fe(III), resulting in an accumulation of Fe(II) outside the cell (86). Dissimilatory metal reduction is not limited to Fe(III); in fact, a wide variety of metals can serve as terminal electron acceptors, including Mn(IV), U(VI), Co(III), V(V), Cr(VI) and Mo(VII) (74).

Electrons can travel only short distances (~10 Å) without the help of redox-active proteins. As such, specialized mechanisms for electron transfer from the surface of a bacterial cell to an external, insoluble acceptor are required. Currently, there are three described strategies used to access insoluble metals by dissimilatory metal reducers. Some bacteria use an indirect mechanism in which soluble electron carriers shuttle electrons from the cell surface to an acceptor (Fig. 1.1A). These soluble compounds are reduced and then diffuse away from the cell and donate electrons to the acceptor, thereby replenishing the pool of oxidized shuttle. One such example of this type of mediator-dependent dissimilatory metal reduction is found in *Shewanella oneidensis. S. oneidensis* secretes and reduces flavins, which diffuse to and reduce an insoluble terminal electron acceptor (92, 135). A second indirect mechanism of metal reduction can also involve chelators that solubilize Fe(III) making it accessible for microbial reduction (Fig. 1.1C).

The third strategy employed by dissimilatory metal-reducers uses a direct mechanism in which cells must be in contact with the electron-accepting surface, allowing electrons to flow from the cell's outer surface directly to the external acceptor (Fig. 1.1B). *Geobacter,* a well-studied metal-reducing species, is capable of direct electron transfer to an insoluble electron acceptor (103). The pathway of electron transfer

from cell to acceptor is not fully understood in *G. sulfurreducens*, but evidence suggests specialized membrane proteins are positioned to directly pass electrons from the outer surface to the acceptor. Microorganisms that rely on the direct mechanism of electron transfer can also benefit from addition of an exogenous shuttle or chelator, further stimulating extracellular electron transfer (78). Likewise, use of an indirect mechanism does not eliminate the direct mechanism, as some microorganisms known to produce a shuttle are also capable of direct electron transfer (7).

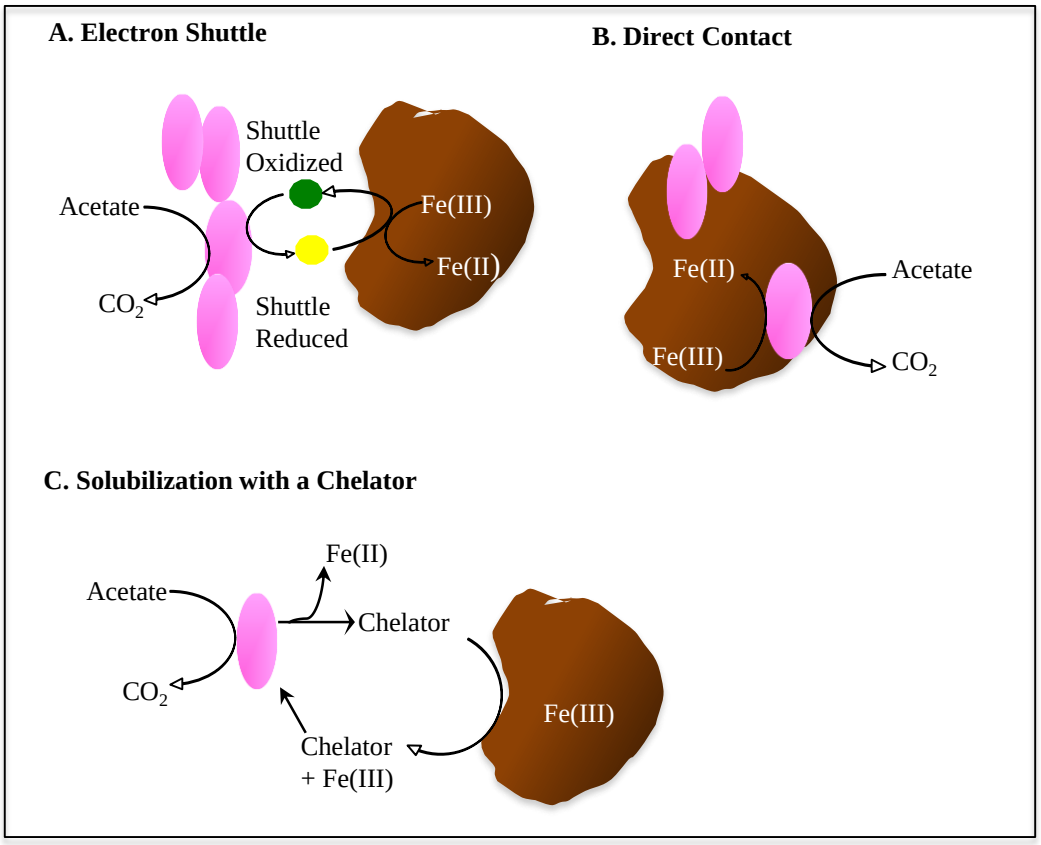

Figure 1.1 Mechanisms of electron transfer to insoluble Fe(III), showing (A) indirect electron transfer using a shuttle, (B) direct electron transfer and (C) transfer using a chelator.

1.2 *Geobacter*

The *Geobacteraceae* family of *Deltaproteobacteria* are highly abundant Fe(III)-reducing organisms found in many anaerobic, neutral pH environments (44, 118, 125). *G. metallireducens* was isolated from Potomac River sediments and represents the first organism known to couple the complete oxidation of organic compounds with the reduction of Fe(III) under anaerobic conditions (79). Fe(III) is used as the terminal electron acceptor during respiration, supporting ATP generation and growth. The most studied member of the *Geobacteraceae, G. sulfurreducens,* was later isolated through enrichments for Fe(III)-reducing organisms from hydrocarbon-contaminated soil in Oklahoma (20).

Geobacter species have long been classified as strict anaerobes, able to respire a variety of metals including Fe(III), Mn(IV), and U(VI) (20, 79). More recently it was shown that *G. sulfurreducens* can grow with oxygen as sole electron acceptor and survive atmospheric levels of oxygen for hours (73). When acetate is provided to stimulate anaerobic metal reduction, *Geobacter* species are the predominant Fe(III)-reducing microorganisms in a variety of subsurface sediments, including those which have recently transitioned from an aerobic environment. Since, Fe(III) is abundant near the oxic-anoxic interface (128), anaerobic microorganisms carrying out Fe(III) reduction in this area are likely to be exposed to oxygen periodically, making the ability to tolerate oxygen advantageous.

While *G. sulfurreducens* typically relies on acetate or hydrogen as electron sources (20), subsurface isolates *G. bemidjiensis* and *G. psychrophilus* are also able to oxidize

ethanol, lactate, pyruvate, malate, and succinate (101), and *G. metallireducens* is able to couple the oxidation of aromatic compounds (toluene, phenol, *p*-cresol) to iron respiration (83). In addition to breakdown of aromatic compounds, the ability of *Geobacter* to precipitate soluble metals, including the radionuclide U(IV) (80), has attracted interest for bioremediation purposes. The electron transfer abilities that allow *Geobacter* to reduce metals also allow for electrical current generation when an electrode serves as sole electron acceptor (13), expanding the potential biotechnological applications. For instance, members of the *Geobacteraceae*, harvesting energy from marine sediments, are able to power small electric devices (12, 127) and generate electricity during wastewater treatment (21, 76).

1.3 Cytochromes and proteins important in *G. sulfurreducens* Fe(III) and electrode reduction

To understand the pathway of electron transfer to an insoluble acceptor in *Geobacter*, type IV pili and *c*-type cytochromes have been extensively studied (18, 47, 54, 70, 71, 75, 98, 112, 113). *c*-type cytochromes play a crucial role in electron transfer reactions in respiration and are associated with metal reduction in *S. oneidensis* (123). Transfer of electrons from central metabolism to the outer surface of a cell and subsequent reduction of an external acceptor involves a series of inner membrane, periplasmic and outer membrane cytochromes. Biochemical studies have shown the majority of the Fe(III)-reductase activity in *G. sulfurreducens* localizes to the membranes, with 80% of this activity associated with the outer membrane (40). The genome of *G. sulfurreducens* encodes over one hundred putative *c*-type cytochromes,

many of these predicted to be associated with the outer membrane (99). To understand potential electron transfer roles, a number of these genes and proteins have been studied through mutant analysis, proteomics, and microarray analysis. These studies have revealed that different cytochromes are expressed at different times, under different conditions, and at different locations throughout the biofilm (31, 32, 37, 43, 51, 55, 102). Phenotypes of important mutants (*c*-type cytochromes, type IV pili, porins) are summarized in Table 1.1.

Table 1.1 Phenotypes of key *Geobacter* mutants

Protein	Mutant phenotype	Putative localization	Reference(s)
OmcB	Decreased soluble and insoluble Fe(III) reduction	Outer membrane	70, 107
OmcE	Decreased insoluble Fe(III) reduction	Extracellular	98
OmcF	Decreased soluble Fe(III) reduction, decreased OmcB and OmcC expression, mislocalization of OmcS and OmcE	Outer membrane	54
OmcG	Decreased soluble Fe(III) reduction, decreased OmcB production	Outer membrane	53
OmcH	Decreased solube Fe(III) reduction, decreased OmcB production	Outer membrane	53
OmcS	Decreased insoluble Fe(III) reduction, decreased OmcT expression	Extracellular/pili	71, 98
OmcT	Decreased insoluble Fe(III) reduction, decreased OmcS expression	Outer membrane	98
OmcZ	Decreased electrode reduction, reduced biofilm thickness	Extracellular	46, 47, 102, 115
OmpJ	Decreased soluble and insoluble Fe(III) reduction, cytochrome content reduced 50%	Outer membrane	1
PilA	Decreased insoluble Fe(III) reduction, Decreased electrode reduction, reduced biofilm thickness	Extracellular	111-113

PpcA	Decreased soluble Fe(III) reduction	Periplasm	75

For extracellular electron transfer to occur, electrons generated through metabolism must cross the inner membrane, periplasm, and outer membrane, likely transported along a chain of cytochromes, before reaching an external electron acceptor, (Fig. 1.2). Characterization of electrode and insoluble Fe(III) reduction phenotypes of *G. sulfurreducens* mutants provides insight into what proteins are required for extracellular electron transfer as these acceptors are external. Soluble Fe(III) citrate is reduced either at the outer membrane or in the periplasm of *G. sulfurreducens* cells (24), requiring at least part of the external electron transfer pathway to be intact. PpcA is a periplasmic *c*-type cytochrome implicated in Fe(III) reduction, with a *ppcA*-deficient mutant showing decreased soluble Fe(III) reduction (75). PpcA and its four homologs (106) may be a bridge for electron transfer between the cytoplasmic membrane and the outer membrane.

Increased expression of a protein designated MacA is found in cells grown using Fe(III) as terminal electron acceptor compared to fumarate (18). Deletion of this protein decreases the ability of *Geobacter* to reduce soluble Fe(III), however transcript and protein levels of an important cytochrome, OmcB, (outer membrane cytochrome B) are also diminished (52). Once thought to be a periplasmic cytochrome, MacA is actually homologous to a known cytochrome *c* peroxidase (42), and is not critical for Fe(III) reduction, as *omcB* expression *in trans* restores Fe(III) reduction to a *macA*-deficient mutant (52).

Once through the periplasm, electrons then must cross the outer membrane to reduce an external acceptor. Likely localized to the outer membrane (107), OmcB has been implicated in reduction of both soluble and insoluble Fe(III). Expression of OmcB increases when using Fe(III) as electron acceptor (32), and an *omcB*-deficient mutant shows impaired ability to reduce both soluble and insoluble Fe(III) compared to wild type *G. sulfurreducens* (70). While polyheme cytochrome OmcC shares 79% identity with OmcB, Fe(III) reduction is not impaired in an *omcC*-deficient mutant (70). An *omcB*-deficient mutant is able to adapt over time to grow using soluble Fe(III) (but not insoluble), as expression of alternate membrane bound cytochromes increases (69). Furthermore, OmcB is thought to play a role in the electron transfer from biofilm to electrode (115), and increased expression of this cytochrome is detected in current-producing biofilms (102).

In addition to MacA, OmcB expression is dependent on the presence of two homologous outer membrane cytochromes, OmcG and OmcH. When deleted in tandem, soluble Fe(III) reduction is inhibited, along OmcB production (53). An abundant porin, OmpJ (outer membrane protein J) is also important for the expression of *c*-type cytochromes. An *ompJ*-deficient strain is able to grow at wild type rates when using fumarate as electron acceptor, but with a 50% reduction in heme content, mutant cells show decreased levels of both soluble and insoluble Fe(III) reduction. An enlarged periplasm (possibly indicating stress reponse and protein degradation) in the absence of OmpJ suggests this porin contributes to maintenance of the periplasmic space needed for cytochrome folding, giving OmpJ an indirect role in Fe(III) reduction (1).

Outer membrane localized OmcF has also been indirectly implicated in soluble Fe(III) reduction, with an *omcF*-deficient mutant showing decreased ability for Fe(III) reduction compared to wild type *G. sulfurreducens* (54). Interestingly, expression of OmcB and OmcC decreases in an *omcF*-deficient mutant and localization of OmcS and OmcE is disrupted, as these extracellular cytochromes are transcribed but not detected at the outer surface (54, 55). OmcF appears necessary for the appropriate expression and localization of specific cytochromes needed for Fe(III) reduction, making it indirectly important in this process. Additionally, over time an *omcF*-deficient mutant can adapt to attain near wild type levels of Fe(III) reduction (54).

Once an electron has crossed the outer membrane, transfer to an extracellular protein(s) that is positioned to reduce an external acceptor can occur. Reduction of insoluble Fe(III) has been linked to the presence of the *c*-type cytochromes OmcS and OmcE (98). Deletion of these cytochromes severely decreases reduction of insoluble Fe(III), with little effect on soluble Fe(III) reduction (98). Accordingly, OmcS is more abundant in cells grown with insoluble Fe(III) compared to cells grown with soluble Fe(III) (31). OmcE is less abundant in Fe(III) oxide grown cells than OmcS, highlighting the importance of OmcS in Fe(III) oxide reduction. Both OmcS and OmcE were thought to be loosely associated with the cell surface as they are released from cells by gentle shearing (98). Recently it was shown that some excreted OmcS is arranged along type IV pili (71). The extracellular localization of these cytochromes suggests they may play a role in electron transfer through the conductive network surrounding *Geobacter* cells. Another cytochrome gene, o*mcT* is located immediately downstream the *omcS* gene and

is expressed as part of the same transcript. An *omcT*-deficient mutant is deficient in reduction of insoluble Fe(III), however *omcS* expression was also reduced. Likewise, *omcT* expression is eliminated in an *omcS* mutant, but restoration of Fe(III) reduction only requires expression of *omcS in trans* (98).

The *c*-type cytochrome OmcZ exists in two forms, 50 kDa $OmcZ_L$ and the 30 kDa cleavage product $OmcZ_S$ (47). Retaining all 8 heme groups, $OmcZ_S$ is the predominant extracellular form of this cytochrome that has been found concentrated near the anode of current-producing biofilms (46). Additionally, this cytochrome is highly expressed in cells grown in current-producing biofilms, with an *omcZ*-deficient mutant severely limited in current production (102). The localization of OmcZ and the phenotype of an *omcZ*-deficient mutant together suggest that this cytochrome may be involved in the final electron transfer from biofilm to anode surface. In contrast, electrochemical analysis suggests that OmcZ participates in electron transfer through the conductive network of the biofilm itself (115).

In addition to specific *c*-type cytochromes, type IV pili are involved in extracellular electron transfer in *G. sulfurreducens.* Pili have been proposed to be the conduit for electron transfer from cell to surface (biological nanowires), and are needed for maximum Fe(III) oxide reduction (111). One hypothesis is that pili promote long range electron transfer through electrode-attached biofilms, as deletion of the gene coding for the structural subunit of pilin greatly reduces current generation (112). While the conductive nature of pili themselves continues to be explored (89), there is also a clear structural role for type IV pili in biofilm formation. Even in the presence of a soluble

electron acceptor, a PilA mutant only forms thin biofilms on glass, Fe(III) oxide-coated surfaces, and poised electrodes, suggesting a potential explanation for its inability to reduce insoluble electron acceptors (113, 115).

In summary, extracellular electron transfer from *Geobacter* to Fe(III) or an electrode is a complex process involving type IV pili and an assortment of cytochromes. Many mutants show low levels of electrode or Fe(III) reduction while others adapt over time to near wild type levels (54, 69, 98, 112, 115). Cytochrome expression levels depend on the terminal electron acceptor, suggesting different roles for cytochromes, and facilitating the use of different electron acceptors. In some cases, increased expression of specific cytochromes can compensate, at least partially, for loss of another. In addition to acceptor specificity, the roles of different cytochromes vary in that some are important for electron transfer between cells while others are important for cell to surface electron transfer. While the pathway of electron transfer to external electron acceptors is not well characterized (Fig. 1.2), it likely relies on a network of bound electron transfer proteins (115) each contributing in a specific way to the process.

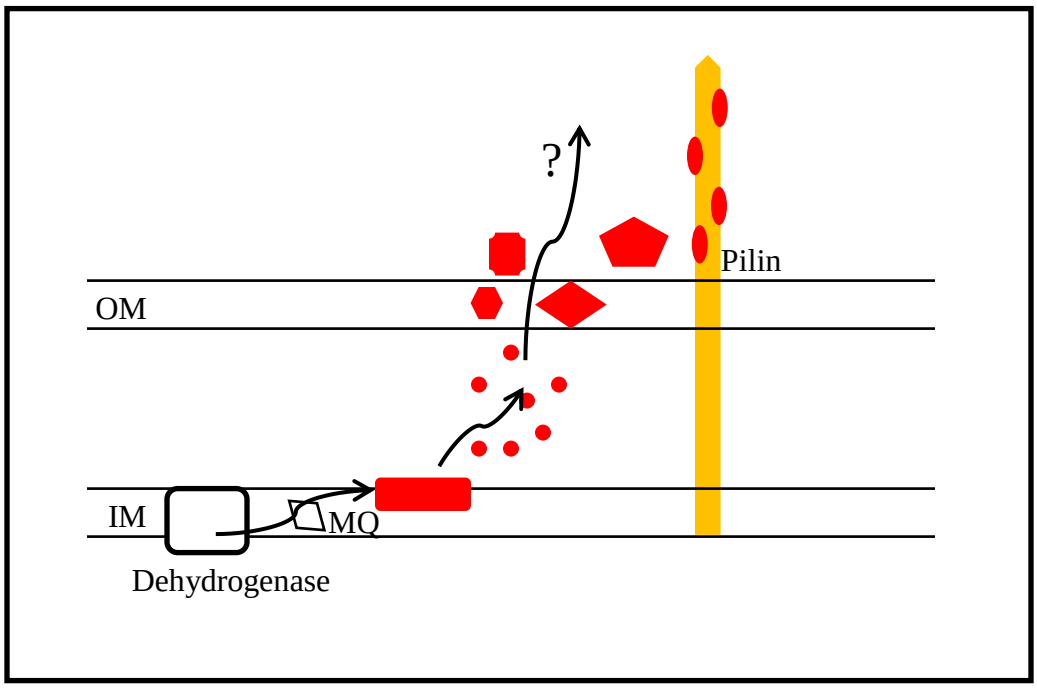

Figure 1.2 Potential pathway for electron transfer in *G. sulfurreducens*, based on previous models (19, 81), with electrons flowing from inner membrane (IM) dehydrogenase through menaquinone (MQ) pool to inner membrane cytochromes (red), periplasmic cytochromes, outer membrane cytochromes, and finally extracellular cytochromes.

1.4 Conductive *Geobacter* biofilms

In addition to transferring electrons from internal oxidative metabolism to external metal oxides, *Geobacter* can use an electrode as its sole electron acceptor (13). In defined laboratory settings, electron transfer in *Geobacter* spp. occurs through a direct mechanism in which contact with the electron accepting surface is required (103). In the case of metal oxides, contact with the acceptor may be transient, but for current

generation on an electrode a biofilm must form on the surface. For reduction of an electrode and continued/increasing current generation by *Geobacter*, multiple steps must occur. First, cells need to make contact with the electrode and attach. Once initial cell-surface attachment has been established, additional cells will attach to this first layer and network, as the only acceptor in this situation is the electrode. Cell-cell attachment is necessary for biofilm growth beyond a monolayer.

For a conductive *Geobacter* biofilm, attached cells need to pass electrons from internal oxidative reactions across the inner membrane, periplasm and outer membrane, to reach an insoluble, external acceptor, such as an electrode. Cells in contact with the electrode pass their electrons directly to it, relying on cell-surface electron transfer. On a polished graphite electrode a *G. sulfurreducens* monolayer has formed once current densities have reached ~75 $\mu A/cm^2$. This first layer of cells initially shows lower rates of electron transfer than subsequent cells as they must first optimize attachment and electron transfer to the surface (94). Subsequent cells that attach to this initial layer must pass their electrons through the biofilm to the distant electrode surface. At this point, electron transfer and cell growth rates increase, reaching levels consistent with reduction of soluble Fe(III) by *G. sulfurreducens.* Once current densities have reached ~ 300 $\mu A/cm^2$, a multi-layer biofilm has formed (~ 10 µm thickness) (94). The increase in current as a biofilm thickens indicates cell to cell electron transfer through the biofilm. Cells distant from the electrode must direct their electrons to this acceptor through a long-range electron transfer mechanism, likely relying on an external network of redox-active proteins. Finally, biofilm growth slows as multiple cell layers are added to the biofilm (~

20 μm thickness), and current densities near 750 μA/cm^2 (94). Electrode-attached biofilms reach a terminal thickness and current density, as biofilm development may be limited by availability of surface for colonization, the ability of electron donors to penetrate the biofilm, or even the pH gradient which develops within current-producing biofilms (38).

Anaerobic three-electrode bioreactors containing a carbon working electrode, platinum counter electrode and calomel reference electrode, controlled by a potentiostat are commonly used to monitor current flow out of *Geobacter* biofilms (Fig. 1.3). Electrochemistry allows the flow of electrons out of a biofilm to be monitored in real time. While metal oxides have variable surface area and redox potentials that change over time, electrodes have well defined surfaces with controlled potentials. Use of poised electrodes allows for sensitive and consistent detection of electron transfer phenotypes. When poised at the correct potential, electrodes can serve as a proxy for Fe(III) oxide as an electron acceptor. Electrochemistry provides insight into the electron transfer mechanisms and capabilities of a microorganism. For example, the presence of an electron shuttle can be detected, supporting the indirect mechanism of electron transfer. Measuring current production over time (chronoamperometry) allows electron transfer capabilities of mutant cells to be assessed. Decreased current generation in a mutant compared to wild type can indicate an electron transfer deficiency. Monitoring current production at varying potentials (cyclic voltammetry) provides insight into the number of redox active species accessible to the electrode or the rate limiting step in external electron transfer. Additionally, electrode-attached biofilms can be visualized through

confocal and electron microscopy, giving an indication of attachment levels and allowing for detection of specific matrix components.

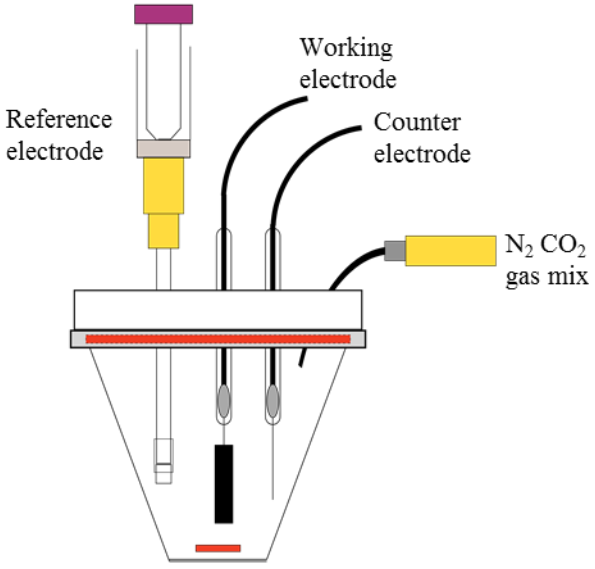

Figure 1.3 Anaerobic 3-electrode bioreactor, adapted from Marsili *et al.*, AEM 2008.

1.5 Complexity of *Geobacter* extracellular electron transfer

The complexity of electron transfer from internal oxidative reactions to external electron acceptors in *G. sulfurreducens* makes characterization of the pathway and determination of the necessary components difficult. First, expression patterns of important electron transfer proteins in *G. sulfurreducens* are dependent on the presence of other proteins. As noted above, OmcB is critical for Fe(III) reduction; however, its expression is often affected by disruption of other genes. Deletion of other outer

membrane cytochromes, a periplasmic cytochrome, and even a porin has been shown to eliminate OmcB expression. Caution is therefore needed when assigning roles to cytochromes in electron transfer to insoluble Fe(III) or electrodes.

Another challenge in the characterization of extracellular electron transfer in *Geobacter* is that many mutants are able to adapt over time, losing their electron transfer phenotypes. For instance, an OmcB mutant has been reported to adapt to near wild type levels of soluble Fe(III) reduction as expression of other outer membrane cytochromes compensate for the loss of OmcB (69). In the case of electrode reduction, there are mutants that initially seem unable to generate current, for example Δ*omcST*. However, given enough time this mutant can reach near wild type levels of current production (115). Adaptations in mutant strains or compensation by expression of alternate cytochromes make it difficult to pinpoint a mutant's true phenotype and determine the degree of involvement of a certain protein in electron transfer. With over 100 cytochromes, redundancy in function is expected, contributing to the complexity of extracellular electron transfer in *Geobacter*.

In addition to deletion of certain genes affecting cytochrome expression patterns, the ability to attach to surfaces and form biofilms can be altered in mutants. Notably, in the PilA mutant, elimination of pili decreased current production on an electrode. However, fewer mutant cells attached to the electrode compared to wild type (115), potentially explaining the decrease in total current. The direct mechanism of electron transfer in *Geobacter* requires that cells are in contact with the electrode for respiration. Fewer attached cells result in less current, regardless of whether the electron transfer

pathway from cell to surface or cell to cell was disrupted. What degree of the current reduction is due to fewer cells and what to the necessity of pili is unknown.

Finally, rates of Fe(III) and electrode reduction by *G. sulfurreducens* vary greatly depending on how a culture is maintained. A strain frequently allowed to grow using Fe(III) oxyhydroxide as sole electron acceptor (between routine culturing with fumarate) demonstrates higher Fe(III) reduction rates than a strain rarely transferred onto insoluble Fe(III). The same is true for electrode reduction, with a culture properly maintained on Fe(III) producing more current. Similarly, a *G. sulfurreducens* variant isolated from a current producing biofilm showed increased levels of current generation compared to the original strain (144). Use of a common background (wild type *G. sulfurreducens* maintained on Fe(III) oxyhydroxide) for mutant construction is critical when Fe(III) and electrode reduction phenotypes are of interest. Overall, for effective analysis of extracellular electron transfer in *Geobacter*, mutant adaptation, cytochrome expression, attachment, and maintenance of parent strain all must be considered.

1.6 Thesis rationale and goals

Type IV pili and *c*-type cytochromes have long been the focus of *Geobacter* research because of their importance in electron transfer and development of a conductive biofilm. How these components network together and promote electron transfer through a multilayer biofilm to a distant, insoluble electron acceptor is not fully understood. The broad goal of this thesis was to discover new genes and proteins necessary for production of a conductive biofilm network in *G. sulfurreducens.* Taking into consideration the complexity of electron transfer and the challenges described above (section 1.5), use of a

well-maintained background strain for mutant construction and attention to biofilm phenotypes were essential to this investigation and the identification of a new component necessary for production of a conductive biofilm by *G. sulfurreducens.*

1.7 Summary of thesis

The focus of this thesis is the discovery of a critical component of a conductive *Geobacter* network. Chapter 2 describes the first reported large-scale mutagenesis of *G. sulfurreducens* along with a system for conjugal transfer of a plasmid in this organism. Through screening of transposon mutants, new genes important in external electron transfer and biofilm formation were identified. Chapter 3 is an in depth study of a mutant (identified through the mutagenesis and screening) defective in the export of polysaccharides to the extracellular matrix. This chapter highlights the importance of extracellular polysaccharides for proper attachment and anchoring of the external *c*-type cytochromes necessary for a conductive biofilm network. Chapter 4 looks at the polysaccharide content of the extracellular matrix of commonly studied cytochrome and type IV pili mutants, showing that defects in cell to cell and cell to surface attachment correlate with levels of extracellular polysaccharides. The identification of proteins associated with the *Geobacter* extracellular matrix through mass spectrometry is detailed in Chapter 5 along with the difficulties in obtaining a sample free of intracellular proteins.

Identification of Genes Involved in Biofilm Formation and Respiration via Mini-*Himar* Transposon Mutagenesis of *Geobacter sulfurreducens.*

Rollefson, J.B., C.E. Levar, and D.R. Bond. Journal of Bacteriology, July 2009, volume 191, p. 4207-4217.

0021-9193/09/$08.00+0 doi: 10.1128/JB.00057-09

Chapter 2: Identification of Genes Involved in Biofilm Formation and Respiration via Mini-*Himar* Transposon Mutagenesis of *Geobacter sulfurreducens*

2.1 Overview

Electron transfer from cells to metals and electrodes by the Fe(III)-reducing anaerobe *G. sulfurreducens* requires proper expression of redox proteins and attachment mechanisms to interface bacteria with surfaces and neighboring cells. We hypothesized that transposon mutagenesis would complement targeted knockout studies in *Geobacter*, and identify novel genes involved in this process. *Escherichia coli* mating strains and plasmids were used to develop a conjugation protocol, and deliver mini-*Himar* transposons, creating a library of over 8,000 mutants that was anaerobically arrayed and screened for a range of phenotypes, including: auxotrophy for amino acids, inability to reduce Fe(III)-citrate, and attachment to surfaces. Following protocol validation, mutants with strong phenotypes were further characterized in a three-electrode system to simultaneously quantify attachment, biofilm development and respiratory parameters, revealing mutants defective in Fe(III)-reduction but unaffected in electron transfer to electrodes (such as an insertion in GSU1330, a putative metal export protein), or defective in electrode reduction but demonstrating wild-type biofilm formation (due to an insertion upstream of the NHL-domain protein GSU2505). An insertion in a putative ATP-dependent transporter (GSU1501), eliminated electrode colonization, but not Fe(III)-citrate reduction. A more complex phenotype was demonstrated by a mutant

containing an insertion in a transglutaminase domain protein (GSU3361), which suddenly ceased to respire when biofilms reached approximately 50% of wild-type levels. As most insertions were not in cytochromes, but rather in transporters, two-component signaling proteins, and proteins of unknown function, this collection illustrates how biofilm formation and electron transfer are separate, but complementary phenotypes, controlled by multiple loci not commonly studied in *Geobacter*.

2.2 Introduction

Geobacter sulfurreducens is a member of the metal-reducing *Geobacteraceae* family, and was originally isolated based on its ability to transfer electrons from internal oxidative reactions to extracellular electron acceptors such as insoluble Fe(III)- or Mn(IV)-oxides (20). *G. sulfurreducens* is also able to use an electrode as its sole electron acceptor for respiration, a phenotype which has many possible biotechnological applications (77, 82), and serves as a useful tool for direct measurement of electron transfer rates (13, 93). As *G. sulfurreducens* was the first *Geobacteraceae* genome sequence available (99), and the only member of this family with a robust genetic system (25), it serves as a model organism for extracellular electron transfer studies.

The proteins facilitating electron transfer to insoluble Fe(III)-oxides by individual *Geobacter* cells, and how these cells interact in multicellular biofilms, are not fully understood. Many genes implicated in Fe(III)- and electrode reduction were identified based on proteomic and microarray analysis of cultures grown with fumarate vs. Fe(III)-citrate as a terminal electron acceptor (32, 51, 100). More recently, similar expression data from Fe(III)-oxide and electrode-grown cultures has also become available (31, 43,

55). In most extracellular electron transfer studies, outer membrane proteins (such as *c*-type cytochromes) have been the focus (18, 70, 75, 98), leading to targeted knockout studies of at least 14 cytochromes to date.

To reduce an insoluble electron acceptor, *Geobacter* must achieve direct contact with the substrate (103). While contact with small Fe(III)-oxide particles may be transient, growth on Fe(III)-coated surfaces or electron-accepting electrodes requires biofilm formation (93, 113). For example, when *G. sulfurreducens* produces an exponentially increasing rate of electron transfer at an electrode, this demonstrates that all newly divided cells remain embedded in the growing, conductive biofilm (13, 93). Thus, in addition to the need for an array of outer membrane cytochromes, there is also a need for control of both cell-cell contact and cell-surface contact.

While a genetic system for *G. sulfurreducens* has been developed, conjugal transfer of a plasmid or a transposon has not been reported (25). The broad-host-range cloning vector, pBBR1MCS-2, has previously been electroporated into *G. sulfurreducens*, but its mobilization capabilities were not utilized (25). Similarly, a number of suicide vectors have been identified for *G. sulfurreducens*, but none have been used to deliver transposons for mutagenesis. *Mariner*-based transposon mutagenesis systems have been successful in a variety of Bacteria and Archaea, producing random insertions (61, 68, 114, 120, 126, 142, 146, 148). For example, genes involved in *Shewanella oneidensis* cytochrome maturation were discovered using the modified transposon, mini-*Himar* RB1 (15).

In this work, we describe a system for the conjugal transfer of the pBBR1MCS family of plasmids from *Escherichia coli* to *G. sulfurreducens*, which allowed transposon mutagenesis based on pMiniHimar RB1. Under strictly anaerobic conditions, a library of insertion mutants was constructed and screened to identify genes putatively involved in attachment and Fe(III)-citrate reduction. Approximately 8,000 insertion mutants were isolated, with insertions distributed throughout the *G. sulfurreducens* chromosome. Subsequent characterization revealed mutants defective in metal reduction but unaffected in all aspects of electrode reduction, as well as mutants able to reduce metals but incapable of electrode reduction. These observations greatly expand the list of *Geobacter* mutants with defects in respiration or biofilm formation, and this library serves as a resource for further screening of extracellular electron transfer phenotypes.

2.3 Materials and Methods

2.3.1 Bacterial strains, plasmids, and culture conditions

Bacterial strains and plasmids used in this study are described in Table 2.1. *G. sulfurreducens* PCA (ATCC #51573) was grown anaerobically at 30°C in a vitamin-free minimal medium containing 20 mM acetate as the electron donor and 40 mM fumarate as electron acceptor (93). *G. sulfurreducens* had been maintained in medium containing 100 mM ferrihydrite as electron acceptor to retain strong biofilm and metal-reduction phenotypes. For *G. sulfurreducens* transposon mutants, 0.01% wt/vol trypticase and 200 µg/ml kanamycin were added to growth medium. *E. coli* WM3064 (122) carrying pMiniHimar RB1 was grown in LB broth containing 50 µg/ml kanamycin and 30 µM 2,6-diaminopimelic acid (DAP) at 37°C. *E. coli* WM3064 carrying pBBR1MCS was

grown in LB broth containing 34 µg/ml chloramphenicol and 30 µM DAP at 37°C, while 50 µg/ml kanamycin was added to cultures of *E. coli* WM3064 carrying pBBR1MCS-2, 100 µg/ml ampicillin was added to cultures carrying pBBR1MCS-4, and 10 µg/ml gentamicin was added to cultures carrying pBBR1MCS-5 (59, 60). *G. sulfurreducens* carrying pBBR1MCS was grown in anaerobic minimal medium containing 10 µg/ml chloramphenicol, while 200 µg/ml kanamycin was added to cultures of *G. sulfurreducens* carrying pBBR1MCS-2, 400 µg/ml ampicillin was added to cultures containing pBBR1MCS-4, and 20 µg/ml gentamicin was added to cultures containing pBBR1MCS-5.

TABLE 2.1 Strains and plasmids used in this study

Strain or plasmid	Relevant characteristics or description	Source
Strains		
G. sulfurreducens	Wild Type (ATC #51573)	20
E. coli WM3064	Donor strain for conjugation: *thrB*1004 *pro thi rpsL hsdS lacZ*ΔM15 RP4-1360 Δ(araBAD)567 ΔdapA1341::[*erm pir*(wt)]	122
E. coli DH5α	Host for *E. coli* cloning	Invitrogen
Plasmids		
pMiniHimar RB1	Plasmid carrying mini*Himar* RBI; *oriR6K*, *oriT*, *lacZ*, Km^r	15
pBBR1MCS	Mobilizable broad-host-range plasmid; *lacZ*, Cm^r	60
pBBR1MCS-2	Mobilizable broad-host-range plasmid; *lacZ*, Km^r	59
pBBR1MCS-5	Mobilizable broad-host-range plasmid; *lacZ*, Gm^r	59
pGCOMP2505	GSU2505 in MCS of pBBR1MCS, Cm^r	This study
pGCOMP1501	GSU1501 in MCS of pBBR1MCS-5, Gm^r	This study
pGCOMP3361	GSU3361 in MCS of pBBR1MCS-5, Gm^r	This study

2.3.2 Conjugal transfer of plasmid

Wild type *G. sulfurreducens* was used in filter mating experiments with *E. coli* WM3064 carrying pBBR1MCS, pBBR1MCS-2, pBBR1MCS-4, or pBBR1MCS-5 (59, 60). *G. sulfurreducens* was grown to an optical density at 600 nm (OD_{600}) of 0.3-0.4. The

donor *E. coli* strain was grown overnight then washed and resuspended in fresh LB to remove antibiotics. Cultures were mixed aerobically in a 1:1 ratio and vacuum filtered on a 0.45 µm filter (Millipore). This filter was incubated on either an LB plate or a vitamin-free minimal medium plate supplemented with fumarate, acetate, and trypticase for 1-24 hours in a MACS MG500 Anaerobic Workstation (Don Whitley Scientific Limited, England) containing 5% H_2, 20% CO_2, and 75% N_2 gas. Filters were then suspended in 3 ml growth medium and vortexed to remove cells. Cells were plated and selected on growth media using the appropriate antibiotic.

2.3.3 Transposon Mutagenesis

Wild type *G. sulfurreducens* was used in filter mating experiments with *E. coli* WM3064 carrying pMiniHimar RB1 (15). *G. sulfurreducens* was grown to an OD_{600} of 0.3-0.4. *E. coli* WM3064 was grown overnight in LB supplemented with 50 µg/ml kanamycin and 30 µM 2,6-diaminopimelic acid (DAP), washed, and resuspended in LB. Cultures were mixed aerobically in a 1:1 ratio and vacuum filtered on a 0.45 µm filter (Millipore). Mating filters were incubated anaerobically on minimal medium containing 0.01% wt/vol trypticase for 4 hours in a MACS MG500 Anaerobic Workstation (Don Whitley Scientific Limited, England) containing 5% H_2, 20% CO_2, and 75% N_2 gas. Filters were then placed in 3 ml growth medium and vortexed to remove cells. The cell suspensions were incubated with occasional shaking for 2 hours, then further diluted in growth medium, plated on minimal medium containing 20 mM acetate, 0.01% (wt/vol) trypticase, and 200 µg/ml kanamycin, and incubated anaerobically at 30°C for 1 week. Isolated colonies were picked anaerobically into 96-well plates containing growth

medium supplemented with 20 mM acetate, 0.01% (wt/vol) trypticase, and 200 µg/ml kanamycin and allowed to grow for one week prior to phenotype screening. In total, over 8,000 transposon mutants were cultured in 96-well plates, and stored at -80ºC. Frozen plates (stored at -80°C) could be revived and re-screened for other phenotypes (such as Fe(III)-oxide reduction) after months of storage.

2.3.4 Phenotype Screening

A bolt replicator (V&P Scientific, San Diego, CA) was used to transfer transposon mutants from a master plate containing growth medium to 96-well flat-bottom polystyrene microtiter plates (Nunc 167008) containing medium specific for auxotroph, biofilm, or Fe(III) reduction screening. Mutants with phenotypes of interest (described below) were streaked for isolation on agar plates to ensure culture purity and re-screened to verify phenotype. OD_{600} was monitored for 72 hours to detect any growth defects and a third phenotype screen performed. Mutants were then transferred to vitamin-free minimal medium containing 25 mM acetate and approximately 100 mM Fe(III)-oxide to test for the ability to reduce insoluble iron.

(i) Auxotroph screen. To screen for amino acid auxotrophs, insertion mutants were transferred to medium lacking trypticase and OD_{600} was measured to identify mutants that were unable to grow in the absence of trypticase.

(ii) Biofilm formation assay. To screen for attachment phenotypes, insertion mutants were grown with minimal medium containing 30 mM acetate for 72 hours at 30°C. To identify mutants with low or high attachment phenotypes compared to wild type, crystal violet (CV) biofilm assays were performed using a modification of a previously described

protocol (104). Cells were stained with 200 µl of a 0.01% (wt/vol) CV solution and allowed to incubate for 15 minutes before wells were rinsed to remove unattached cells. Remaining cells were dried for 20 minutes at room temperature, then the CV was solubilized with 200 µl 100% DMSO. OD_{600} was measured to identify mutants with low or high growth compared to wild type. Prior to screening, electron donor and acceptor concentrations were optimized for *G. sulfurreducens* surface attachment. Acceptor limitation (30 mM acetate, 40 mM fumarate) resulted in greater attachment to the wells of a 96-well plate than donor limitation.

(iii) Fe(III)-reduction. To screen for the inability to reduce Fe(III)-citrate, insertion mutants were transferred to minimal medium containing 10 mM acetate as electron donor and 55 mM Fe(III)-citrate as electron acceptor. Clearing of the medium was monitored as indication of Fe(III)-citrate reduction.

In addition, sequenced transposon mutants were tested for the ability to reduce Fe(III)-oxide. Mutants were transferred to minimal medium containing 20 mM acetate as the electron donor and 100 mM ferrihydrite as the electron acceptor. After two successive transfers (to remove potentially chelating citrate that could rescue certain mutations), cultures were inoculated into the same medium and samples collected over 10 days and diluted 10-fold in 0.5N HCL. To monitor production of Fe(II) over time, 50 µl samples were analyzed in microtiter wells with 300 µl 2g/L ferrozine in 100 mM HEPES buffer, followed by A_{562} measurement (85).

2.3.5 DNA sequencing

For sequencing of transposon insertion sites directly from *G. sulfurreducens* genomic DNA, chromosomal DNA was isolated from mini-*Himar* RB1 mutants after overnight growth using the Wizard Genomic DNA Purification Kit (Promega, Madison, WI). Purified DNA was precipitated in ethanol and resuspended in nuclease free water. Sequencing was performed at the Biomedical Genomics Center at the University of Minnesota. Approximately 3-4 µg of DNA was submitted as template with 12 pmol primer DRB05-27 (TGACGAGTTCTTCTGAGCGG), using the following cycling parameters: 95ºC for 5 min, followed by 99 cycles of 95ºC for 30 s, 55 ºC for 20 s, and 60 ºC for 4 min.

2.3.6 Identification of transposon insertion site

To determine the site of mini-*Himar* RB1 insertion, DNA sequences obtained from transposon mutant genomic DNA were compared to the complete genome of *G. sulfurreducens* (available at the Department of Energy Joint Genome Institute [http://www.jgi.doe.gov/]) using the BLASTN algorithm. The site of insertion in each mutant was confirmed using PCR with primers designed to amplify DNA spanning the insertion.

2.3.7 Construction of complemented mutants

GSU2505 was amplified from wild type *G. sulfurreducens* using primers NHLF (GCAAGCTTATGAGACAAATCGGCAACCG; HindIII site underlined) and NHLR (TAGGATCCTCAGTCGTGCGTTACCTTGA; BamHI site underlined), GSU1501 was amplified from wild type *G. sulfurreducens* using primers 1501S

(CGAAGCTTATGGGTACGTTCATCAATGG; HindIII site underlined) and 1501E (TAGGATCCTCATTCCGGCCCGTTAGACT; BamHI site underlined), and GSU3361 was amplified using primers 3361S (TTAAGCTTTTGCGTGCCGTTCGACGAGAG; HindIII site underlined) and 3361E (TAGGATCCCTACCTCATCTCAACCACCC; BamHI site underlined) The following conditions were used for each: 30 cycles of 94°C for 1 min, 55ºC for 1 min, 72ºC for 1.5 min, then a final extension at 72ºC for 10 min. Each product was digested with HindIII and BamHI. The GSU2505 produced was inserted into the HindIII and BamHI sites of pBBR1MCS, creating the vector pGCOMP2505. This construct was mated into the GSU2505 mutant (*G. sulfurreducens* with insertion coordinate 2762032) and selected on chloramphenicol. The GSU1501 product was inserted into the HindIII and BamHI sites of pBBR1MCS-5, creating the vector pCGOMP1501. This construct was mated into the two GSU1501 mutants (*G. sulfurreducens* with insertion coordinate 1646730 or 1646910) and selected on gentamicin. The GSU3361 product was inserted into the HindIII and BamHI sites of pBBR1MCS-5, creating the vector pCGOMP3361. This construct was mated into the two GSU3361 mutants (*G. sulfurreducens* with insertion coordinate 3693699 or 3694136) and selected on gentamicin.

2.3.8 Electrochemical Analysis

Carbon electrodes were polished using P1500 grit sandpaper (3M, Minneapolis, MN) and prepared as previously described (93). Bioreactors containing a carbon working electrode, platinum counter electrode, and saturated calomel reference electrode connected via a salt bridge were prepared as previously described (93). Sterile growth

medium was added to autoclaved bioreactors, with anaerobic conditions generated by constant flow of humidified N_2:CO_2 (80:20 v/v). Reactors were placed in 30ºC water bath and connected to a 16-channel potentiostat (VMP®, Bio-Logic USA, Knoxville TN) with software (EC-Lab V.9.41) able to run differential pulse voltammetry (DPV), cyclic voltammetry (CV) and chronoamperometry (CA) as previously described (93). Bioreactors were inoculated with 50% (v/v) of *G. sulfurreducens* approaching stationary phase (OD_{600} = 0.40 – 0.55), and incubated for 4-120 hours with a potential of 0.24 V vs. standard hydrogen electrode (SHE) applied.

2.3.9 Confocal Analysis

A Nikon C1 Spectral Imaging Confocal Microscope (Nikon, Japan) was used to image biofilm covered electrodes. Immediately after harvest, biofilms were washed with growth medium and stained with propidium iodide and SYTO 9, from a LIVE/DEAD® *Bac*light™ Bacterial Viability Kit (Invitrogen Corp., Carlsbad, CA). SYTO 9 is membrane-permeable, and stains cells in a population green, while propidium iodide stains cells with damaged membranes red. Electrodes in medium were placed on microscope slides with the coverslips elevated above the thickness of the electrode and viewed using the 488 and 561 nm lasers.

2.3.10 Biomass Measurement

Biomass attached to electrodes was determined using the Pierce bicinchoninic Protein Assay Kit (Thermo Scientific, Rockford, IL). Immediately after electrochemical analysis, carbon working electrodes were dipped in growth medium to remove planktonic cells. The carbon working electrode was then removed from the platinum wire and

incubated in 1 ml of 0.2 M NaOH at 96°C for 20 minutes to remove the attached biomass. The protein present in the 1 ml NaOH sample was measured, indicating the biomass attached to the electrode.

2.4 Results

2.4.1 Development of a transposon mutagenesis system in *G. sulfurreducens*

A system for conjugal transfer of plasmids into *Geobacter* has not been described. However, the broad host range plasmid pBBR1MCS-2, which has been electroporated into *G. sulfurreducens* (25), can be mobilized by E. *coli* WM3064, as this DAP auxotroph contains mobilization genes on its genome. Filter matings between E. *coli* WM3064 carrying pBBR1MCS-2 and *G. sulfurreducens* were successful when filters were incubated on either LB or *Geobacter* medium plates, with highest numbers of transconjugants (>10^7 from a mating of 10^9 *G. sulfurreducens*) occurring when matings were performed in an anaerobic chamber on *Geobacter* medium supplemented with trypticase. Related plasmids (pBBR1MCS-1, pBBR1MCS-4, and pBBR1MCS-5) were also transferred into *G. sulfurreducens* using the appropriate antibiotic selection.

G. sulfurreducens is typically described as a strict anaerobe, but recent data have shown an ability to both tolerate and even utilize small amounts of oxygen (73). This tolerance was exploited in developing a protocol in which *Geobacter* cultures were captured on a filter with *E. coli*. The filter could be aerobically rinsed free of antibiotics and other medium, placed on solid medium and transferred into an anaerobic chamber. Anaerobic incubation beyond 4 hours did not significantly increase the number of transconjugants. After matings, cells were recovered on selective medium, and putative

transconjugants picked and inoculated into liquid medium (in 96-well plates) in an anaerobic chamber.

Matings between *G. sulfurreducens* and *E. coli* WM3064 carrying pMiniHimar RB1 (a non-replicating plasmid in *G. sulfurreducens*) were performed using the conditions developed for conjugal transfer (4 hour anaerobic filter matings, anaerobic colony picking), producing up to10^5 mutants (containing insertion of the 2.2 kb transposable element) in a single mating. Some preliminary sequencing using genomic DNA to identify the location of transposon insertions produced mixed sequencing data, suggesting either mixed cultures, or clonal cultures carrying multiple insertions. Thus, after mating, filters were shaken gently in kanamycin-free medium for 2 hours (less than half the doubling time of *G. sulfurreducens*) to facilitate separation of cells before dilution and plating. In addition, all mutants were re-isolated from single colonies and phenotypes re-verified before sequencing. These steps dramatically reduced the occurrence of mutants with ambiguous sequencing results. If cultures produced poor sequencing data, or insertion sites were uncertain in any way, mutants were discarded prior to characterization. Transposon locations determined via direct sequencing of genomic DNA averaged ~900 bp, which was sufficient to locate the insertion site. Insertions were verified via PCR, using primers spanning the putative insertion site.

2.4.2 Construction and screening of a mini-*Himar* RB1 insertion library in *G. sulfurreducens*

To verify the method's ability to produce insertional mutations with identifiable phenotypes, mutants were screened for an inability to grow in the absence of trypticase.

Putative auxotrophs were re-streaked and re-isolated, and DNA from these cultures used to test protocols for identifying the transposon insertion site. For example, a mutant (13A2) was identified that was unable to grow in the absence of trypticase, with a transposon insertion in GSU3097. This gene was annotated as *hisH* (a component of imidazole glycerol phosphate synthase), in a cluster of proteins putatively involved in histidine biosynthesis (Fig. 2.1A). PCR of this region confirmed the presence of a 2.2 kb insertion in this mutant (data not shown). Addition of histidine restored growth, which was consistent with a defect in histidine biosynthesis (Fig. 2.1B). No mutants recovered from the auxotroph screen were in similar regions of the genome, suggesting random incorporation of the transposable element (Table 2.2).

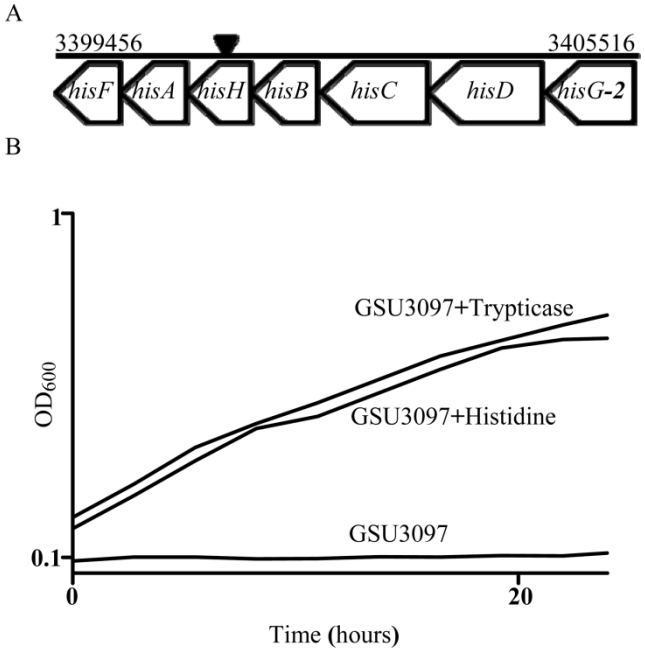

Figure 2.1 A) View of *G. sulfurreducens* chromosomal DNA with coordinates 3399456-3405516, showing location of transposon insertion for mutant

GSU3097, located among putative histidine biosynthesis genes (*hisF* – imidazole glycerol phosphate synthase subunit, *hisA* – phosphoribosylformimino-5-aminoimidazole carboxamide ribotide isomerase, *hisH* – imidazole glycerol phosphate synthase subunit, *hisB*-imidazoleglycerol-phosphate dehydratase, *hisC* – histidinol phosphate aminotransferase, *hisD* – histidinol dehydrogenase, and *hisG-2* – ATP phosophribosyltransferase). B) Growth curves (representative of 3 replicates) for GSU3097 mutant in presence and absence of 0.01% wt/vol trypticase or supplemented with 0.01% wt/vol histidine. Lines connect data points collected automatically every 2.75 hours by a spectrophotometer housed inside an anaerobic glove box.

TABLE 2.2A pMiniHimar transposon mutants isolated in this study

Mutant	GSU locus[a]	Annotation[b]
13A2	3097	hisH
13D8	3253	Response Regulator
51G10	0785	Nickel dependent hydrogenase, large subunit
54B11	0782	Nickel dependent hydrogenase, small subunit
21B3	0685	Radial SAM domain protein
48B1	1074	Hypothetical protein
56F4	1197	RNA methyltransferase
58F8	0506	Methylamine utilization protein
59C5	0007	PAS/PAC signal transduction histidine kinase
63E10	1330	Metal ion efflux protein
70B1	0274	Cytochrome C family protein
70B4	1486	MttB family protein, TatC
2C3	2505*	NHL repeat domain protein
7A2	1012	Hypothetical protein
13B6	0881	Sensor histidine kinase
15E9	1999	Hfq protein
47D9	1928	Sensor histidine kinase/response regulator

63H3	2889	Hypothetical protein
70A12	1665	Rhomboid family protein
71F12	1508	Hypothetical protein
79G11	2759	Potassium efflux system protein
13E5	1492	Twitching motility protein PilT
20B5	1501	ABC transporter, ATP binding protein
20C6	2948	Hypothetical protein
21H3	0170	GreA/GreB family protein
22G11	1499	Hypothetical protein
26D6	2898	High molecular weight cytochrome C
26E12	1226	Hypothetical protein
33B8	3361	Transglutaminse domain protein
34E4	3129	MATE efflux family protein
36H2	0351	NADH Dehydrogenase 1, N Subunit
61C5	1891	Response Regulator
62F6	1891	Response Regulator
67B2	1501	ABC transporter, ATP binding protein
68D1	0599	Sensor histidine kinase
68H10	2925	Hypothetical protein
72B5	1432	TPR domain protein
73F4	3361	Transglutaminse domain protein
77B8	3438	Hypothetical protein

[a] GSU locus designation assigned by JGI For the ORF disrupted by the pMiniHimar RBI transposon

[b] Annotation assigned by JGI

TABLE 2.2B pMiniHimar transposon mutants isolated in this study

Mutant	Coordinate[c]	Attachment[d]	Fe(III)-citrate[e]	Fe(III)-oxide[f]
13A2	3401903	+	+	+
13D8	3566024	+	-	+
51G10	846918	+	-	+
54B11	843038	+	-	+
21B3	722345	+	-	+
48B1	1163782	+	-	+
56F4	1300712	+	-	+
58F8	537753	+	-	+
59C5	11967	+	-	+
63E10	1455965	+	-	+

70B1	283160	+	-	+
70B4	1629929	+	-	+
2C3	2762032	-	+	+
7A2	1094418	-	+	+
13B6	941495	-	+	+
15E9	2191532	-	+	+
47D9	2109312	-	+	+
63H3	3175621	-	+	+
70A12	1829414	-	+	+
71F12	1653572	-	+	+
79G11	3038775	-	+	+
13E5	1636675	++	+	+
20B5	1646730	++	+	-
20C6	3247587	++	+	+
21H3	187315	++	+	+
22G11	1645371	++	+	-
26D6	3186221	++	+	+
26E12	1329442	++	+	+
33B8	3693699	++	+	+
34E4	3430078	++	+	-
36H2	381393	++	+	+
61C5	2068995	++	+	+
62F6	2068944	++	+	+
67B2	1646910	++	+	-
68D1	631524	++	+	+
68H10	3225163	++	+	+
72B5	1569891	++	+	+
73F4	3694136	++	+	+
77B8	3783890	++	+	+

[c] Coordinate of the transposon insertion in the *G. sulfurreducens* genome
[d] High (++) or low (-) biofilm adhesion in crystal violet assay compared to wild type (+)

[e] Ability to reduce Fe(III)-citrate

In this report, we detail results from two phenotypic screens; attachment and Fe(III)-citrate reduction. Mutants were screened for deficiencies in adhesion to 96-well plates using a crystal violet assay (104), following incubation under electron acceptor-limited conditions. After determination of OD_{600} (to identify low-growth cultures which could produce false negatives), mutants with attachment levels as high as 275%, and as low as 35% of wild-type were identified (Fig. 2.2). To identify genes involved in Fe(III)-reduction, mutants were cultivated in Fe(III)-citrate, and detected based on the color difference between Fe(III) and fully reduced Fe(II) after 10 days.

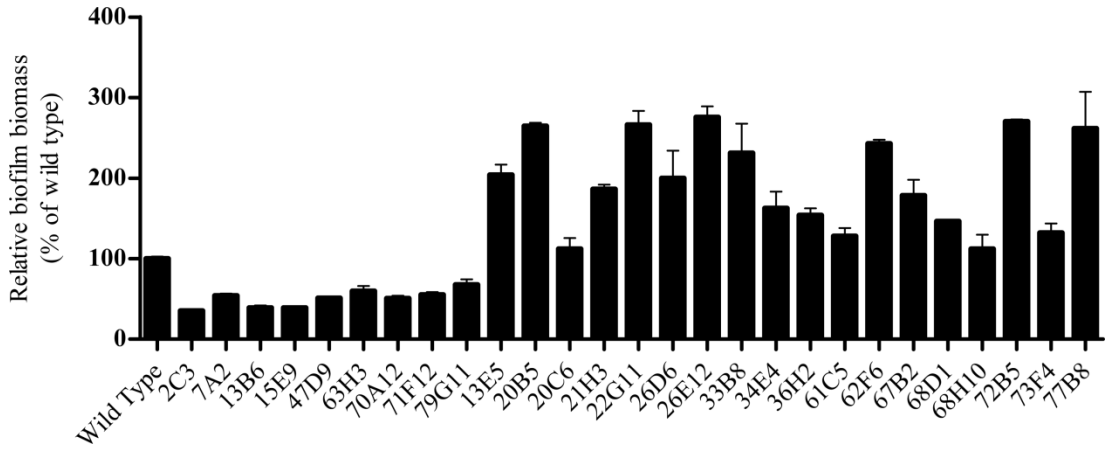

Figure 2.2 Biofilm formation by *G. sulfurreducens* attachment mutants, based on crystal violet staining of cells adherent to 96-well plates after 72 hours of growth in fumarate-limited medium in an anaerobic glove box. The mean absorbance of each mutant in a minimum of three trials is expressed relative to that for wild type *G. sulfurreducens* (mean absorbance was ~ 0.39). Error bars are the standard errors of the mean for 3 replicates.

Approximately 500 cultures were initially identified with detectable alterations in these two phenotypes. After a second round of re-isolation, re-screening, sequencing and PCR verification, 39 mutants were retained with strong, consistent phenotypes of interest to the current study. An additional factor in choosing mutants for further study was measurement of growth rates and yield (OD_{600}) in 96-well plates using a spectrophotometer housed in an anaerobic chamber (Fig. 2.3). This additional screen allowed for identification of mutants with general metabolic deficiencies. An example of a mutant with markedly slower growth and final optical density is shown in Fig. 2.3 (brown trace, containing an insertion in GSU0170), compared to other mutants which demonstrated near wild-type behavior. While some genes or gene clusters were disrupted more frequently than others, no mutant was isolated with an identical insertion, and alignment of insertion regions from 15 sequenced mutants revealed only a TA-motif at the insertion site (as noted by (65, 66)). A list of phenotypes and corresponding sites is shown in Table 2.2.

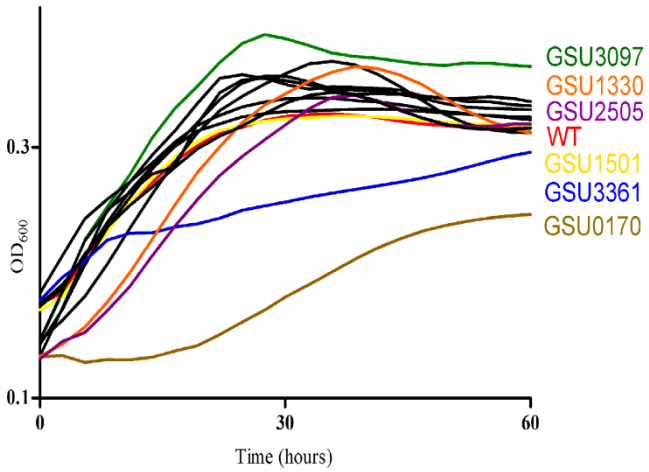

Figure 2.3 Growth curves showing screening process used to identify metabolic defects in the initial library of transposon mutants. Wild type *G.*

sulfurreducens is shown in red, and a selection of transposon mutants discussed in subsequent sections are shown, including GSU1330 (orange), GSU1501(yellow), GSU2505 (purple), GSU3097 (green), and GSU3361 (blue). Examples of mutants with growth rates similar to wild type are shown in black, while a mutant (GSU0170) with a decreased growth rate is shown in brown.

2.4.3 Electrochemical analysis and confocal microscopy of selected transposon mutants

The screening tools used to discover mutants were based on general consequences of respiration or cell surface alterations. However, electron transfer to solid electron acceptors by *Geobacter* is a complex process requiring initial attachment, followed by proper networking of daughter cells within the biofilm matrix (113). Improper localization of proteins on cell surfaces can also interfere with reduction of insoluble electron acceptors (97), and these intertwined phenotypes are difficult to study using heterogeneous electron acceptors such as Fe(III)-oxides. Use of an electrode surface as an electron acceptor offers a consistent, geometrically defined surface, which can be poised at a fixed potential to act as a homogenous electron acceptor. Defects in initial attachment can be separated from defects in cell-cell attachment, and both biofilm characteristics and respiration rates can be directly measured.

First, wild type *G. sulfurreducens* was analyzed by inoculating cultures into bioreactors containing polished carbon electrodes, which were poised to act as electron

acceptors at +0.24 V vs. SHE. After inoculation of a wild type electron acceptor-limited culture, chronoamperometry revealed an exponentially increasing rate of electron transfer to the electrode, as has been described previously (13, 93). To prepare a baseline set of images for comparison to mutant cultures, electrodes were harvested during growth and imaged using confocal laser scanning microscopy (CLSM). The use of polished (1500 grit), flat electrodes caused biofilms to be highly similar at all imaged locations, with the exception of sites at the very edge of the electrode, near the magnetic stir bar. For each electrode, multiple stacks near the center of each electrode were collected (two independent electrodes analyzed per time point) and representative images are shown spanning early to late growth.

A series of CLSM images collected over a span of 120 hours allowed for a demonstration of events occurring as current production rates at electrodes increased (Fig. 2.4). Within the first 24 hours of colonization, electrodes appeared completely covered with at least a monolayer of cells. As biofilms became thicker, films remained uniform, with no clear 'pillars' or higher order structures appearing. During the first 48 hours, the rate of electron transfer to electrodes increased exponentially, indicating that each new layer of cells attached to the growing biofilm was also capable of donating electrons to the electrode. After 72 hours, the rate of electron transfer did not increase further, as has been reported previously (93). However, the biofilm continued to thicken over the next 48 hours, indicating that beyond a certain level, additional cells could not contribute to additional electron transfer to the surfaces.

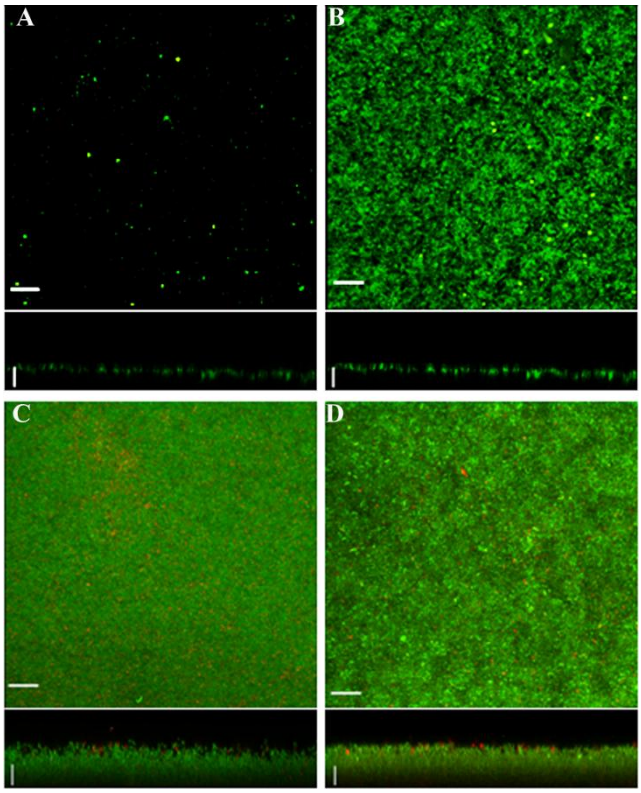

Figure 2.4 CLSM of wild type biofilm formation by *G. sulfurreducens* grown using a carbon electrode as the electron acceptor (+0.24 V vs. SHE). Cells are shown at A) 4, B) 18, C) 72, and D) 120 hours after inoculation. Images similar to wild type film formation at intermediate time points can be seen in Fig. 5 G-H and Fig. 6 D-E. Top panels are maximum projections (bar = 20 μm), bottom panels are side projections (bar = 10 μm). 'Live' cells stain green, while permeable cells stain red.

Mutants with strong biofilm or Fe(III) reduction phenotypes were then analyzed using the same electrochemical approach, and imaged using CLSM. In addition, voltammetry data (cyclic voltammetry and differential pulse voltammetry, described previously (93)), were collected for each mutant for comparison with wild-type behavior.

Each mutant was grown in at least four independent replicate electrode experiments, with representative data and confocal images shown in Figs 2.5 and 2.6.

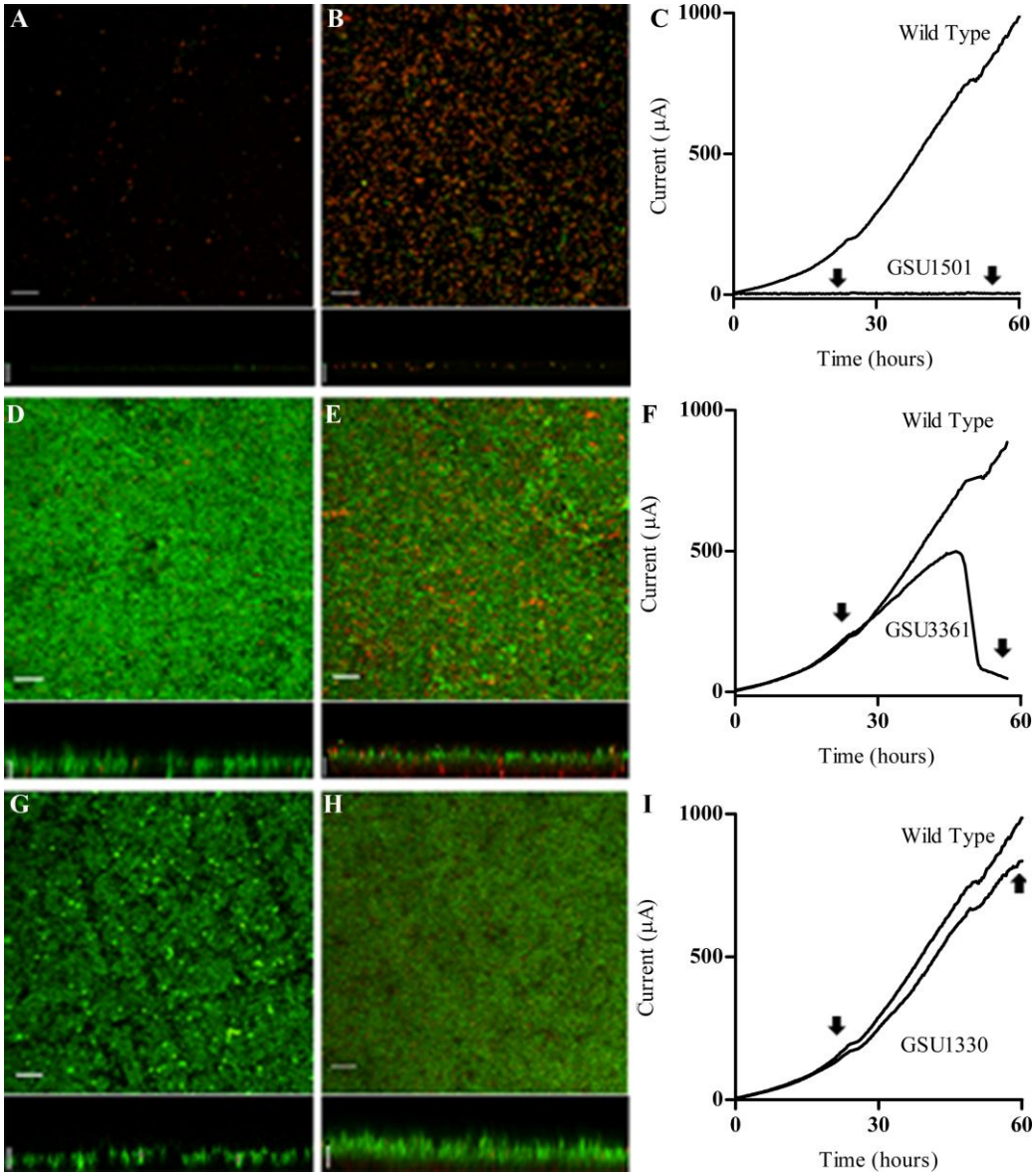

Figure 2.5 Representative CLSM images and chronoamperometry of biofilm formation by *G. sulfurreducens* transposon mutants on carbon electrodes poised at +0.24 V vs. SHE. GSU1501 mutant at A) 24 and B) 48 hours,

GSU3361 mutant at D) 24 and E) 60 hours, GSU1330 mutant at G) 24 and H) 60 hours. Top panels are maximum projections (bar = 20 μm), bottom panels are side projections (bar = 10 μm). 'Live' cells are green, while permeable cells are red. Chronoamperometry for each mutant is shown in the right column (C, F, I) along with wild type *G. sulfurreducens*. Arrows indicate CLSM timepoints.

For example, two separate mutants were identified in the crystal violet assay as having a high level of attachment (~260% that of wild type), but no defect in Fe(III)-citrate reduction. Both of these mutations mapped to separate regions of open reading frame GSU1501. This gene encoded a putative ATP-binding protein, in a gene cluster containing a permease domain for a hypothetical ABC transporter. While the GSU1501 mutant was identified based on a strong attachment phenotype (in 96-well plates), it failed to demonstrate any significant capacity for electron transfer to the electrode surface (maximum of 10 μA, compared to nearly 900 μA in wild-type) (Fig. 2.5C). Both insertion mutants were tested separately for growth on electrodes and produced identical phenotypes.

Imaging of electrodes at different time points showed very few GSU1501 mutant cells attached to electrodes at 24 and 48 hours, in contrast to wild type *G. sulfurreducens* (Fig. 2.4, Fig. 2.5A-B). In addition, most mutant cells attached to the electrodes were permeable to the propidium iodide stain (red cells in Fig. 2.5), which suggested that these cells were not viable. When biomass was recovered from electrodes and used to express

electron transfer rates as a function of attached protein, the GSU1501 mutants produced a maximum of only 100 μA/mg protein, compared to a maximum of over 4000 μA/mg protein produced by wild type cultures. Consistent with this strong defect in electron transfer to an electrode surface was the observation that these mutants were unable to reduce Fe(III)-oxides (even though this mutant reduced Fe(III)-citrate at wild-type levels).

While the same open reading frame (GSU1501) was disrupted in two separate mutants, complementation with this gene alone did not restore wild-type phenotype. When GSU1501 was expressed *in trans* with a constitutive promoter, complemented strains only marginally increased their maximum rate of current production (~20 μA maximum, data not shown). The presence of multiple genes up- and downstream of GSU1501, including additional ATP binding cassette subunits, suggested that the insertion was polar, producing the observed phenotype as the sum of multiple defects in this cluster.

Another gene identified more than once in the initial screen, based on a high level of attachment in the crystal violet assay (230% of wild type), also demonstrated unexpected behavior when grown as a biofilm with an electrode as the electron acceptor. Both mutants contained insertions located in different sites within a gene (GSU3361) encoding a protein putatively attached to the inner membrane by a single transmembrane domain, with a periplasmic domain bearing similarity to transglutaminases. After 24 hours of growth, each of these mutants colonized electrode surfaces, and demonstrated electron transfer rates similar to wild type (Fig. 2.5D).

However, in all incubations (for both mutants), there was a sudden decrease in electron transfer rate by 48 hours (Fig. 2.5F). Imaging of biofilms prior to this sudden decrease showed films of similar thickness and morphology to wild type cultures, but imaging of biofilms immediately after the decrease revealed the layer of cells closest to the electrode was permeable to propidium iodide. This indicated a sudden event which damaged the membranes of cells closest to electrodes, triggered at a time when biofilms reached an electron transfer rate ~50% of maximum (Fig. 2.5E). This event was highly repeatable in both mutants, and biofilms could not be restored to high rates of electron transfer after this precipitous drop occurred (e.g., by addition of electron donor, changing of medium, or further incubation).

Complementation with only GSU3361 *in trans* with a constitutive promoter produced cultures which did not display this catastrophic decline in electron transfer. The current production rate slowed as cultures approached ~50% of wild type rates, and only reached current densities of ~70% of wild type (see supplementary Fig 2.S1). Confocal images of these complemented strains also confirmed that cells throughout the biofilm consistently stained as viable. However, biofilms formed by the complemented strains appeared more compact at the base, and extended in tufts for as much as 40 μm beyond the base of the biofilm. This intermediate response, which was not seen in any other wild type or mutant culture, could be due to improper expression levels of GSU3361 from the constitutive promoter, or residual polar effects from the small hypothetical gene downstream of GSU3361.

An example of a mutant which demonstrated a strong phenotype in liquid culture, but not on electrode surfaces, contained an insertion in GSU1330. This mutant was initially identified as having a decreased ability to reduce Fe(III)-citrate. As GSU1330 was similar to outer membrane metal ion efflux proteins (most similar to Cu(I)/Ag(I) RND exporters) (36, 36, 48), the kinetics of metal reduction were investigated further. In liquid culture, metal reduction slowed as Fe(II) accumulated above 10 mM, and ceased at levels above 35 mM; however, this mutant was able to reduce Fe(III)-oxide at wild type levels and rates (data not shown). As free Fe(II) does not accumulate in Fe(III)-oxide medium, but rather adsorbs to Fe(III) surfaces and leads to formation of magnetite (103), this further argued that GSU1330 was part of an Fe(II) export system. Consistent with a role for this protein in metal ion export rather than respiration, this mutant colonized electrodes and demonstrated peak electron transfer rates similar to wild type cultures (Fig. 2.5G-I).

Some mutants originally identified as having a decreased level of attachment in the crystal violet assay also had altered respiratory phenotypes. A mutant containing an insertion upstream of GSU2505 (part of a cluster of outer membrane *c*-type cytochromes including OmcS (GSU2504) and OmcT (GSU2503)) (98), was able to reduce Fe(III)-citrate, but electrochemical analysis showed a defect in the maximum rate of electron transfer. While wild type cultures always produced maximum rates >800 µA/electrode, the GSU2505 mutant produced a maximum value of approximately 200 µA (Fig. 2.6C). Unlike the behavior of mutants such as GSU1501, CLSM imaging showed only slightly altered levels of attachment and biofilm formation on electrodes compared to wild type,

suggesting that the defect was not related to the ability of cells to attach to surfaces or to each other, but to transfer electrons within films (Fig. 2.6B). When corrected for attached biomass, the GSU2505 mutant generated a maximum of approximately 1500 µA/mg protein, also consistent with high levels of attachment but poor rates of long distance electron transfer.

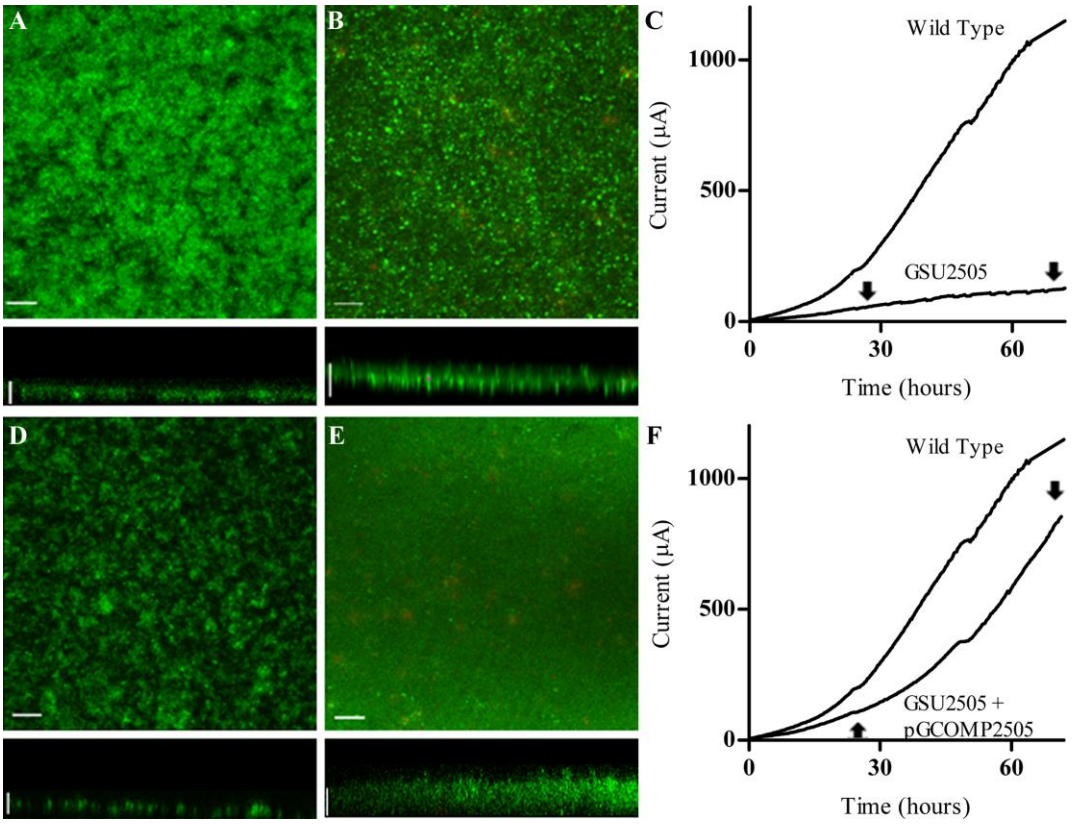

Figure 2.6 Representative CLSM images of biofilm formation of the GSU2505 mutant and complemented strain on carbon electrodes poised at +0.24 V vs. SHE. Both strains were imaged at (A and D) 24 and (B and E) 72 hours. Top panels are maximum projections (bar = 20 µm), bottom panels are side projections (bar = 10 µm). 'Live' cells are green, while permeable

cells are red. Chronoamperometry for C) GSU2505 mutant and D) complemented strain is shown in comparison to wild type *G. sulfurreducens*. Arrows indicate CLSM timepoints.

Unlike the other mutants, the insertion site of the GSU2505 mutant was upstream of an open reading frame, rather than within a coding sequence. DNA containing only GSU2505, the first gene downstream of the insertion, was expressed *in trans* with a constitutive promoter in the transposon mutant. Complementation with this fragment restored electron transfer, and also produced biofilms with similar morphology (less dense and clumped cells) (Fig. 2.6D-F). Based on biomass recovered from electrodes, the rate of electron transfer in the complemented mutant increased to 3800 μA/mg protein, nearly that of wild type.

The mutant containing an insertion upstream of GSU2505 was the only strain which also demonstrated altered phenotypes in the more detailed electrochemical analyses (e.g., slow scan rate cyclic voltammetry). Wild type *G. sulfurreducens* has been shown to respond to applied potential in what is commonly described as a wave, rising steeply at a characteristic midpoint potential at all stages in biofilm growth (93). When the derivative of this wave is plotted, three peaks are evident in wild type biofilms, at approximately -0.25 V, -0.15 V and -0.05 V. The GSU2505 mutant demonstrated a similar midpoint potential, and peak width at half-height, of the primary catalytic feature at -0.15 V (Fig. 2.7). However, differences in the two other regions of the current-potential curve were evident. Both features were regained in the complemented strain,

namely, the small peak at -0.25 V and the broad shoulder at higher potential (-0.05, Fig. 2.7). These observations suggested alterations in levels of redox-active proteins accessible to the electrode, but not a change in the rate-controlling step (at -0.15 V).

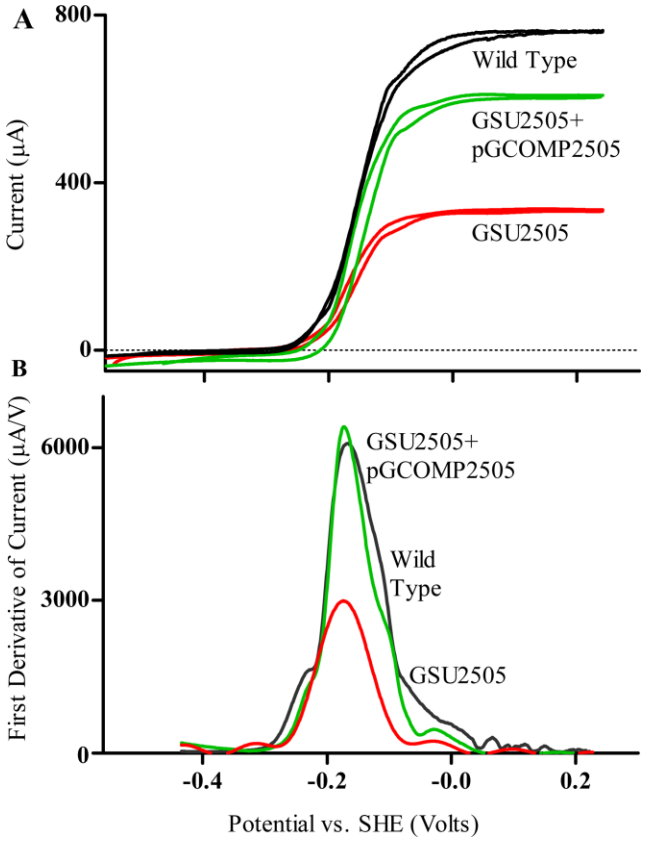

Figure 2.7 A) Cyclic voltammetry of *G. sulfurreducens* biofilms 72 hours after inoculation, showing wild type (black), GSU2505 mutant (red), and complemented mutant (blue). B) First derivatives of cyclic voltammograms of biofilms.

2.5 Discussion

A system for the introduction of plasmids through conjugation, coupled with an efficient transposon mutagenesis method for *G. sulfurreducens,* has increased the number of known genes linked to extracellular electron transfer and biofilm formation. In addition, the use of a poised electrode surface has demonstrated that these phenotypes can be separated from each other, resulting in mutants with defects in one aspect (electron transfer) but not the other (biofilm formation).

As transposon mutagenesis has not been reported in this organism, preliminary experiments were performed to verify the method, and maximize the likelihood of single random insertions causing observed phenotypes. For example, additional cell separation and re-isolation steps were essential to obtaining pure cultures, and all mutants were screened for metabolic defects (by measurement of growth rates and yields) which could confound interpretation of attachment and respiration data. The method identified amino acid auxotrophs (such as the histidine auxotroph with an insertion in GSU3097), as well as mutants with biofilm and electron transfer phenotypes, and produced a library which can be used in future experiments.

Some disrupted genes have been identified and discussed in previous *Geobacter* work, such as GSU0785 and GSU0782 which are predicted to encode large and small subunits (*hybL* and *hybS*,) of a nickel dependent hydrogenase necessary for hydrogen-dependent reduction of Fe(III) (26). As the Fe(III)-reduction screen was conducted in the presence of hydrogen, this phenotype was expected. Another example of a previously studied locus was GSU1492, coding for the PilT subunit of one of the pili clusters of *G.*

sulfurreducens. This mutant demonstrated increased attachment to surfaces, suggesting that pilT (typically involved in retraction of type IV pili) could also be involved in release of *Geobacter* from surfaces (6).

While these findings show how mutagenesis may complement other approaches, most mutants were identified with insertions in genes never described as significantly abundant or differentially regulated in genome-wide studies (31, 32). Notable among these was a mutant in the *c*-type cytochrome GSU0274, which was identified based on a defect in Fe(III)-citrate reduction. This cytochrome has never been described as differentially regulated or essential in any other microarray or proteomic experiments. The overall lack of identified cytochrome genes was not surprising, as we selected for mutants unable to demonstrate any Fe(III) reduction over a long period of time, and many cytochrome mutants in *Geobacter* show residual background activity, or an ability to adapt via expression of other cytochromes to rescue their phenotype (54, 69).

The mutants chosen for further characterization also demonstrated how the 96-well-based attachment assay was not a predictor of electrode-attached biofilm phenotypes in *Geobacter,* but did detect cells with altered outer surfaces. For example, both of the GSU1501 mutants were identified based on a 'high attachment' crystal violet phenotype, but showed almost no attachment to a carbon electrode. As these mutants were able to reduce Fe(III)-citrate, but unable to reduce Fe(III)-oxide, the inability to transfer electrons to the surfaces of carbon electrodes and Fe(III)-oxide may require similar attachment mechanisms which are facilitated by this gene cluster. While strong defects in metal- or electrode reduction in *Geobacter* are typically due to deletions of key

cytochromes, or in protein export pathways, GSU1501 was a component of an ABC transporter not identified in any previous study. A substrate-binding domain was not located near this transporter (suggesting a role for this protein in export) (109), which indicates for the first time that export of a small molecule may be involved in assembly or localization of proteins involved in biofilm formation and metal reduction.

Similarly, both of the GSU3361 mutants, first identified by their 'high attachment' phenotype, did not display increased attachment to electrodes, or enhanced current generation (Fig. 2.5D-F). In these mutants, growth and respiration were initially similar to wild type, followed by a sudden decrease, which correlated with the apparent death of cells nearest the electrode (Fig. 2.5E-F). Recent studies have shown that the interior of a thick *Geobacter* biofilm can represent a markedly different environment than the exterior (e.g., lower pH at the base) (38, 130), which may explain the dependence on biofilm age in triggering the striking phenotype. A drop in cell wall or membrane integrity could be related to the predicted periplasmic-targeted transglutaminase domain in GSU3361, which is similar to domains implicated in protein cross-linking (145), and strengthening of cell walls and membranes (49, 138). In addition, the fact that the entire flux of electrons to the electrode was compromised, when only the cells closest to the electrode were damaged, provides an independent observation of the importance of the cell-electrode interface layer in transmitting electrons to the surface from cells more distant from the electrode.

A mutant with a reduced capacity for Fe(III)-citrate reduction that generated wild type current levels (GSU1330), was also identified. Past studies had suggested that

GSU1330 played a role in electron transfer to electrodes, as it is part of a gene cluster strongly upregulated in cells grown on the anode of a microbial fuel cell (43). In addition, GSU1330 was downregulated in an outer membrane cytochrome mutant with a decreased capacity for current production (55). However, no effect on electron transfer was observed when the GSU1330 mutant was examined under our controlled electrode-growth conditions (Fig. 2.5I). The hypothesis that the disruption was in an Fe(II)-efflux protein was supported by the observation that the GSU1330 mutant was only defective in reduction of soluble Fe(III) (where high levels of Fe(II) accumulate), but not insoluble Fe(III) (where solube Fe(II) binds the iron oxide). Based on these observations, not all genes significantly up- or down-regulated when cells are grown on electrodes are necessarily involved in electrode respiration.

An example of the opposite phenotype (a mutant deficient in current generation but not in Fe(III) reduction) was also characterized (GSU2505) (Fig. 2.6C). The nearest gene downstream of the insertion was annotated as containing a putative NHL domain protein, but was located just upstream of genes for the well-studied outer membrane cytochromes OmcS and OmcT. Deletion of *omcS* has been reported to reduce rates of current production in microbial fuel cells (43, 98). In this study, the GSU2505 transposon mutant was also partially defective in respiration to electrodes. Electrodes held at constant potential, combined with biofilm imaging and electrochemical analyses, were able to show that this was not due to an attachment or biofilm defect *per se*, nor was it due to a defect in the primary mechanism of transferring electrons to the outer surface (e.g., as evidenced by the similar midpoint potentials in cyclic voltammetry). Instead,

data pointed to a defect in electron transfer between cells. As complementation with only GSU2505 (which contains no putative redox-active domains) restored respiration, electrochemistry, and attachment phenotypes (Fig. 2.6E-F), and the phenotypes of this mutant and OmcS mutants were similar, GSU2505 may be needed for proper expression or assembly of proteins such as OmcS.

2.6 Implications

A reliable and efficient method for transposon mutagenesis and screening under anaerobic conditions in *G. sulfurreducens* using mini-*Himar* RB1 was used to identify many genes previously not known to be involved in biofilm formation and Fe(III) reduction. We have also demonstrated how these two phenotypes can be separated by analysis using poised-potential electrodes and biofilm imaging. This library extends the study of extracellular electron transfer beyond key cytochromes, implicating such factors as RNA processing, two-component regulatory networks, small exported molecules, and post-translational processing in electron transfer. Expansion and further screening of this same library for mutants defective in reduction of insoluble metals, reduction of compounds relevant to bioremediation (such as U(VI)), and attachment to more environmentally relevant surfaces will complement ongoing studies aimed at understanding the physiology of *Geobacter*.

2.7 Supplementary data

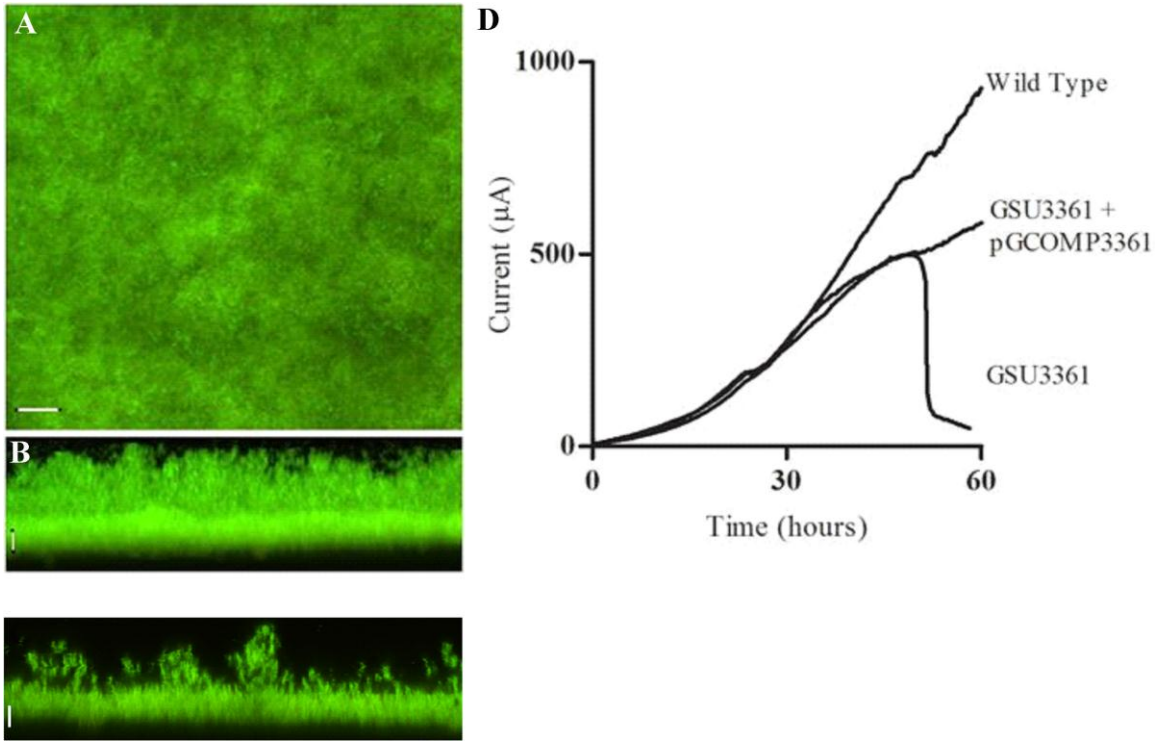

Figure 2.S1 A-C) Representative CLSM images of biofilm formation of a GSU3361 complemented mutant on carbon electrodes poised at +0.24 V vs. SHE. Strain was imaged at 60 hours. Maximum projections from A) above the biofilm (bar = 20 μm), and B) viewed from the side of the biofilm (bar = 10 μm) are shown. Image in C) is a single vertical slice of biofilm formed by the GSU3361 complemented mutant, showing how vertical pillars of cells (bar = 10 μm) produce the additional 'height' in the maximum projection in (B). 'Live' cells are green, while permeable cells are red. D) Chronoamperometry for GSU3361 complemented mutant is shown in comparison to wild type *G. sulfurreducens*, and the transposon insertional mutant.

Identification of an Extracellular Polysaccharide Network Essential for Cytochrome Anchoring and Biofilm Formation in *Geobacter sulfurreducens.*

Rollefson, J.B., C.S., Stephen. M. Tien, and D.R. Bond. Journal of Bacteriology, March 2011, volume 192, p. 1023-1033.

0021-9193/11/$12.00 doi: 10.1128/JB.01092-10

Chapter 3: Identification of an Extracellular Polysaccharide Network Essential for Cytochrome Anchoring and Biofilm Formation in *Geobacter sulfurreducens*

3.1 Overview

Transposon insertions in *G. sulfurreducens* GSU1501, part of an ATP-dependent exporter within an operon of polysaccharide biosynthesis genes, were previously shown to eliminate insoluble Fe(III) reduction and use of an electrode as electron acceptor. Replacement of GSU1501 with a kanamycin resistance cassette produced a similarly defective mutant, which could be partially complemented by expression of GSU1500-1505 *in trans*. The Δ1501 mutant demonstrated limited cell-cell agglutination, enhanced attachment to negatively charged surfaces, and poor attachment to positively charged poly-D-lysine or Fe(III)-coated surfaces. Wild type and mutant cells attached to graphite electrodes, but when electrodes were poised at an oxidizing potential inducing a positive surface charge (+0.24 V vs. SHE), Δ1501 cells detached. Scanning electron microscopy revealed fibrils surrounding wild type *G. sulfurreducens* which were absent from the Δ1501 mutant. Similar amounts of Type IV pili and pili-associated cytochromes were detected on both cell types, but shearing released a stable matrix of *c*-type cytochromes and other proteins bound to polysaccharides. Matrix from the mutant contained 60% less sugar and was nearly devoid of *c*-type cytochromes such as OmcZ. Addition of wild type extracellular matrix to Δ1501 cultures restored agglutination and Fe(III) reduction. The polysaccharide binding dye Congo red preferentially bound wild type cells and

extracellular matrix material compared to the mutant, and Congo red inhibited agglutination and Fe(III) reduction by wild type cells. These results demonstrate a crucial role for the *xap* (extracellular anchoring polysaccharide) locus in metal oxide attachment, cell-cell agglutination, and localization of essential cytochromes beyond the *Geobacter* outer membrane.

3.2 Introduction

Many dissimilatory Fe(III)-reducing bacteria are able transfer electrons from cytoplasmic respiratory oxidation reactions to external Fe(III) oxyhydroxides. The predominant Fe(III)-reducing organisms in a variety of anaerobic neutral pH environments belong to the *Geobacteraceae* family of Deltaproteobacteria (44, 118, 125). The genetically tractable representative *Geobacter sulfurreducens* (25) can transfer electrons to soluble electron acceptors such as fumarate and Fe(III) citrate, as well as insoluble electron acceptors such as Fe(III) and Mn(IV) oxyhydroxides (20). Like most *Geobacteraceae,* it can also use properly poised electrodes as electron acceptors, and will form 20-40 μm thick biofilms on such surfaces, with each cell layer able to direct electrons to the electrode via a long-range electron transfer mechanism (13, 93, 94).

To reduce an external electron acceptor such as Fe(III) or an electrode, *Geobacter* must construct a chain of redox proteins linking the outer membrane to the electron-accepting surface (103). Additionally, formation of a network allowing electron transfer between cells is necessary for growth of daughter cells not in contact with Fe(III) particles, or to allow new cell layers to grow at a distance from an electrode (93, 94). Genetic studies (18, 70, 75, 98) strongly suggest that *c*-type cytochromes are involved in

this process, and electrochemical analysis of electron transfer through electrode-attached biofilms is consistent with a diffusional mechanism involving electron hopping through this biofilm network (39, 93, 94, 115). However, how cytochromes are anchored between cells in a three-dimensional network to create such redox conductivity remains unclear.

G. sulfurreducens Type IV pili and outer membrane *c*-type cytochrome mutants were a focus of early electron transfer and attachment studies, and it was suggested that pili mediated both attachment and long-distance electron conduction (18, 70, 75, 98, 111-113). However, mutants in the structural protein of the Type IV pilus (*pilA*) still form thin biofilms and reduce electrodes, showing that other factors contribute to early attachment events and cell-surface electron transfer. As *Geobacter* pili are now known to be coated with the hexaheme cytochrome OmcS (71), and the octaheme cytochrome OmcZ is consistently found on material between cells (46, 47), there is increasing evidence that cytochromes localized well beyond the cell membrane play key roles in long-distance electron transfer.

Recently, a library of *G. sulfurreducens* transposon mutants was screened for biofilm and Fe(III)-reduction defects (116), revealing new genes required for attachment and electron transfer. In particular, a class of biofilm mutants that was unable to reduce insoluble Fe(III) oxyhydroxides and graphite electrodes was identified (116). This class differed from most *c*-type cytochrome and pili mutants, as mutants did not show any residual electron transfer activity on electrodes, and did not show an ability to adapt or evolve to regain metal reduction phenotypes. These mutants contained insertions in open reading frame GSU1501, encoding part of a multisubunit ABC transporter within an

operon containing a putative undecaprenyl attachment protein and a series of glycosyltransferase genes, and could not be complemented by expression of just GSU1501 *in trans* (116).

Cuthbertson *et al.* recently reviewed the role of gene clusters with similar components in synthesis and export of cell surface polysaccharides (28). Variations in outer surface polysaccharides can have pleiotropic effects; sugars can modify surface charge to alter surface attachment, provide an anchor for retention of peripheral proteins, and/or control cell-cell recognition events (8, 35, 57, 58, 72, 124). A complex relationship between extracellular polysaccharides, Type IV pili and biofilm growth is found in *Myxococcus xanthus*, a relative of *Geobacter* with a well-characterized multicellular lifestyle. Fibrils extending from *Myxococcus* cells are comprised of a highly stable protein:polysaccharide matrix, which is required for cell-cell cohesion and social gliding motility (4, 8). Mutants unable to produce this matrix, as well as wild type cells exposed to Congo red (a carbohydrate binding dye that inhibits fibril polymerization), are blocked in most aspects of cell-cell agglutination and gliding motility (4, 5). Type IV pilus retraction by *M. xanthus* is stimulated by matrix binding, and defects in pili inhibit matrix synthesis via the *dif* signal transduction network (10, 72, 143).

In this work, we describe the phenotype of a newly constructed *G. sulfurreducens* Δ1501 mutant, and provide evidence that this mutation disrupts an operon responsible for synthesis of sugars that serve as extracellular anchors for *c*-type cytochromes essential in cell-surface electron transfer. The Δ1501 mutant also displayed an attachment preference for surfaces with a negative charge, further limiting interactions with Fe(III)

oxyhydroxides and positively poised electrodes. We report new methods for imaging and isolating a matrix of protein and polysaccharides from *G. sulfurreducens,* and show it is both decreased in sugar content and nearly devoid of *c*-type cytochromes in the Δ1501 mutant. This genetic region, containing genes for synthesis of extracellular anchoring polysaccharides (*xapA-K*), is conserved in all sequenced metal-reducing *Geobacteraceae*. While much work has focused on redox proteins anchored to the membrane, this shows a role for extracellular polysaccharides as attachment sites for peripheral redox proteins that enable multicellular communities to transfer electrons to distant acceptors.

3.3 Materials and Methods

3.3.1 Bacterial strains, plasmids, and culture conditions

Bacterial strains and plasmids used in this study are described in Table 3.1. *G. sulfurreducens* PCA (ATCC 51573) was routinely grown at either 25°C or 30°C in anaerobic mineral media, with 20 mM acetate as electron donor and 40 mM fumarate as electron acceptor (93). To maintain the replacement mutant phenotype, cultures of the Δ1501 mutant were supplemented with kanamycin (200 µg/ml). The Δ1501 mutant containing pGCOMP1500-5 was maintained using gentamicin (20 µg/ml). *Escherichia coli* WM3064, the donor strain used for conjugation (122), was grown in LB broth containing 30 µM 2,6-diaminopimelic acid (DAP) at 37°C, with 10 µg/ml gentamicin present when carrying pBBR1MCS-5 or pGCOMP1500-5.

TABLE 3.1. Strains, plasmids, and primers used in this study

Designation	Relevant characteristics or sequence (5'-3')	Reference or usage
G. sulfurreducens		
Wild Type	ATC #51573	20
20B5	pMiniHimar RB1 insertion at 1646730, Km^r	116
67B2	pMiniHimar RB1 insertion at 1646910, Km^r	116
Δ1501	Kanamycin resistance gene replacing GSU1501, Km^r	This study
E. coli		
WM3064	Donor strain for conjugation: *thr*B1004 pro thi rpsL hsdS lacZΔM15 RP4-1360 Δ(araBAD)567 ΔdapA1341::[erm pir(wt)]	122
Plasmids		
pBBR1MCS--2	Mobilizable broad-host-range plasmid; *lacZ*, Km^r	59
pBBR1MCS-5	Mobilizable broad-host-range plasmid; *lacZ*, Gm^r	59
pGCOMP1500-5	GSU1500-1505 in MCS of pBBR1MCS-5, Gm^r	This study
Primers		
JR03	TGATCTGTTGGAATACGGGATGAAGTACCG	PCR amplification of sequence upstream GSU1501
JR04	GAAATTCCCCTCTTCAGTTATTCTGAACTC	
JR05	TTGTGAGCTTCCAAGCATTTCTAAGGATCT	PCR amplification of sequence downstream GSU1501
JR06	CACACTGAGGAAGAGCCAGCTCGATATCGG	
JR07	*TAACTGAAGAGGGGAATTTC* AGCGAACCGGAATTGCCAGCT	PCR amplification of kan^r from pBBR1MCS-2 with overhangs homologous to JR04 and JR05 in italics
JR08	*GAAATGCTTGGAAGCTCACAA* TCAGAAGAACTCGTCAAGAAGGC	
JR09	GTCCAACAAAGGGAACTGCT	QPCR detection of GSU1501
JR10	CCTCCGCAGAGAGGTAATCA	
JR11	AGTTCTCGACGTACGCCACT	QPCR detection of *rpoD*
JR12	TCAGCTTGTTGATGGTCTCG	
JR13	CACCGGCATAATCTCCAAGT	QPCR detection of *recA*
JR14	TTGAGGGATGCGATCTTGCG	
JR15	TAC*TCTAGA*AATGGTGCCGTTCACCGACCA	PCR amplification of GSU1500-1505, XbaI and SacI sites in italics
JR16	GAC*GAGCTC*TCATAAACGAACCTCGTCCC	

3.3.2 Construction of the Δ1501 mutant

Single-step gene replacement (75) was used to insert a gene for kanamycin resistance (Kan^r) into *G. sulfurreducens*, replacing GSU1501, with all primers listed in Table 3.1. Recombinant PCR was used to generate a 2 kb DNA fragment containing Kan^r flanked by approximately 0.5 kb of sequence upstream and downstream of GSU1501. Kan^r was amplified from pBBR1MCS-2 (59) using primers JR07F and JR08R and the following conditions: 30 cycles of 94°C for 1 minute, 55°C for 1 minute, and 72°C for 2 minutes, followed by a final extension at 72°C for 10 minutes. The sequence upstream of GSU1501 was amplified from *G. sulfurreducens* genomic DNA using primers JR03F and JR04R, and the sequence downstream GSU1501 was amplified using JR05F and JR06R. The following conditions were used for each: 30 cycles of 94°C for 1 minute, 52°C for 1 minute, 72°C for 1 minute, and a final 10 minute extension at 72°C. The products of these three PCR reactions were used as templates in a primer-less PCR reaction, producing the 2 kb linear DNA fragment, using 15 cycles of 96°C for 40 seconds, 47°C for 1 minute, 72°C for 5 minutes, then a final extension at 72°C for 10 minutes. The 2 kb fragment was then amplified using 30 cycles of the same reaction conditions and primers JR03F and JR06R. This linear DNA fragment was electroporated into wild type *G. sulfurreducens* (25), and recombinants were selected on mineral media containing 200 µg/ml kanamycin. Putative mutants were re-streaked on selective medium, and isolated colonies checked for proper deletions using primers spanning the region. Optical density at 600 nm (OD_{600}) of wild type and the Δ1501 mutant (using fumarate as electron

acceptor) was monitored for 72 hours to verify there were no growth defects when using fumarate, a soluble electron acceptor.

3.3.3 Construction of a complemented Δ1501 mutant

GSU1500-1505 was amplified from wild type *G. sulfurreducens* using primers JR15F and JR16R listed in Table 3.1 using the following conditions: 30 cycles of 94°C for 1 minute, 58°C for 1 minute, and 72°C for 6 minutes, followed by an additional 72°C for 10 minutes. The ~ 6 kb fragment was digested and inserted into the XbaI and SacI sites of pBBR1MCS-5, creating the vector pGCOMP1500-5. This construct was mated into the Δ1501 mutant and transformants selected on gentamicin (116).

3.3.4 Fe(III) reduction

Wild type *G. sulfurreducens,* the Δ1501 mutant, and the complemented strain (Δ1501 + pGCOMP1500-5) were each transferred to mineral medium containing 10 mM acetate as electron donor and 55 mM Fe(III) citrate or Fe(III) oxyhydroxide as the electron acceptor. Some cultures containing Fe(III) oxyhydroxide as the electron acceptor were supplemented with 5 µM of the electron shuttle anthraquinone-2,6-disulfonate (AQDS). After inoculation, samples were taken every 2-6 hours until most Fe(III) had been reduced. A modified colorimetric ferrozine assay was used to measure production of Fe(II) over time (84). Ferrozine reagent (2 g ferrozine/L in 100 mM HEPES, pH 7) was combined with sample (dissolved in 1 N HCl) and absorbance at 562 nm (A_{562}) was determined. Fe(III) reduction was also monitored in the presence of 50 µg/ml Congo red and 7µg protein/ml sheared extracellular matrix material where described, with samples taken every 24 hours.

3.3.5 Electrochemical analysis

Electrochemical bioreactors were prepared as previously described (93), containing a graphite working electrode, platinum counter electrode, and saturated calomel reference electrode. Reactors were incubated in a 30°C water bath and connected to a 16-channel potentiostat (VMP; Bio-Logic, Knoxville, TN) with EC-Lab software to run chronoamperometry as previously described (93). Anaerobic bioreactors, receiving humidified N_2/CO_2 (80:20 [vol/vol]), were inoculated with 50% (vol/vol) *G. sulfurreducens* entering stationary phase (OD_{600} 0.4 – 0.5) and mineral media containing 40 mM acetate (no electron acceptor) and incubated for 24-48 hours at a potential of +0.24 V or -0.24 V vs. the standard hydrogen electrode (SHE). Bioreactors containing two working electrodes were used when the applied potential was varied over the course of the experiment. Bioreactors were first inoculated with 50% (vol/vol) of either wild type *G. sulfurreducens* or the Δ1501 mutant, approaching stationary phase (OD_{600} 0.4 – 0.5), in mineral medium containing 40 mM fumarate and 20 mM acetate (potential for acetate oxidation: -0.28 V vs. SHE). Cells were allowed to incubate for 24 hours at 30°C without an applied potential, after which one of the working electrodes was removed for confocal analysis. Medium was then removed from the bioreactor and replaced with mineral medium containing only 20 mM acetate (no electron acceptor). Electrodes were then poised at either +0.24 V or -0.24 V vs. SHE for 4-24 hours at 30°C, after which the second electrode was removed for confocal analysis. Electrode-attached biofilms were stained using a LIVE/DEAD *Bac*Light bacterial viability kit (Invitrogen Corp., Carlsbad,

CA), and imaged using a Nikon C1 spectral imaging confocal microscope (Nikon, Japan).

3.3.6 Biofilm formation assays

To detect attachment phenotypes, cells were grown in mineral medium containing 30 mM acetate for 72 hours at 30°C as previously described (116). Attachment to the wells of either a Nunclon^{TM} Δ (Nunc 167008) or a poly-D-lysine coated (Nunc 152039) polystyrene, flat bottom, 96-well microtiter plate were determined using a modified crystal violet (CV) assay (104). Cells (or sheared extracellular material) were stained with 0.1% CV for 15 minutes, plates were rinsed to remove planktonic cells, and remaining CV was solubilized with dimethyl sulfoxide. OD_{600} was measured as an indicator of attachment level.

3.3.7 Quantitative RT-PCR analysis

Total RNA was isolated from fumarate grown cells during exponential (OD_{600} = 0.35) and stationary (OD_{600} = 0.60) growth phases and from electrode grown cells while current was increasing exponentially and once current had reached plateau using the RNAqueous®-Micro kit (Ambion, Austin, TX). The DyNAmo^{TM} SYBR® Green 2-Step qRT-PCR kit (Finnzymes, Woburn, MA) was used for cDNA synthesis and qPCR reactions using the manufacturer's protocol and a 7900HT Fast Real-Time PCR System (Applied Biosystems, Foster City, CA), with *rpoD* and *recA* as internal controls, using primers listed in Table 1.

3.3.8 Agglutination assay

To test for agglutination phenotypes, cells were grown anaerobically in mineral medium (with excess acetate and limiting fumarate) at 25°C for 72 hours, conditions which promote cell aggregation. OD_{600} was first determined for cells which remained in suspension. Then cell aggregates were broken apart by vortexing and OD_{600} was measured and compared to the initial OD_{600} of the cell suspension to assess the degree of agglutination (113). Additionally, cultures were incubated with Congo red (10-50 µg/ml) or extracellular material (7µg/ml) to test for inhibition and restoration of agglutination respectively.

3.3.9 Isolation of sheared proteins

To isolate pili, cultures of wild type *G. sulfurreducens* and the Δ1501 mutant were pelleted and resuspended in 1/100 volume 1X phosphate buffered saline (PBS, 137 mM NaCl, 2.7 mM KCl, 4.3 mM Na_2HPO_4, 1.47 mM KH_2PO_4). Suspensions were vortexed vigorously for 2 minutes to shear loosely bound proteins, then cells were removed by centrifugation at 16,000 x g for 5 minutes. Supernatants were removed and centrifuged for an additional 25 minutes, after which the supernatant was collected and 0.1 M $MgCl_2$ was added (from a 1 M stock) to facilitate precipitation of proteins. After an overnight incubation at 4°C, samples were centrifuged at 30,000 x g for 1 hour at 4ºC (134). To enhance the depolymerization of pili, pellets were resuspended in a small volume of 8M urea, 50 mM Tris-HCl pH 8, prior to boiling at 100ºC in SDS loading buffer for 15 minutes or they would not enter the SDS-PAGE gel. To confirm the identity of isolated pili, bands were excised for in-gel trypsin digestion followed by liquid chromatography-

mass spectrometry at the University of Minnesota Center for Mass Spectrometry and Proteomics.

3.3.10 Detection of proteins

Sodium dodecyl sulfate-polyacrylamide gel electrophoresis (SDS-PAGE) (64) in 15% Tris-HCl gels under non-reducing conditions was used to analyze isolated proteins. Samples were boiled at 100ºC for 15 minutes in SDS loading buffer (and treated with urea where indicated), as the longer denaturing times were necessary to visualize pili proteins and some matrix-bound cytochromes. To detect putative *c*-type cytochromes via peroxidase activity, gels were incubated in 6.3 mM 3,3',5,5'– tetramethylbenzidine (TMBZ) in methanol (3 parts TMBZ mixed with 7 parts 0.25 M sodium acetate, pH 5.0) for 2 hours as previously described (129), after which 30 mM hydrogen peroxide was added. Alternatively, a Pro-Q$^{(R)}$ Emerald 300 Glycoprotein Gel and Blot Stain Kit (Invitrogen Corp., Carlsbad, CA) was used to visualize glycosylated proteins that had been separated by SDS-PAGE following the manufacturer's procedure. The Colloidal Blue Staining Kit (Invitrogen Corp., Carlsbad, CA) was used to visualize total protein.

3.3.11 Fe(III)-coated slides

A solution containing 1% agarose and 0.4 M Fe(III) oxyhydroxide (ferrihydrite) was applied to acid-washed glass slides and allowed to solidify. These Fe(III)-coated slides were then incubated vertically in cultures of wild type *G. sulfurreducens* or the Δ1501 mutant for 4 hours. Attached cells were stained with 100 μg/ml 4',6-diamidino-2-phenylindole (DAPI) for 5 minutes and visualized by confocal laser scanning microscopy (CLSM).

3.3.12 Safranin O staining and scanning electron microscopy (SEM) analysis

A graphite electrode was placed in mineral medium (containing 20 mM acetate and 40 mM fumarate) which was then inoculated with wild type *G. sulfurreducens* or the Δ1501 mutant. After 48 hours of growth at 30°C, electrode-attached cells were fixed in 2% glutaraldehyde, 0.15M sodium cacodylate pH 7.4, for at least 24 hours. To help stabilize extracellular polysaccharides, some samples were also fixed in the presence of 0.15% safranin O (34). Samples were then post-fixed for 2 hours in 1.5% osmium tetroxide and dehydrated in ascending ethanol concentrations [25, 50, 75, 95 (2x), 100% (3x) 5 minutes each] prior to drying by treatment in hexamethyldisilazane (HMDS) [50% (v/v) HMDS in 100% ethanol, 100% HMDS (2x) for 5 minutes each] (3). Samples were mounted on adhesive carbon films and coated with a thin layer of gold using a Fullam sputter coater (Ernest Fullam Inc., Schenectady, NY) followed by imaging with a Hitachi S3500N variable pressure scanning electron microscope (Hitachi Inc, Toronto, Canada).

3.3.13 Isolation of extracellular matrix

Extracellular material was isolated using a modification of a procedure previously described for *Myxococcus* (22). Briefly, cells were pelleted and resuspended in 1/5 volume TNE (10 mM Tris-HCl pH 7.5, 100 mM NaCl, 5 mM EDTA) and blended at low speed for 1 minute in a Waring Commercial Blender (Waring Products, Inc., Torrington, CT). Cells were lysed by the addition of SDS (0.1% final concentration) and stirred at room temperature for 5 minutes. This lysate had to be further sheared by 5 passes (~30 seconds each) through an 18 gauge needle, then centrifuged at 17,000 x g for 15 minutes to obtain a pellet. This pellet was resuspended in Tris-HCl pH 7.5, pelleted and

resuspended 5 times to remove SDS. The bicinchonicic acid (BCA) protein assay was used to detect protein (Thermo Scientific, Rockford, IL), and the phenol sulfuric acid method was used to detect carbohydrate with glucose as the standard (95).

3.3.14 Congo red assay

A modification of a previously described Congo red binding assay was used to detect extracellular polysaccharide (67). Suspensions of wild type *G. sulfurreducens* and the Δ1501 mutant (OD_{600} = 2.0) or extracellular material (100 µg protein/ml) were incubated in the dark with 15 µg/ml Congo red for 30 minutes at room temperature. Cells were then removed by centrifugation and absorbance at 490 nm (A_{490}) of the supernatant was measured. Congo red binding was also observed by growing cells on 1.7% (w/v) agar plates containing 0.01% (w/v) Congo red. Clearing zones around colonies were measured after 5 days of anaerobic growth at 30ºC.

3.3.15 Detection of cytochrome reduction

Absorbance of equal concentrations of wild type, Δ1501 mutant, and Δ1501+pGCOMP1500-5 extracellular material was measured using wavelengths spanning 400-600 nm. To reduce cytochromes, a few crystals of sodium dithionite were added to each sample and absorbance measured.

3.3.16 OmcZ antibody production and purification

Peptides HTSPAAVAKD and DSPNAANLGTVKPGL were selected from the OmcZ protein sequence using an online hydropathicity plots program to identify hydrophilic and antigenic regions (www.vivo.colostate.edu). Subsequently, the peptide sequences were searched against a non-redundant protein database in NCBI Protein

BLAST to ensure that the peptides only matched OmcZ in *G. sulfurreducens* PCA. A cysteine residue was added to the amino terminus of the first peptide and the carboxyl terminus of the second peptide for conjugation to a carrier protein for antibody production. The peptides were synthesized at Penn State Hershey Macromolecular Core Facility. Polyclonal antibodies to OmcZ were produced in a New Zealand White rabbit (Covance Custom Immunology Services Inc., Princeton, NJ). The peptides were covalently linked to the Sulfolink Coupling Resin (Pierce Biotechnology, Rockford, IL) via the cysteine residues according to the manufacturer's protocol and used to affinity purify the OmcZ antibodies from the antiserum. The following modifications for affinity purification of the antibodies were obtained from the Pikaard Lab (Washington University): the resin was washed with 20 ml 1X PBS with 250 mM NaCl, pH 7.2, then 10 ml of 100mM glycine, pH 2.5 elution buffer, and finally with 20 ml 1X PBS, pH 7.2. The antiserum was diluted with an equal volume of 1X PBS, pH 7.2 and allowed to incubate overnight with the Sulfolink resin at 4^0C with gentle rotation. After binding of the antibodies, the resin was washed with 20 ml 1X PBS, pH 7.2 and 10 ml 1X PBS, pH 7.2 with 250 mM NaCl. The antibodies were eluted with 5 ml of elution buffer, in 500 µl aliquots and neutralized with 50 µl of 1M Tris, pH8. Aliquots containing the antibody were detected using the Bradford reagent (16). OmcZ specificity was tested via Western blotting of *G. sulfurreducens* biofilm grown cells, showing only one cross-reactive band.

3.3.17 Detection of OmcZ in extracellular material

Protein content of wild type and Δ1501 extracellular material was determined using the Lowry protein assay (88). For SDS-PAGE, 28 µg of protein was suspended in

sample buffer and boiled for 15 minutes, prior to electrophoresis on a 12% gel (64). The proteins were then transferred onto a nitrocellulose membrane and probed with 1:100 dilution of affinity-purified OmcZ antibody. The blot was then developed using a BCIP/NBT solution (Amresco, Solon, OH).

3.4 Results

3.4.1 Identification of the extracellular anchoring polysaccharide (*xap*) gene cluster and construction of a GSU1501 replacement mutant

Previous screening of a transposon library for increased surface adherence in a 96-well crystal violet assay identified two mutants with transposon insertions in open reading frame GSU1501 (Fig. 3.1) that demonstrated a growth impairment with Fe(III) oxyhydroxides and graphite electrodes as electron acceptors (116). The original GSU1501 transposon mutants could not be complemented through re-introduction of GSU1501 (116), consistent with the location of this gene within a larger transcriptional unit (62, 108). For further work with this locus, a new mutant was constructed via complete deletion of GSU1501, and replacement with a kanamycin resistance cassette. Fe(III) oxyhydroxide reduction, and attachment to electron-accepting electrodes could not be restored in the Δ1501 mutant via expression of GSU1501 alone, or by expression of GSU1500-1502. However, expression of multiple genes from this cluster (GSU1500-1505) in the Δ1501 mutant restored most phenotypes, such as Fe (III) oxyhydroxide reduction and surface attachment, to within 50% of wild type (detailed in Fig. 3.S1).

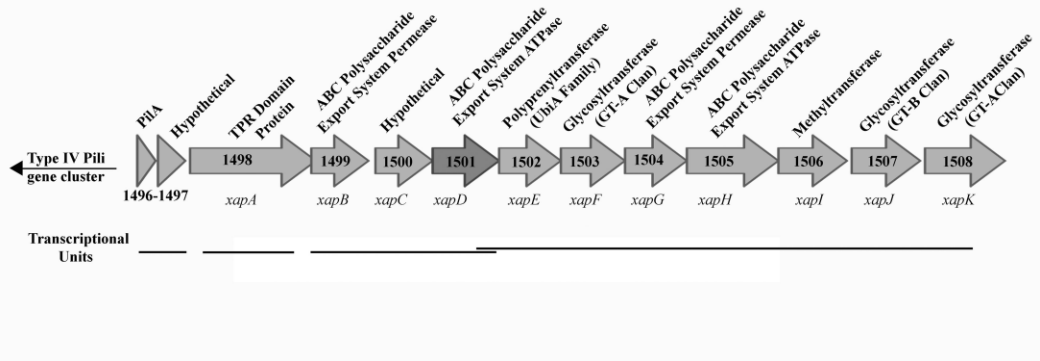

Figure 3.1 *G. sulfurreducens* extracellular anchoring polysaccharide (*xap*) cluster (GSU1498-1508) showing putative gene products and transcriptional units. GSU1501-1502 (*xap D-E*) overlap both transcriptionally and translationally (Qiu *et al*., 2010).

3.4.2 Altered cell-cell agglutination and lack of binding to positively charged surfaces

During routine cultivation it was observed that, unlike wild type *G. sulfurreducens*, the Δ1501 mutant failed to aggregate and accumulate at the bottom of culture tubes upon reaching stationary phase with fumarate as the electron acceptor. This difference was more pronounced at 25°C, a temperature previously reported to facilitate agglutination of *G. sulfurreducens* (111, 113). At 25°C, 5-fold more wild type cells agglutinated compared to the Δ1501 mutant (Fig. 3.2). The ability to agglutinate was partially restored through expression of GSU1500-1505 (Fig. 3.S1A). This defect in cell-cell attachment was surprising as the mutant was first identified based on an increased biofilm formation phenotype.

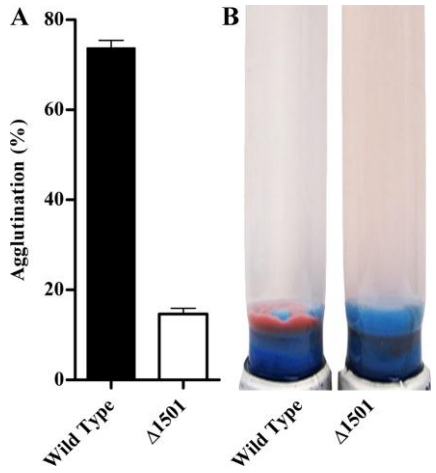

Figure 3.2 (A) Percent agglutination in wild type *G. sulfurreducens* and the Δ1501 mutant as determined by change in OD_{600} before and after aggregate disruption. Error bars are standard errors of the mean for three replicates. (B) Agglutinated cells after 72 hours of growth at 25ºC.

Adherence to 96-well plates was re-examined, comparing negatively charged and positively charged poly-D-lysine coated wells. The mutant demonstrated nearly 3-fold higher attachment to negatively charged plates, compared to positively charged poly-D-lysine coated plates (Fig. 3.3A). Attachment, measured using crystal violet, reflected actual biomass on the surfaces, as similar results were obtained with a protein assay (data not shown). This suggested that the mutant was highly attracted to negatively charged surfaces in comparison to the wild type, which explained its identification in the transposon screen.

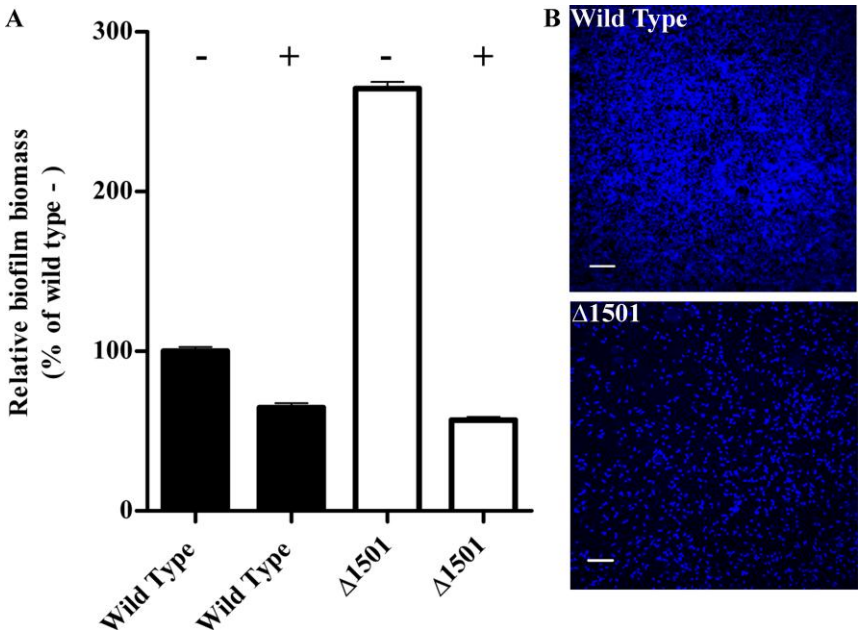

Figure 3.3 (A) Biofilm formation based on CV staining of cells adherent to negatively (-) or positively (+) charged 96-well plates, with mean absorbance expressed relative to wild type attachment to negatively charged plates. Error bars are standard errors of the mean for three replicates. (B) Representative CLSM images of wild type *G. sulfurreducens* and Δ1501 mutant attachment to Fe(III) oxyhydroxide-coated glass slides after four hours of attachment. Panels are maximum projections (bar = 20 μm) of attached cells stained with DAPI.

Fe(III) oxyhydroxides are known for their positive surface charge, a property that makes them excellent materials for sorption of AsO_4^{3-} and PO_4^{3-} ions (2, 110). When

attachment to vertically positioned Fe(III)-coated slides was investigated, very few Δ1501 mutant cells attached to Fe(III)-coated slides in comparison to wild type (Fig. 3.3B). Consistent with this observation, when the mutant was cultivated with Fe(III) oxyhydroxide as an electron acceptor, less than 5 mM Fe(III) was reduced after 7 days, compared to 50 mM by the wild type (Fig. 3.4). In the presence of only 5 µM AQDS, an electron shuttling compound able to transfer electrons from multiple membrane- and surface-associated redox proteins to Fe(III) oxyhydroxides (136), the mutant was capable of wild type rates of Fe(III) reduction (Fig. 3.4). Along with the observation that the mutant exhibited wild type rates of soluble Fe(III) citrate reduction (116) this suggested that the phenotype was not due to a defect in electron transfer proteins bringing electrons to the outer membrane, but rather was related to cell:surface attachment or electron transfer events beyond the cell membrane.

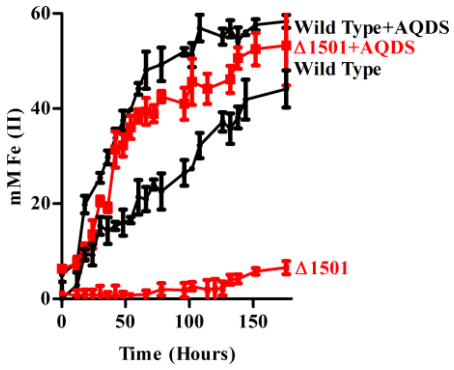

Figure 3.4 Iron reduction curves showing Fe(III) oxyhydroxide reduction over time as indicated by accumulation of Fe(II) in the presence and absence of soluble electron shuttle AQDS (5 µM). Error bars are standard errors of the mean for three independent replicates.

3.4.3 Electrode binding deficiency is also linked to surface charge

Previous work showed that GSU1501 transposon mutants failed to produce electrical current when provided with electrodes as electron acceptors (116). Since this mutation did not affect the mutant's ability to transfer electrons to soluble metals and AQDS, we hypothesized that the electrode phenotype was also linked to attachment. When bare electrodes were used in an attachment assay, but not poised to act as electron acceptors, both wild type *G. sulfurreducens* and the Δ1501 mutant attached (Fig. 3.5A, D). As cells remained attached after rinsing in fresh medium, incubation in another change of buffer for staining, and mounting for imaging, these experiments initially appeared to contradict the hypothesis that the mutant was unable to attach to electrodes.

However, when these same electrodes were poised to act as oxidizing electron acceptors (at +0.24 V vs. SHE), a condition which withdraws electrons and alters the surface charge to become more positive, Δ1501 mutant cells rapidly detached. Figure 3.5 shows an example experiment, where unpoised electrodes were pre-colonized for 24 hours, planktonic cells were washed from the reactor, and a subset imaged (Fig. 3.5A, D). Electrode surfaces were then poised at +0.24 V vs. SHE for only 4 hours before imaging (Fig. 3.5B, E). During this time, wild type cells remained attached to electrodes, while the number of attached mutant cells severely decreased (Fig. 3.5B vs. E).

When pre-colonized electrode surfaces were poised at a negative potential (-0.24 V vs. SHE), for as long as 24 hours, both the wild type and the Δ1501 mutant remained attached (Fig. 3.5F,G). The ability to attach to a positively charged electrode was restored

when GSU1500-1505 were re-introduced to the Δ1501 mutant (Fig. 3.S1B). These experiments further demonstrated that attachment of the Δ1501 mutant was a function of electrode surface potential.

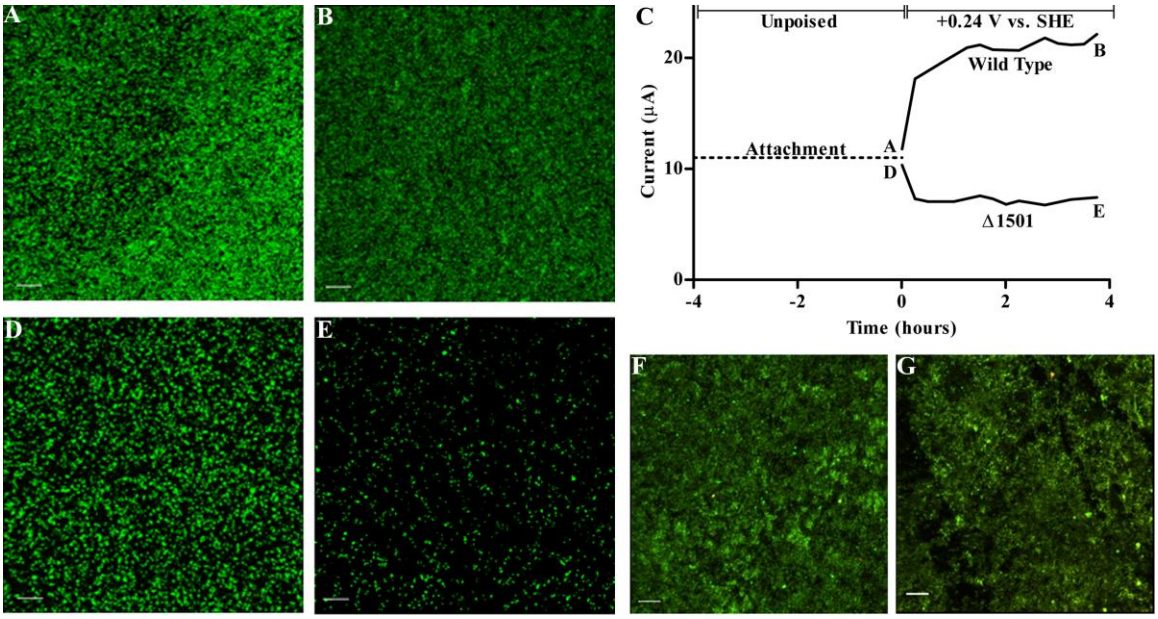

Figure 3.5 CLSM images of biofilm formation by (A) wild type *G. sulfurreducens* and the (D) Δ1501 mutant after 24 hours of attachment to unpoised graphite electrodes, followed by images taken of (B) wild type and (E) Δ1501 mutant after 4 additional hours with electrodes poised at +0.24 V vs. SHE. (C) Current production during 4 hours poised at +0.24 V vs. SHE, letters indicate CLSM timepoints. CLSM images of (F) wild type and (G) Δ1501 mutant after 24 hours with electrode poised at -0.24 V vs. SHE. CLSM images are maximum projections (bar = 20 μm) of electrode-attached biofilms stained with a LIVE/DEAD kit.

3.4.4 GSU1501 expression is similar during planktonic exponential growth with fumarate and biofilm growth with electrodes

GSU1501 mRNA expression levels were measured via quantitative RT-PCR to determine if this gene was specifically induced during growth with different electron acceptors, using both *rpoD* and *recA* as standards. GSU1501 expression was not significantly higher when cells were grown as biofilms (in exponential phase) on oxidizing electrodes, when compared to exponentially grown fumarate-reducing cultures. Regardless of the electron acceptor, expression dropped as cells entered into stationary phase (decreasing 80-fold as planktonic cells abruptly entered stationary phase due to fumarate depletion). These wild type *G. sulfurreducens* mRNA expression levels showed that solid-phase electron acceptors were not needed to induce GSU1501 expression, and were consistent with the fact that cells pre-grown with fumarate demonstrated the strong phenotypes of poor attachment and cell-cell agglutination.

3.4.5 SEM evidence that Δ1501 mutants lack an extracellular fibrillar matrix

GSU1501 is a component of a putative ATP-dependent exporter within an operon annotated to have a series of glycosyltransferases similar to those used to assemble extracellular polysaccharides (Fig. 3.1). As *Geobacter* lacks O-antigen side chains (133), we hypothesized that this cluster was involved in synthesis and export of sugars to the cell exterior, leading to a change on the mutant cell surface, or on exposed proteins, that prevented electron transfer to metals or electrodes.

Recent work with pathogens such as *Enterococcus faecalis* has shown that common fixation methods for scanning electron microscopy fail to preserve delicate outer surface structures, but that treatment with some dyes can enhance stabilization and visualization of extracellular fibrils (34). After screening a range of commonly used agents, we found that if *Geobacter* cells were fixed in the presence of the small molecular weight dye safranin O, which is typically used to stain negatively charged mucopolysaccharides (119), significantly more detail was preserved.

The first set of SEM images shown in Figure 6 compares mutant and wild type cells attached to unpoised graphite surfaces, using standard SEM preparation protocols (Fig. 3.6A,B). The second series of images shows biofilms prepared using safranin O in the fixative (Fig. 3.6 C,D). In both cases, individual cells attached to the electrode surface were visible, but safranin preserved a dense network of extracellular material surrounding wild type cells (Fig. 3.6C). This fibrillar network was absent from the Δ1501 mutant under all conditions tested (Fig. 3.6B,D).

When biofilms were imaged using a more sensitive 2.5 kV field emission scanning electron microscope, fibrils surrounding wild type cells could also be seen in preparations lacking stabilizing dyes (Fig. 3.6E). Even with this more sensitive microscope, no fibrils or material were detected around the mutant (Fig. 3.6F). In all cases, the diameter of these fibrils was larger than what has been reported for *Geobacter* pili (20-40 nm) (111).

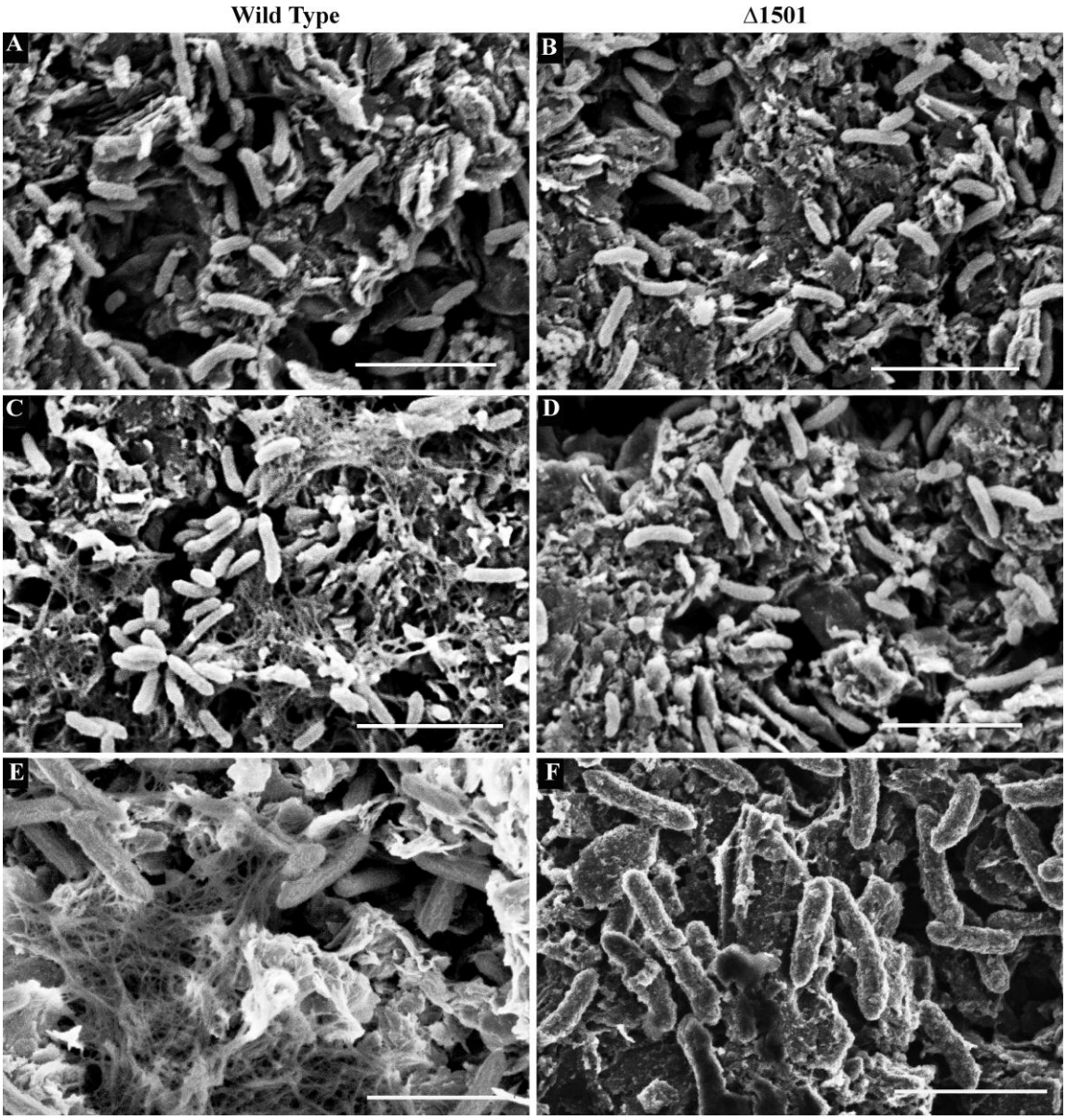

Figure 3.6 SEM images of (A) wild type *G. sulfurreducens* and (B) Δ1501 mutant biofilms and (C) wild type and (D) Δ1501 mutant biofilms fixed in the presence of cationic dye safranin O (bar = 5 μm). Field emission SEM images of (E) wild type and (F) Δ1501 mutant biofilms. All biofilms grown on unpoised graphite electrodes (bar = 2 μm).

As mutations in Type IV pili are known to affect agglutination, Fe(III) reduction and electrode growth (111-113), and pili could aggregate to form larger fibrils during preparation for SEM, cells were sheared to obtain pili. Sheared fractions from both mutant and wild type cultures had to be re-solubilized in 8 M urea to visualize individual proteins by SDS-PAGE. Urea-solubilized pellets from wild type and mutant cultures produced similar bands corresponding to the predicted 6 kDa size of processed PilA subunits. Mass spectrometry revealed that processed PilA protein represented the dominant sequence recovered from this 6 kDa band in all cases (data not shown).

Staining to label putatively glycosylated proteins, using safranin O or periodic acid oxidation and labeling with fluorescent detection reagents, consistently stained this PilA subunit band as well as an unidentified 15 kDa protein in both preparations (data not shown). In addition, all pili preparations contained a large amount of a 50 kDa protein that stained positive for heme, consistent with the recent discovery that the 50 kDa OmcS cytochrome coats *Geobacter* Type IV pili (71). As we could detect no difference in the abundance of pili, their glycosylation state, or in pili-associated proteins, these results indicated that the fibril material missing in the Δ1501 mutant was not related to Type IV pili. Abundant fibrils extending from cells have also been observed in *Geobacter* mutants lacking the pilin protein PilA (56), further supporting this conclusion.

3.4.6 Congo red binding evidence for an extracellular polysaccharide matrix defect in Δ1501

In the related Deltaproteobacterium *M. xanthus*, polysaccharide fibrils polymerize to form a matrix anchoring proteins to the outer surface, and this matrix also acts as a

signal for cell-cell recognition and pili retraction (8, 72, 124). Polysaccharide-binding dyes such as Congo red adhere to this matrix, and have the notable effect of preventing fibril polymerization and cell-cell agglutination (4, 5). Based on the hypothesis that the Δ1501 mutant was defective in production of a similar kind of matrix, the effect of dye binding to cells was investigated.

On agar plates supplemented with Congo red, wild type *G. sulfurreducens* colonies developed clearing zones, extending as much as 0.37 (± 0.041) cm from colony edges, while little clearing was observed around colonies of the Δ1501 mutant (Fig. 3.7A). As clearing zones could indicate either reductive fission to aromatic amines, or binding of Congo red, a non-respiratory binding assay was performed (67). After growth to stationary phase in liquid culture, wild type *G. sulfurreducens* bound twice as much Congo red compared to the Δ1501 mutant (Fig. 3.7B), even after pelleting and resuspension in aerobic buffer, showing that this Congo red-binding material was cell-associated, and did not require respiration for the phenotype.

Growth of wild type *G. sulfurreducens* in medium containing Congo red did not affect growth rate or final cell density, but supplementation of 50 µg/ml Congo red inhibited cell-cell agglutination by the wild type nearly to the level seen in the Δ1501 mutant without Congo red (Fig. 3.7C). As little as 10 µg/ml Congo red eliminated what agglutination remained in the Δ1501 mutant. In addition, Fe(III) oxyhydroxide reduction by wild type cultures was decreased in the presence of Congo red, with only 20 mM Fe(II) produced after 7 days, compared to 50 mM when Congo red was not present.

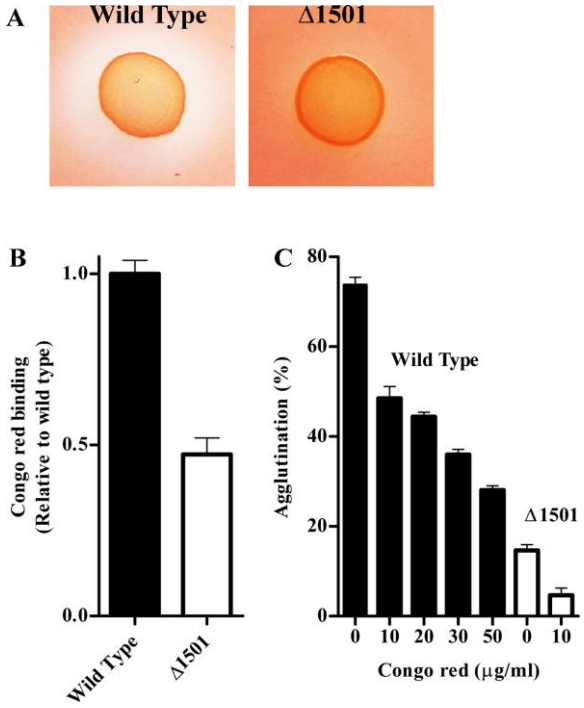

Figure 3.7 (A) Colonies of wild type *G. sulfurreducens* and Δ1501 grown on agar plates supplemented with Congo red. (B) Congo red binding as an indicator of relative levels of extracellular material. (C) Inhibition of wild type agglutination with increasing concentration of Congo red, compared to agglutination in the Δ1501 mutant. Error bars are standard errors of the mean for three replicates.

3.4.7 Isolation of the extracellular matrix from wild type and Δ1501 mutant cultures

Using a protocol based on methods used to extract *Myxococcus* fibrils, involving mechanical shearing, SDS treatment, and pelleting of high-molecular weight material, a thick red pellet was obtained from wild type *G. sulfurreducens* cells. Analysis of three

independent preparations showed that this material contained both protein and polysaccharide in a nearly 1:1 ratio in the wild type, and an average of 7.5 mg (on a protein basis) was obtained from one liter of *G. sulfurreducens* stationary phase fumarate-grown culture (~150 mg protein). In contrast, the mutant produced less total material, the isolated matrix contained approximately 60% less polysaccharide per unit protein (0.57:1), and it was largely absent of color (Fig. 3.8A). Expression of GSU1500-5 in the Δ1501 mutant resulted in an increased matrix polysaccharide content per unit protein (0.77:1) and restoration of the color of wild type matrix material (Fig. 3.S1C).

Consistent with whole-cell Congo red binding assays, Δ1501 extracellular material bound less Congo red than wild type (20%, per unit protein). The extracellular matrix from the Δ1501 mutant also showed a preference for binding negatively charged surfaces, compared to matrix from the wild type. Using bound protein as a measure of attachment, nearly 2-fold more matrix material from the Δ1501 mutant attached to negatively charged surfaces than wild type material (data not shown). Taken together, this data revealed the presence a high molecular weight extracellular matrix, which retained a protein component even in the presence of SDS, that was significantly altered in the Δ1501 mutant in sugar content, charge, and Congo red binding.

Both in-gel peroxidase staining and UV/vis spectral analysis revealed that extracellular material from the Δ1501 mutant was nearly devoid of *c*-type cytochromes compared to wild type (Fig. 3.8B,D). In fact, to detect residual cytochromes in mutant preparations, twice as much material had to be loaded onto PAGE gels (e.g., Fig 3.8B, lane 4). In studying this isolated matrix, we also noted that, in order to release proteins

for separation and visualization, much longer (15 minute) boiling times at 100°C in SDS loading buffer were required, otherwise the majority of the material remained in the well or near the top of the gel. When properly separated, the most abundant heme-positive protein in wild type matrix had an estimated size of 25-30 kDa, a size range suggesting the processed form of the *c*-type cytochrome OmcZ (46, 47, 102), as well as the *c*-type cytochrome OmcE (98).

Western blot analysis of isolated matrix material from wild type cells confirmed the presence of the processed OmcZ, and found significantly less OmcZ in the Δ1501 matrix (Fig 3.8B). Additionally, when using a high concentration of antisera, a faint band for the 50 kDa form of OmcZ could be seen, but only in Δ1501 matrix. These results confirmed that OmcZ was a major constituent missing from the Δ1501 matrix, and what little OmcZ protein remained was processed differently. Unidentified cytochromes in the ~90 kDa, 15 kDa, and 8 kDa ranges were also missing, suggesting that multiple cytochromes were typically anchored in this network.

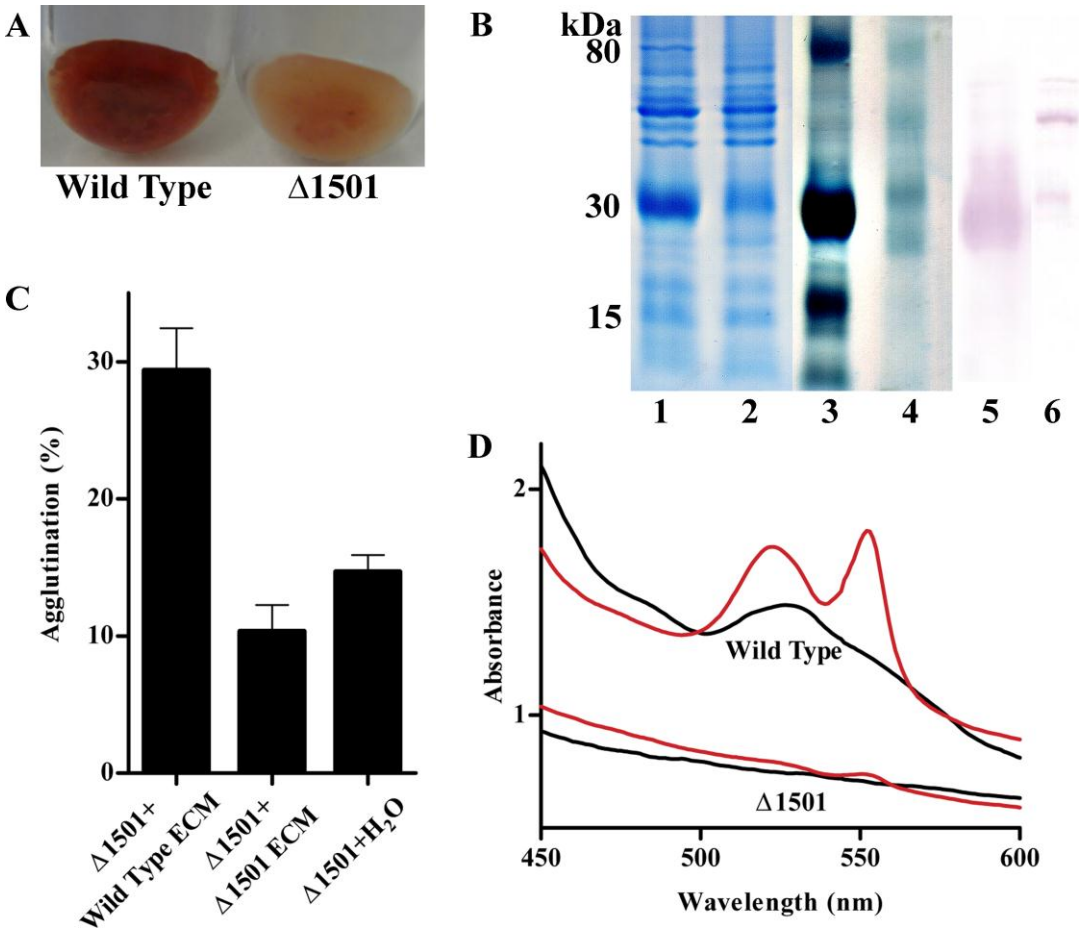

Figure 3.8 (A) Extracellular material isolated from wild type and Δ1501 mutant. (B) Stain of total extracellular protein in wild type (lane 1) and Δ1501 mutant (lane 2) and heme-stain of wild type (lane 3) and Δ1501 (lane 4), and anti-OmcZ western blot of wild type (lane 5) and Δ1501 mutant (lane 6), 20 µg protein loaded in lanes 1-3, 40 µg in lane 4 and 28 µg in lanes 5-6. (C) Percent agglutination of Δ1501 mutant with the addition of extracellular material (7 µg/ml) isolated from either wild type or the mutant. Error bars are standard errors of the mean for 4 replicates. (D) UV/visible spectra of

isolated extracellular material, oxidized shown in black, dithionite reduced in red.

3.4.8 Wild type extracellular matrix added to the Δ1501 mutant partially restores key phenotypes

Extracellular material, sheared from cells in the presence of SDS, then washed to remove detergent (Fig. 3.8A), was added back to cultures at physiological concentrations (7.5 mg/l). Even though this material had been sheared and washed in detergent, the addition of wild type matrix restored the mutant to ~40% of wild type agglutination levels (Fig. 3.8). In contrast, addition of the same material isolated from the Δ1501 mutant did not increase agglutination of either the wild type or the mutant, even at twice these added levels (data not shown). Similarly, addition of wild type matrix material to Fe(III) oxyhydroxide medium partially restored the ability of the mutant to reduce Fe(III), with 30 mM Fe(II) produced after 1 week compared to only 5 mM produced by cultures of Δ1501 mutant, even in the presence of additional matrix from the mutant (data not shown).

3.5 Discussion

This work demonstrated that an extracellular matrix, rich in cytochromes and polysaccharides, is produced by *G. sulfurreducens*. Deletion of a gene (Δ1501) within a cluster of putative polysaccharide biosynthesis proteins (Fig. 3.1) led to defects in the sugar content, charge, and dye-binding properties of this matrix, as well as the cytochrome content. Because this gene cluster (GSU1498-1508) was implicated in

production of extracellular anchoring polysaccharides, we proposed the designation *xap* for this locus. Along with the ATP-dependent exporter disrupted by the *xapD* mutation, this region also contains a complement of GT-A family (NDP-utilizing) glycosyltransferases, a UbiA-like prenyltransferase likely used to anchor polysaccharide chains to undecaprenyl carriers in the cytoplasmic membrane, and a periplasmic TPR-domain containing protein weakly similar to proteins found in protein glycosylation pathways (63) and polysaccharide export pathways (50).

Many *Geobacter c*-type cytochrome mutants and pili mutants remain able to attach to surfaces, transfer electrons to electrodes, or adapt over time to achieve wild type reduction rates (43, 69, 98, 102, 112). In contrast, the Δ1501 (*xapD*) mutant failed to form even thin biofilms on electron-accepting electrodes, never demonstrated more than 1% of wild type electron transfer rates (5 $\mu A/cm^2$) at an electrode, and retained this phenotype regardless of extended exposure to Fe(III) or electrodes. Mutant cells still produced pili, as well as cytochromes attached to the pili, and retained the ability to transfer electrons to external, soluble acceptors. This stable phenotype suggested the *xap* locus represented a central, yet previously unstudied aspect of *G. sulfurreducens* electron transfer that was unrelated to transmembrane electron transfer, or pili.

It was previously noted that attachment in the 96-well plate-based biofilm assay was not a good predictor of the ability to form electrode-attached biofilms (116). This can now be explained by the positive surface charge of the electrode when poised, in contrast to the negatively charged polystyrene plates used to discover increased adherence in most screening assays. Surface charge of a bacterial cell and electrostatic interactions are

factors known to be important in biofilm formation, with the charge of the surface itself critical in the initial attachment stage (23, 29, 90, 96, 105). The surface of wild type *G. sulfurreducens* has been reported to be electronegative, with a zeta potential similar to most *Shewanella* species (57), which likely evolved for contact with positively charged metal oxyhydroxides, and may explain why many *Geobacter* strains easily attach to commonly used anode surfaces.

Polysaccharides located outside the bacterial membrane are common agents used to mediate surface attachment and cell to cell biofilm interactions (30, 35, 45, 137, 139), as they are cheap to polymerize (compared to the ATP cost of peptide bond synthesis), and easy to modify. The fibrils occasionally visualized extending from *Geobacter* cells have been the subject of speculation, most commonly that they represent pili or pseudopili-based structures (56). However, we found that this fibril network surrounding wild type *G. sulfurreducens* bound polysaccharide-binding cationic dyes, and that disruption of the *xap* polysaccharide biosynthesis locus (which did not appear to affect pili) eliminated these fibrils.

It would seem counterintuitive for *Geobacter*, which depends upon extracellular electron transfer events between membrane proteins and surfaces, to coat itself in a layer of potentially insulating sugars. Our demonstration that this matrix is rich in *c*-type cytochromes, in particular OmcZ (46, 47, 102), suggests that this matrix is not insulating, and is instead a scaffold for electron transport proteins. Such a framework for tethering cytochromes is consistent with multiple electrochemical studies demonstrating that electrons hop through the *Geobacter* biofilm network according to semi-infinite

diffusional kinetics (39, 93, 94, 115). Along with the recent demonstration that *G. sulfurreducens* Type IV pili are coated in cytochromes (71), this provides further evidence that electron transfer from *G. sulfurreducens* to surfaces requires cytochromes localized well beyond the cell membrane. The anchoring of cytochromes in extracellular matrix may be a general characteristic of metal-reducing microorganisms, as *S. oneidensis* MR-1 cytochromes have also been detected beyond the cell and in extracellular matrix (87, 91).

While the *xap* mutation did not appear to alter pilus assembly, the *xap* cluster is located immediately downstream of the Type IV pili operon in all sequenced *Geobacter* strains, suggesting a secondary interaction, or coordination between pili and this component of the *Geobacter* extracellular matrix. In particular, GSU1500-1501 (*xapC-D*) are highly conserved in six recently analyzed *Geobacter* genomes, with reciprocal orthologs in each (19). A similar genetic linkage also exists in *M. xanthus*, which has a cluster of ATP-dependent transporter genes (sharing as high as 40% identity with *xapBDE*) necessary for cell-cell cohesion and multicellular development immediately downstream of *M. xanthus* Type IV pili (141).

The production of extracellular fibrils composed of protein and carbohydrate extending from *M. xanthus* is tightly regulated by pili interactions, via a complex signaling network known as the *dif* chemosensory pathway. Isolated matrix from *M. xanthus* causes pili to retract upon binding, and pili retraction signals the *dif* pathway to increase matrix biosynthesis (10, 11, 72, 143). Comparative genomics of *Geobacter* has revealed a cluster of methyl-accepting chemotaxis proteins in the same gene order which

are homologous to the *dif* proteins of *Myxococcus* (131). Future studies should focus on whether components of the *Geobacter xap* matrix signal Type IV pili to retract, as this would have the benefit of bringing cells closer together for between-cell electron transfer. Also, if pili have an influence on *xap* matrix biosynthesis in *Geobacter*, then pili mutants would be hypothesized to also be altered in this essential extracellular matrix that mediates cell-surface attachment and cytochrome anchoring.

3.6 Supplementary data

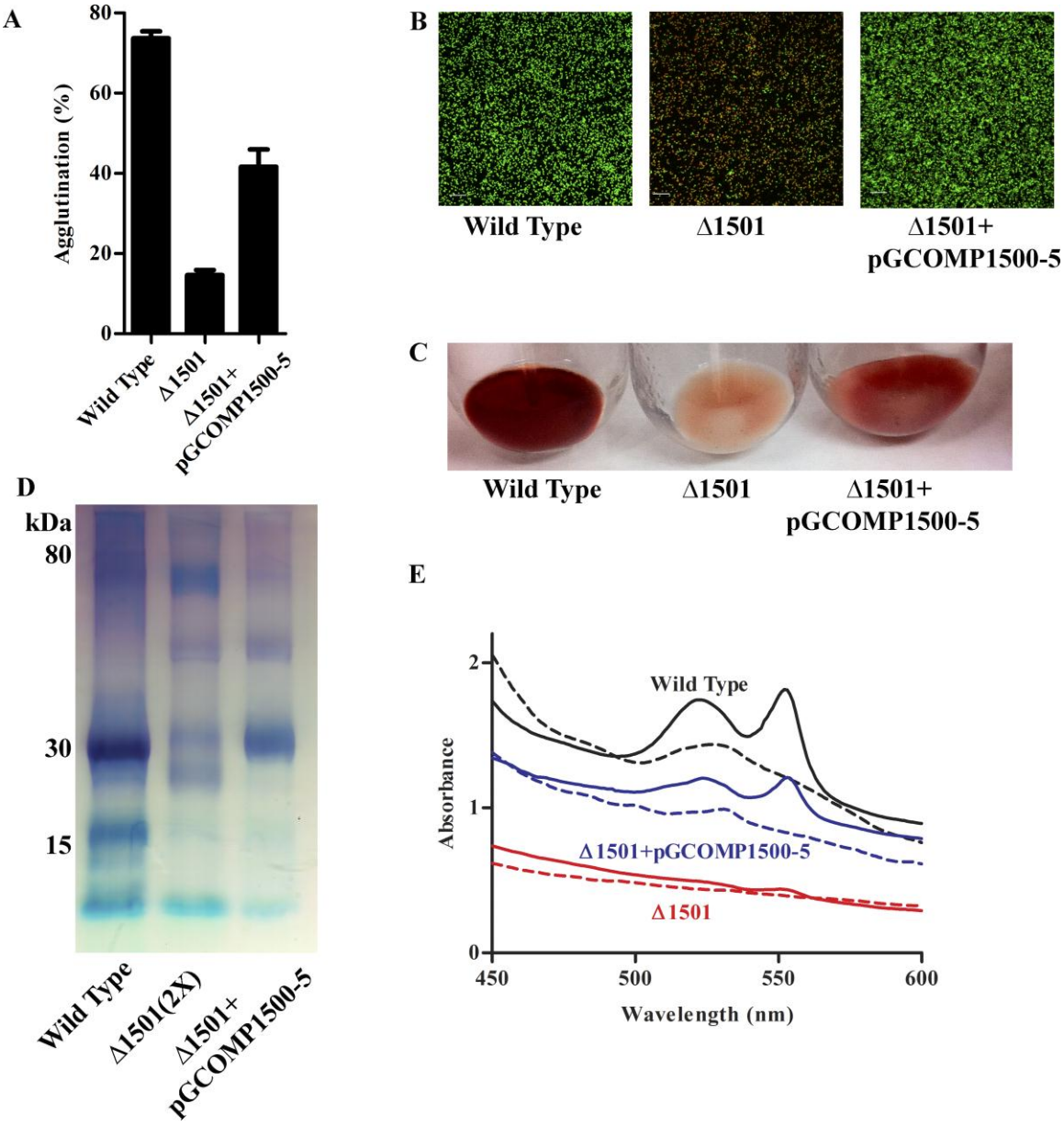

Figure 3.S1 Complementation of the Δ1501 mutant required expression of multiple genes from the *xap* cluster. (A) Percent agglutination in wild type *G. sulfurreducens*, Δ1501 mutant, and complemented mutant

(Δ1501+pGCOMP1500-5) as determined by change in OD_{600} before and after aggregate disruption. Error bars are standard errors of the mean for three replicates. (B) CLSM images of wild type, Δ1501 mutant, and Δ1501+pGCOMP1500-5 after 24 hours with electrode poised at +0.24 V vs. SHE. CLSM images are maximum projections (bar = 20 μm) of electrode-attached biofilms stained with a LIVE/DEAD kit. (C) Extracellular material isolated from wild type, Δ1501 mutant, and Δ1501+pGCOMP1500-5. (D) Stain of total extracellular heme-containing protein in wild type (lane 1), Δ1501 mutant (lane 2) and Δ1501+pGCOMP1500-5 (lane 3), 10 μg protein loaded in lanes 1 and 3, 20 μg protein loaded in lane 2. (E) UV/visible spectra of isolated extracellular material, oxidized shown by dashed lines, dithionite reduced as solid lines.

Chapter 4: Disrupted Extracellular Polysaccharide Network in *Geobacter sulfurreducens* Pili and Cytochrome Mutants

4.1 Overview

Disruption of polysaccharide export in *Geobacter* influences surface attachment as well as reduction of external acceptors which depend on cell-surface contact. Many of the commonly studied *G. sulfurreducens* mutants share phenotypes similar to a polysaccharide export mutant. Investigation of the extracellular material of *c*-type cytochrome mutants and type IV pili mutants revealed decreased extracellular polysaccharide content, which correlated with key phenotypes such as agglutination, surface attachment, and concentration of extracellular cytochromes. Defects in many of these phenotypes were rescued by the addition of isolated extracellular material, suggesting that phenotypes previously attributed to disruption of a cytochrome of pili subunit may also be the result of a disrupted extracellular matrix.

4.2 **Introduction**

Respiration of insoluble acceptors (minerals, electrodes) requires mechanisms for transfer of electrons from internal oxidative reactions to the outer surface of a bacterium followed by transfer from the cell surface to the acceptor. While some microbes use electron shuttles to achieve the final cell-acceptor transfer (14, 92), *G. sulfurreducens* uses a direct mechanism of transfer with no soluble electron carriers (103). Recent studies suggest that *Geobacter* uses type IV pili (71) or extracellular polysaccharides (117) to

position important *c*-type cytochromes in an extracellular network that facilitates electron transfer to insoluble acceptors.

The extracellular matrix surrounding *G. sulfurreducens* contains polysaccharides tightly associated with proteins. A mutation disrupting polysaccharide export (disruption of *xapD*, part of a polysaccharide export system) influenced both the polysaccharide and protein content of this matrix, with retention of important extracellular *c*-type cytochromes decreasing with lower matrix polysaccharide content. Along with a roughly 50% reduction in extracellular polysaccharides, the Δ*xapD::kan* (Δ1501) mutant showed reduced attachment to specific surfaces, including Fe(III) oxyhydroxide and graphite electrodes poised at oxidizing potentials (117). In addition to surface attachment, the Δ*xapD::kan* mutant was deficient in some of the commonly studied phenotypes previously associated with *Geobacter* pili or cytochrome mutants, such as agglutination and electrode or Fe(III) reduction. The similarity of the Δ*xapD::kan* mutant's phenotype and that of a type IV pili mutant (112, 113) in particular prompted an examination of the extracellular polysaccharide content of previously studied *Geobacter* mutants.

In addition to polysaccharides, specific *c*-type cytochromes and type IV pili may play structural (as well as functional) roles in the *Geobacter* extracellular matrix. The impact of disruption of these genes on the structure and composition of the extracellular matrix was investigated. An association between type IV pili and the extracellular matrix has been well described in another proteobacterium, *Myxococcus xanthus,* in which extracellular polysaccharides are thought to trigger pilus retraction and additional matrix production (10, 72). In the *M. xanthus* genome, homologs to the *xap* cluster of *Geobacter*

are located immediately downstream of type IV pili. The similar genetic arrangement in *G. sulfurreducens* may suggest a similar functional relationship.

When the extracellular matrix of *Geobacter* was disrupted (in the Δ*xapD::kan* mutant), the presence of cytochromes (ex. OmcZ, OmcS, OmcE) found in this matrix significantly decreased. In addition to a functional role as electron transfer proteins, extracellular cytochromes may contribute to the overall structure of the extracellular matrix. For example, an extracellular cytochrome, OmcZ, known to be critical for current production in a microbial fuel cell (102) is also the dominant heme-containing protein found in the extracellular material of *G. sulfurreducens* (46, 117). The extracellular localization of OmcS along type IV pili (71) may indicate a structural role for this cytochrome in the extracellular matrix as well. Disruption of matrix-associated cytochromes may influence properties of the matrix itself, resulting in phenotypes due to a disrupted network. This work shows a new relationship between extracellular proteins (cytochromes and pili) and polysaccharides, with the presence or absence of one affecting the concentration of the other.

4.3 Materials and Methods

4.3.1 Bacterial strains, plasmids and culture conditions

G. sulfurreducens PCA (ATCC 51573) was grown anaerobically at 30°C in a mineral media containing 20 mM acetate as electron donor and 40 mM fumarate as electron acceptor (93). Cultures were maintained using media containing Fe(III) oxyhydroxide as the electron acceptor. *G. sulfurreducens* kanamycin replacement mutants were supplemented with kanamycin (200 µg/ml), while complemented

replacement mutants were supplemented with gentamicin (20 µg/ml). *Escherichia coli* WM3064 was grown in LB broth containing 30 µM 2,6-diaminopimelic acid (DAP) at 37°C, with the addition of kanamycin (50 µg/ml) when carrying pBBR1MCS-2 or gentamicin (10 µg/ml) when carrying pBBR1MCS-5 (59).

4.3.2 Construction of replacement mutants

Single-step gene replacement (75) was used to insert a gene for kanamycin resistance (kan^r) into the *G. sulfurreducens* genome, replacing target genes, with primers for each mutant listed in Table 4.1. Recombinant PCR was used to create a ~2 kb fragment containing kan^r and approximately 0.5 kb of sequence upstream and downstream of the gene targeted for deletion. For each mutant, kan^r was amplified from pBBR1MCS-2 using the appropriate primer set listed in Table 4.2 (PilA1 and PilA2, PilT1 and Pilt2, OmcZ1 and OmZ2, OmcS1 and OmcS2, or OmcE1 and OmcE2) and the following reaction conditions: 30 cycles of 94°C for 1 min, 60°C for 1 min, 72°C for 1 min, and then a final extension at 72°C for 5 min. The upstream and downstream regions of each gene to be replaced were amplified using the appropriate primer sets listed in Table 4.2 (PilA3 and PilA4, PilA5 and PilA6, PilT3 and PilT4, PilT5 and PilT6, OmcZ3 and OmcZ4, OmcZ5 and OmcZ6, OmcS3 and OmcS4, OmcS5 and OmcS6, OmcE3 and OmcE4, OmcE5 and OmcE6) and the following reaction conditions: 30 cycles of 94°C for 1 min, 55°C for 1 min, 72°C for 1 min, and then a final extension at 72°C for 5 min.

For each replacement mutant, the three PCR products were used as templates in a primer-less PCR reaction, resulting in ~2 kb DNA fragments containing kan^r flanked by the upstream and downstream regions of genes targeted for replacement. To create these

linear fragments, two rounds of PCR were used, first 15 cycles of 96°C for 40 seconds, 47°C for 1 min, 72°C for 5 min, then a final extension at 72°C for 10 min. Then the 2 kb fragment was further amplified using 30 cycles of the same reaction conditions with the addition of the outermost primers listed in Table 4.2 (PilA3 and PilA6, PilT3 and PilT6, OmcZ4 and OmcZ5, OmcS4 and OmcS5, OmcE3 and OmcE6). Linear DNA fragments were electroporated into wild type *G. sulfurreducens* (25), and recombinants selected on mineral media containing 200 µg/ml kanamycin, resulting in the following replacement mutants: Δ*omcS::kan,* Δ*omcE::kan,* Δ*omcZ::kan,* Δ*pilT::kan,* Δ*pilA::kan* (Table 4.1).

Table 4.1 Strains and plasmids used in this study

Strain or plasmid	Relevant characteristics	Reference
G. sulfurreducens		
Wild Type	ATCC 51573	20
Δ*xapD::kan*	Kanamycin resistance gene replacing GSU1501	117
Δ*omcE::kan*	Kanamycin resistance gene replacing GSU0618	This study
Δ*omcS::kan*	Kanamycin resistance gene replacing GSU2504	This study
Δ*omcZ::kan*	Kanamycin resistance gene replacing GSU2076	This study
Δ*pilA::kan*	Kanamycin resistance gene replacing GSU1496	This study
Δ*pilT::kan*	Kanamycin resistanc gene replacing GSU1492	This study
Δ*xapD::kan*+pG1500-5	Complemented Δ*xapD::kan* mutant	117
E. coli		
WM3064	Donor strain for conjugation	122
Plasmids		
pBBR1MCS-2	Mobilizable broad-host-range plasmid, Km^r	59
pBBR1MCS-5	Mobilizable broad-host-range plasmid, Gm^r	59
pG0618	GSU0618 in MCS of pBBR1MCS-5, Gm^r	This study
pG2504	GSU2504 in MCS of pBBR1MCS-5, Gm^r	This study
pG2076	GSU2076 in MCS of pBBR1MCS-5, Gm^r	This study
pG1496	GSU1496-7 in MCS of pBBR1MCS-5, Gm^r	This study
pG1492	GSU1492 in MCS of pBBR1MCS-5, Gmr	This study

Table 4.2 Primers used in this study

Primer	Sequence (5' to 3')	Use
OmcE1	*ACGTGAAAGGAGAACGCAGA* AAGCGAACCGGAATTGCCAGCT	Amplify Kan^r, homologous to OmcE4 in italics
OmcE2	*TTTTCCCGGAGAGGAACCCC* TCAGAAGAACTCGTCAAGAAGGC	Amplify Kan^r, homologous to OmcE5 in italics
OmcE3	TGTGTCGACTTGTGCAGGTTAATGG	Amplify sequence upstream GSU0618
OmcE4	TCTGCGTTCTCCTTTCACGTGAGTAC	Amplify sequence upstream GSU0618
OmcE5	GGGGTTCCTCTCCGGGAAAAGGGTG	Amplifiy sequence downstream GSU0618
OmcE6	GCACTGACGGAGGGGTTGTAGTTGG	Amplify sequence downstream GSU0618
OmcS1	*CAACCAAAATGGAGGAAATG* AAGCGAACCGGAATTGCCAGCT	Amplify Kan^r, homologous to OmcS3 in italics
OmcS2	*CAACATCAGATTGTGGCAAGA* TCAGAAGAACTCGTCAAGAAGGC	Amplify Kan^r, homologous to OmcS6 in italics
OmcS3	CATTTCCTCCATTTTGGTTGGTTTCTCCG	Amplify sequence upstream GSU2504
OmcS4	CCACGGGGATCGCGGTTGACGGCCT	Amplify sequence upstream GSU2504
OmcS5	ACCCAGCTGTAGGTCTTCTTGAGCC	Amplify sequence downstream GSU2504
OmcS6	TCTTGCCACAATCTGATGTTGTGTGAT	Amplify sequence downstream GSU2504
OmcZ1	*CAAGAAAGGAGCAGAAAGGA* AAGCGAACCGGAATTGCCAGCT	Amplify Kan^r, homologous to OmcZ3 in italics
OmcZ2	*GCCCCGTTGGTCGGAAAGGTA* TCAGAAGAACTCGTCAAGAAGGC	Amplify Kan^r, homologous to OmcZ6 in italics
OmcZ3	TCCTTTCTGCTCCTTTCTTGTGAAG	Amplify sequence upstream GSU2076
OmcZ4	GCTAGTTATATGCAGTAAAATAGCGTA	Amplify sequence upstream GSU2076
OmcZ5	AACCTGGTCGGCACCGATGTGCTGC	Amplify sequence downstream GSU2076
OmcZ6	TACCTTTCCGACCAACGGGGCAGGG	Amplify sequence downstream GSU2076
PilA1	*TTTAAGGATTAAACGGATAA* AAGCGAACCGGAATTGCCAGCT	Amplify Kan^r, homologous to PilA4 in italics
PilA2	*TCCAGTATGTATTTAATCAA* TCAGAAGAACTCGTCAAGAAGGC	Amplify Kan^r, homologous to PilA5 in italics
PilA3	TGAAGCTGCTCATGTCATACGGATT	Amplify sequence upstream GSU1496
PilA4	TTATCCGTTTAATCCTTAAACGTTA	Amplify sequence upstream GSU1496
PilA5	TTGATTAAATACATACTGGAGGAAA	Amplify sequence downstream GSU1496
PilA6	AAATCATTGATGGATTTTATCTTTT	Amplify sequence downstream GSU1496
PilT1	*TTGTAACGGAGAACATCATA*	Amplify Kan^r, homologous to PilT4 in italics

	AAGCGAACCGGAATTGCCAGCT	
PilT2	*ACAGATCGATCCGGCGGCGG* TCAGAAGAACTCGTCAAGAAGGC	Amplifiy Kan^r, homologous to PilT5 in italics
PilT3	TGAACCTGATTACCGCCCAGCGTCT	Amplify sequence upstream GSU1492
PilT4	TATGATGTTCTCCGTTACAAAATGTC	Amplify sequence upstream GSU1492
PilT5	CCGCCGCCGGATCGATCTGTACACA	Amplify sequence downstream GSU1492
PilT6	TCAGGATTGTGTCGAGGATGCCGCC	Amplify sequence downstream GSU1492

4.3.3 Construction of complemented mutants

Each kanamycin replacement mutant was complemented through expression of the replaced gene on pBBR1MCS-5 (59). To complement the Δ*omcZ::kan* mutant, GSU2076 was amplified from wild type genomic DNA using primers ZFor (CTC*GGATCC*ATGAAGAAAAAGGTACTGATTGG; BamHI site in italics) and ZRev (CGC*CTGCAG*TTACCGTTTGACTTTCTTCG; PstI site in italics). GSU1496-1497 was amplified using PilAFor (CAT*GGATCC*TTGGCCAATTACCCCCATAC) and PilARev (ATA*CTGCAG*CTACTGCGACTTCCACTCGG) to complement the Δ*pilA::kan* mutant. To complement the Δ*omcE::kan* mutant, GSU0618 was amplified using EFor (CGC*GGATCC*ATGAGAAGCGAAGTAAAAATCG) and ERev (CTA*CTGCAG*CTACTTCTTGTGGCAACCCAG). GSU2504 was amplified using SFor (CGC*GGATCC*ATGAAAAAGGGGATGAAAGTAAG) and SRev (ATT*CTGCAG*TTAGTCCTTGGCGTGGCACTTG) to complement the Δ*omcS::kan* mutant. Primers PilTF (CAG*GGTACC*ATGGCCAACATGCATCAACTCC; KpnI site in italics) and PilTR (ACA*CTGCAG*TTACCTCATCTGAGGGCGCTG) were used to amplify GSU1492. For each reaction the following conditions were used: 30 cycles of 94°C for 1 min, 55°C for 1 min, 72°C for 2 min, and then a final extension at 72°C for 5

min. Products were digested and inserted in either the BamHI and PstIor the KpnI and PstI sites of pBBR1MCS-5. Complementation plasmids (Table 4.1) where then transformed into mating strain *E. coli* (WM3064) and introduced into the appropriate *G. sulfurreducens* replacement mutants through conjugation (116), and selected for with gentamicin.

4.3.4 Isolation of extracellular matrix

Extracellular material was isolated using a previously described protocol (22). Cells were grown to OD_{600} = 0.6, pelleted and resuspended in 1/10 volume TNE (10 mM Tris-HCl pH 7.5, 100 mM NaCl, 5 mM EDTA) before shearing in a commercial blender (Waring Products, Inc., Torrington, CT) for 1 min at low speed. Sheared cells were lysed by the addition of SDS (0.1% final concentration) with stirring for 5 min at room temperature. This lysate was centrifuged at 17,000 x g for 10 min then washed 5 times in Tris-HCl, pH 7.5. Protein concentration of the matrix material was determined using a bicinchonicic acid (BCA) protein assay (Thermo Scientific, Rockford, IL), and the total polysaccharide content was determined using the phenol sulfuric acid method, with glucose as a standard (95).

For isolation of the polysaccharide component of the extracellular material, the above protocol was used with slight modifications (72). After treatment with 0.1% SDS, lysate was incubated with Pronase E (1 mg/ml) for 180 min at 37°C. Protease treated lysate was then pelleted as above and washed 4 times with 0.1% SDS to inactivate the protease, before 5 washes in Tris-HCl, pH 7.5. To isolate any polysaccharides loosely associated with the matrix material, cells were grown to OD_{600} = 0.6, and resuspended in

TNE. After shearing and cell lysis, supernatants were collected and proteins and polysaccharides precipitated with 2 volumes cold ethanol at 4°C overnight.

4.3.5 Reduction of extracellular cytochromes

Absorbance of equal volumes of wild type and mutant extracellular material (cultures grown to same OD, ECM resuspended in same volume) was measured using wavelengths spanning 400-600 nm. To reduce cytochromes, sodium dithionite was added to each sample and absorbance measured. To determine relative extracellular cytochrome content, the difference between absorbance at 552 and 562 nm was calculated.

4.3.6 Fe(III) reduction

Wild type *G. sulfurreducens* and the type IV pili and cytochrome mutants grown with fumarate were each transferred (1% inoculation) to mineral medium containing Fe(III) oxyhydroxide as electron acceptor and 20 mM acetate as donor. Samples were taken after 7 days, diluted in 1N HCl, and a modified ferrozine assay was used to measure Fe(II) production (85).

4.3.7 Biofilm formation assays

To determine attachment phenotypes, cells were grown for 72 h in 96-well plates (Nunc 167008) as previously described (116). A modified crystal violet assay was used in which cells were stained with crystal violet, planktonic cells removed, and dimethyl sulfoxide used to solubilize crystal violet from attached cells (104). Crystal violet absorbance at 600 nm (A_{600}) was measured as an indicator of attachment. Where described, extracellular material (10 µg polysaccharide/ml) or protease treated extracellular material (polysaccharides, 10 µg/ml) was added at time of inoculation.

4.3.8 Agglutination assays

To determine agglutination phenotypes, cells were grown for 48 h at 30°C with mineral media containing acetate and fumarate. Optical density at 600 nm (OD_{600}) was first measured for suspended cells, then cell aggregates were disrupted by vortexing and OD_{600} measured again to determine levels of agglutination (113). Where described, isolated extracellular material or polysaccharides (10 µg/ml) was added to culture at time of inoculation, with material added to non-inoculated medium serving as a control.

4.3.9 Electrochemical and confocal analysis

Electrochemical bioreactors containing a graphite working electrode, platinum counter electrode, and saturated calomel reference electrode were prepared as previously described (93), and incubated in a 30°C water bath connected to a 16-channel potentiostat (VMP; Bio-Logic, Knoxville, TN) with EC-Lab software to run chronoamperometry. Anaerobic bioreactors (receiving humidified N_2/CO_2 [80:20 vol/vol]) were inoculated with 50% (vol/vol) *G. sulfurreducens* (OD_{600} = 0.5) and mineral media containing 40 mM acetate. Inoculated bioreactors incubated for 24 h at a potential of +0.24 V vs. the standard hydrogen electrode (SHE) then electrode-attached biofilms were stained using a LIVE/DEAD *Bac*Light bacterial viability kit (Invitrogen Corp., Carlsbad, CA), and imaged using a Nikon C1 spectral imaging confocal microscope (Nikon, Japan).

4.4 Results

4.4.1 Decreased cytochrome and polysaccharide content of mutant extracellular material

Previous work showed that the extracellular matrix of the Δ*xapD::kan* mutant (a polysaccharide export mutant) had decreased polysaccharide content and was nearly devoid of *c*-type cytochromes (117). We hypothesized that disruption of other extracellular appendages or proteins would disrupt the matrix, decreasing levels of polysaccharides and cytochromes recovered in the matrix material of mutant cells. Extracellular matrix material was isolated from equal volumes of wild type and mutant cells (grown to the same OD) for comparison. When using fumurate, mutant cells did not show any defects in growth rate or final OD.

Type IV pili and *c*-type cytochrome mutants differed in the quantity and composition of pelleted extracellular material (Fig 4.1A). Matrix material isolated from the Δ*omcS::kan* and Δ*omcE::kan* mutants was similar to wild type in color and quantity. The Δ*pilT::kan* mutant's extracellular material also showed a high cytochrome content, with a slight reduction in quantity. In contrast, the Δ*omcZ::kan* mutant matrix was almost white in color, while the Δ*pilA::kan* mutant extracellular material was red, but significantly reduced in quantity compared to wild type.

The differences in color and quantity of extracellular material were supported by the relative cytochrome content in the extracellular material of mutants. Cytochrome content was determined based on the spectral signature of reduced cytochromes using equal volumes of extracellular material (isolated from 1L of cells grown to $OD_{600} = 0.6$).

Wild type *G. sulfurreducens* showed the highest levels of extracellular cytochromes (difference in absorbance between 552 and 562 nm) with lower levels detected in the Δ*omcS::kan,* Δ*omcE::kan,* and Δ*pilT::kan* mutants. Mutants with more severe defects in extracellular matrix polysaccharide content (Δ*pilA::kan,* Δ*xapD,* Δ*omcZ::kan*) had greatly reduced cytochrome content, indicating fewer extracellular cytochromes per liter cells (Fig. 4.1C).

Extracellular polysaccharide content was quantified for each mutant, with matrix material isolated from the Δ*omcS::kan* mutant having roughly the same concentration of polysaccharides (~5-6 mg/L) as wild type cells. Deletion of this *c*-type cytochrome, shown to be aligned on type IV pili (71), did not significantly alter polysaccharide content. However, when *c*-type cytochromes OmcE and OmcZ (a cytochrome recently shown to be localized to the extracellular matrix (46, 117) were disrupted, polysaccharide content decreased to approximately 70% of wild type (Fig. 4.1B).

Disruption of type IV pili had the greatest influence on the levels of polysaccharides recovered in the extracellular matrix. Disruption of the protein responsible for pili retraction (pilT) brought matrix polysaccharide content down to the level found in the Δ*xapD::kan* mutant (~50% of wild type). Disruption of the pilin structural subunit (*pilA*) resulted in the greatest decrease, with only 30% the polysaccharides of wild type found in the matrix of this mutant (Fig. 4.1B).

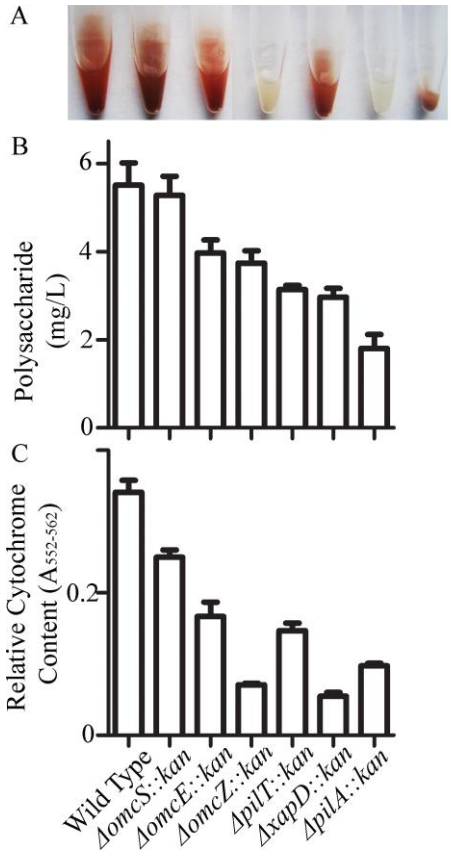

Figure 4.1 (A) Pelleted extracellular material from 100 ml cells grown to OD_{600} = 0.6. (B) Total polysaccharides present in the extracellular material isolated from 1L wild type and mutant cells grown to OD_{600} = 0.6, using glucose as a standard. (C) Relative extracellular cytochrome content based on the difference between absorbance measured at 552 and 562 nm of equal volumes dithionite reduced extracellular material. Error bars are standard errors of the mean for three independent replicates.

4.4.2 Increased surface attachment correlates with extracellular polysaccharide content

The charge of a surface influences attachment of *Geobacter* cells, in particular when extracellular polysaccharides are depleted, as previously demonstrated in the Δ*xapD::kan* mutant. This mutant (with roughly 50% the extracellular polysaccharides of wild type) showed increased attachment to negatively charged surfaces, but very little attachment to positively charged surfaces in comparison (117). We hypothesized the matrix contained negatively charged proteins or polysaccharides in the wild type (absent in the Δ*xapD::kan* mutant) that resulted in this attachment preference.

A trend of increased attachment to negatively charged surfaces with decreasing extracellular polysaccharide content was also observed with the pili and cytochrome mutants (Fig. 4.2A). Attachment assays using negatively charged surface coatings were performed to compare mutant and wild type behavior. A mutant with roughly the same level of extracellular polysaccharides as wild type (Δ*omcS::kan*) showed similar attachment in negatively charged 96 well plates. In contrast, mutants with fewer extracellular polysaccharides demonstrated higher attachment to the negative surface. The mutant with the lowest polysaccharide content (Δ*pilA::kan*) had the highest level of attachment, over twice that of wild type cells, while mutants with intermediate extracellular polysaccharide levels (Δ*omcE::kan,* Δ*omcZ::kan*) showed intermediate levels of attachment (170-190% of wild type) to negatively charged wells (Fig. 4.2A). In each case, decreased polysaccharide levels in the mutants correlated with increased attachment to a negatively charged surface.

High attachment to negatively charged surfaces was observed in all mutants with decreased extracellular polysaccharides. In all cases, the addition of isolated extracellular material from wild type cells to the growth medium decreased attachment by these mutants. Attachment was decreased to near wild type levels in the Δ*omcE::kan,* Δ*omcZ::kan,* Δ*xapD::kan,* and Δ*pilA::kan* mutants (Fig. 4.2B). A slight decrease in attachment was also observed in wild type and Δ*omcS::kan* cells with the addition of extracellular material. Additionally, when replacement mutants were complemented through expression of the appropriate gene(s) *in trans*, the attachment phenotypes were restored to wild type levels (Fig. 4.2C).

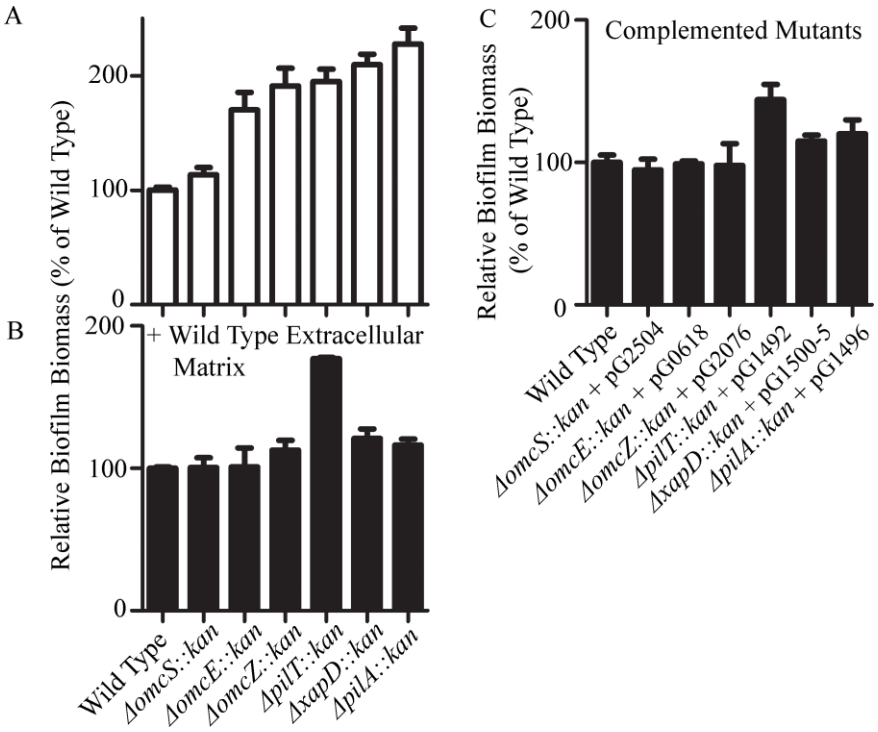

Figure 4.2 (A) Biofilm formation based on CV staining of cells adherent to negatively charged 96-well plates, with mean absorbance expressed

relative to wild type attachment. (B) Biofilm formation with the addition of 10 µg/ml extracellular material (isolated from wild type) to growth medium of mutants. (C) Biofilm formation by complemented mutants relative to wild type levels. For each, error bars are standard errors of the mean for three replicates.

4.4.3 Cell-cell agglutination decreases with extracellular polysaccharide content

The ability for cells to agglutinate has been linked to the presence of type IV pili, as a *pilA* mutant has little ability to agglutinate (113). Recently it was shown that agglutination might be dependent on the presence of extracellular polysaccharides. The Δ*xapD::kan* mutant, which had decreased extracellular polysaccharide content, only agglutinated at ~20% of wild type cells (117). In this study agglutination in wild type *G. sulfurreducens* and the Δ*pilA::kan* mutant was tracked for 120 h (at 25 or 30°C) to determine the incubation length and temperature where defects would be most prominent. Within 48 hours, differences in agglutination between mutant and wild type were evident, and remained relatively constant through 120 hours. However, final OD dropped in cultures incubated over 48 hours as cells lysed. A 48 h incubation at 30°C was used for subsequent tests as differences between mutant and wild type were quickly evident and little cell lysis had occurred.

The mutant with similar levels of extracellular polysaccharides as wild type (Δ*omcS::kan*) was not significantly defective in agglutination (Fig. 4.3A), while mutants with lower polysaccharide content showed lower levels of agglutination. For example,

the Δ*omcE::kan* mutant, which had ~70% the extracellular polysaccharides of wild type, was able to agglutinate to ~60% of wild type levels. A mutant with a more severe defect in polysaccharide content, Δ*pilA::kan*, was only able to agglutinate to ~30% wild type levels (Fig. 4.3A). The Δ*pilT::kan* and Δ*omcZ::kan* mutants, which also had decreased levels of extracellular polysaccharides, showed defects in agglutination, with Δ*pilT::kan* able to agglutinate to roughly 60% that of wild type and Δ*omcZ::kan* having the least agglutination ability (~25% of wild type). In general, cells with more extracellular polysaccharides showed greater levels of cell to cell agglutination.

The addition of extracellular matrix material isolated from wild type cells was previously shown to partially restore agglutination in the Δ*xapD::kan* mutant (117). The Δ*pilA::kan* and Δ*omcZ::kan* mutants showed the most severe defects in agglutination, but in each case, the addition of extracellular matrix isolated from wild type was also able to partially restore agglutination. The level of agglutinated cells doubled for each mutant, with the Δ*pilA::kan* mutant able to achieve almost 80% wild type agglutination (Fig. 4.3B). Mutants with intermediate agglutination phenotypes (Δ*omcE::kan,* Δ*pilT::kan*) also showed increased agglutination in the presence of wild type extracellular material. While the Δ*omcS::kan* mutant showed little defect in agglutination, addition of isolated extracellular material still increased agglutination in this mutant (Fig. 4.3B).

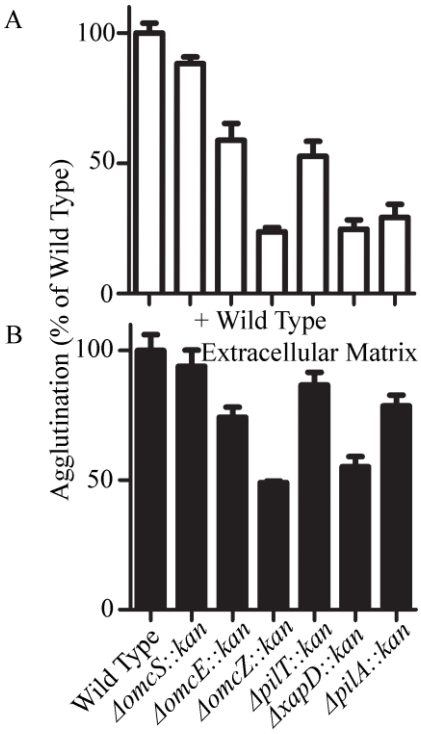

Figure 4.3 (A) Percent agglutination in wild type *G. sulfurreducens* and replacement mutants as determined by change in OD_{600} before and after aggregate disruption. (B) Percent agglutination in wild type and mutants with the addition of 10 µg/ml extracellular material (isolated from wild type) to growth medium of mutants. Error bars are standard errors of the mean for three replicates.

4.4.4 Fe(III) oxyhydroxide reduction and electrode binding linked to extracellular polysaccharide levels

For reduction of Fe(III) oxyhydroxide by *Geobacter*, contact between surface and cell (likely the extracellular matrix) is needed. Decreased levels of Fe(III) oxyhydroxide reduction were seen with the Δ*xapD::kan* mutant (which also showed decreased

attachment to Fe(III)-coated glass slides) suggesting that correct networking of extracellular polysaccharides was needed. With the exception of the Δ*omcS::kan* mutant, Fe(III) oxyhydroxide reduction generally decreased with decreasing polysaccharide content of the extracellular matrix (Fig. 4.4A). After 7 days, when wild type had reduced ~25 mM Fe(III) oxyhydroxide, the Δ*omcE::kan* mutant which had only slightly less extracellular polysaccharides had reduced ~20 mM. The mutants with the greatest reduction in extracellular polysaccharides, Δ*xapD::kan,* Δ*pilA::kan,* and Δ*pilT::kan*, showed the lowest levels of Fe(III) oxyhydroxide reduction, with 12-14 mM produced after 7 days. Despite having decreased extracellular polysaccharides, Δ*omcZ::kan* was not severely inhibited in reduction of insoluble Fe(III).

Current production by the pili, cytochrome, and matrix mutants was measured for 24 h on an electrode poised at +0.24 V vs. SHE. While all mutants studied showed reduced current generation, mutants with reduced levels of extracellular polysaccharides showed the lowest levels. After 24 h, the Δ*xapD::kan,* Δ*pilA::kan*, and Δ*omcZ::kan* mutants produced only 5 µA, compared to the 150 µA by wild type (Fig. 4.4B). Current production by *Geobacter* is dependent on the ability to attach to a properly poised electrode (a surface with a positive surface charge). In contrast to attachment to the negatively charged 96 wells plates, electrode attachment generally decreased with decreasing polysaccharide content (Fig. 4.4C). High levels of electrode attachment were seen with the Δ*omcS::kan* mutant (Fig. 4.4C), which also had the highest current production (Fig. 4.4B) and polysaccharide content (Fig 4.1B) of all the mutants. Mutants

with fewer extracellular polysaccharides (Δ*pilA::kan* and Δ*omcZ::kan*) formed thin electrode-attached biofilms, consistent with past reports (115).

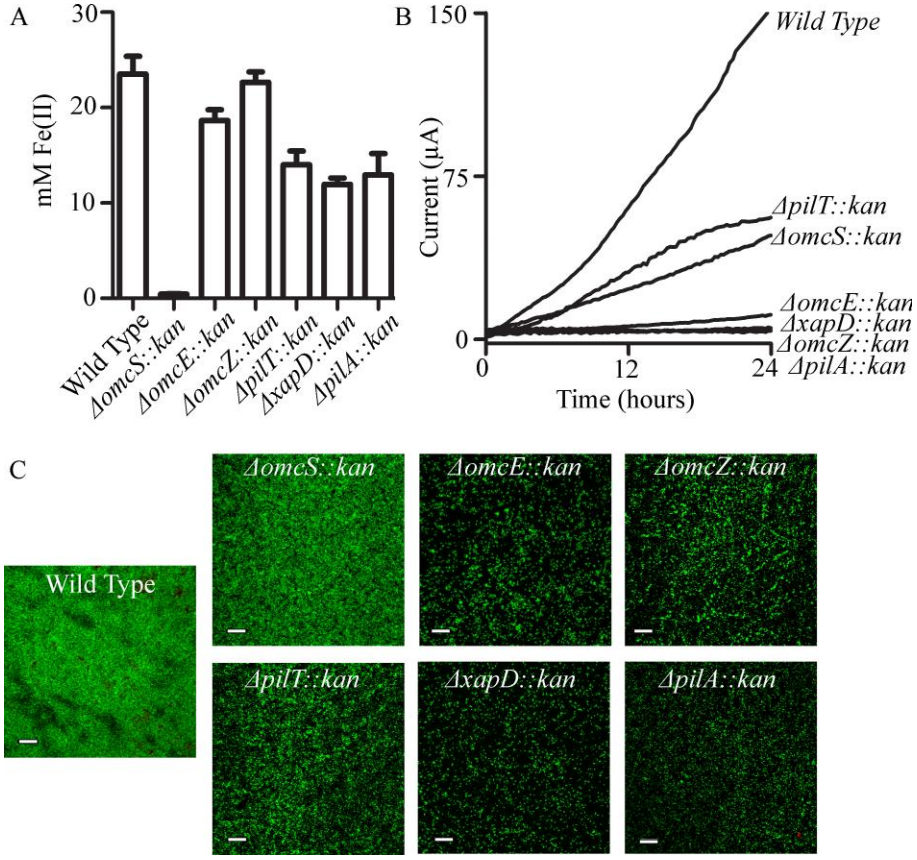

Figure 4.4 (A) Reduced Fe(III) oxyhydroxide as indicated by accumulation of Fe(II) after 7 day incubation of 1% inoculation. Error bars are standard errors of the mean for three independent replicates. (B) Current produced over 24 hours by wild type and mutants (C) Confocal images (maximum projections, bar = 20 μm) of electrode-attached biofilms after 24 hours.

4.4.5 Complementation with Δ*pilA::kan* mutant extracellular material

To test if type IV pili in the wild type extracellular material were responsible for restoring key phenotypes, the growth medium of the Δ*pilA::kan* mutant was supplemented with extracellular material isolated from itself. Attachment returned to near wild type levels in the presence of additional Δ*pilA::kan* extracellular material (Fig. 4.5A), and agglutination also increased with the addition of Δ*pilA::kan* extracellular material (Fig. 4.5B). For both phenotypes, additional extracellular material brought the mutant to levels similar to what was observed in the complemented strain.

To determine if a protein in the extracellular material was involved in the restoration of attachment and agglutination, wild type extracellular material was protease treated and Δ*pilA::kan* cultures were supplemented with the remaining polysaccharides at time of inoculation. Attachment to a negatively charged 96 well plate returned to near wild type levels, similar to what was observed in the complemented mutant (Fig. 4.5A). Similarly, agglutination increased in the Δ*pilA::kan* mutant in the presence of protease treated extracellular material (Fig. 4.5B). These experiments showed that attachment and agglutination are not dependent on type IV pili, and instead may rely on the presence of extracellular polysaccharides.

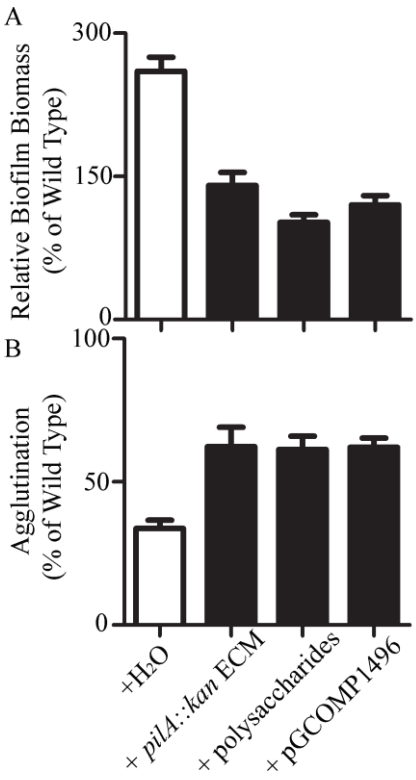

Figure 4.5 (A) Biofilm formation and (B) agglutination by the complemented Δ*pilA::kan* mutant and the Δ*pilA::kan* mutant with the addition of Δ*pilA::kan* extracellular material or polysaccharides (10 µg/ml), relative to wild type levels.

4.4.5 Loosely tethered polysaccharides recovered in supernatants

To test whethere polysaccharides were loosely associated with the pelleted extracellular matrix, material was precipitated from wild type and Δ*pilA::kan,* and Δ*xapD::kan* mutant supernatants. Few polysaccharides (3-4 mg/L) were recovered from wild type and Δ*xapD::kan* supernatants, while higher levels (nearly 7 mg/L) of loosely

bound polysaccharides were detected in Δ*pilA::kan* supernatants. When polysaccharide levels in the matrix pellet and the supernatant were totaled, the Δ*pilA::kan* mutant appeared to produce similar quantities of extracellular polysaccharides as wild type, while the Δ*xapD::kan* remained deficient.

4.5 Discussion

Extracellular respiration in *Geobacter* relies on tight interactions between the cell surface and an insoluble electron acceptor. These interactions are governed in part by outer surface characteristics such as charge. Defects in surface attachment, cell to cell agglutination, and to a lesser extent Fe(III) oxyhydroxide reduction by *G. sulfurreducens* occur when the extracellular matrix is deficient in polysaccharides. Decreased levels of extracellular polysaccharides were previously observed in a polysaccharide export mutant (Δ*xapD::kan*), resulting in an altered surface charge and inability to reduce Fe(III) oxyhydroxide or electrodes (117). This work demonstrated that defects in specific *Geobacter* phenotypes track with the levels of extracellular polysaccharides and these polysaccharide levels are affected by a number of extracellular mutations.

The extracellular matrix of *G. sulfurreducens* is a complex network of type IV pili, *c*-type cytochromes and polysaccharides.Disruption of multiple extracellular proteins impacted overall matrix properties. Most mutants in which type IV pili and extracellular cytochromes had been disrupted had lower levels of extracellular polysaccharides. Polysaccharides are known to play a critical role in bacterial biofilm structure, viablility, and initial attachment (9, 41, 117). In this case, decreased matrix polysaccharides increased attachment to negatively charged surfaces, suggesting a charge difference in the

extracellular material of mutants. A more positive surface charge possibly created by loss of negative polysaccharides could limit contact of mutant cells with Fe(III) oxyhydroxide, decreasing Fe(III) reduction levels. The change in surface charge of mutant cells also decreased the cell to cell contact necessary for agglutination. The levels of matrix bound *c*-type cytochromes, as indicated by the spectral signature of reduced cytochromes and the appearance of pelleted extracellular material, also tracked with matrix polysaccharides, with cytochrome content decreasing with decreasing polysaccharide content. In general, mutants with the greatest decreases in extracellular polysaccharides exhibited the most severe phenotype defects, while mutants with extracellular polysaccharides near wild type levels had phenotypes similar to wild type.

The inability of a PilA mutant to agglutinate has been reported, suggesting type IV pili are necessary for agglutination (113). The finding that addition of extracellular material isolated from the Δ*pilA::kan* mutant (material lacking pili) restores agglutination in this mutant suggests pili are not in fact necessary. The addition of polysaccharides alone to the Δ*pilA::kan* mutant also partially restoring agglutination suggests that polysaccharides may be the primary component. In contrast to the Δ*pilA::kan* mutant, agglutination could not be recovered in the Δ*xapD::kan* mutant by addition of its own extracellular material (even though it could be rescued by wild type matrix material) (117). This may indicate that the reduction in extracellular polysaccharides in the Δ*xapD::kan* mutant is due to the absence of a specific polysaccharide or set of polysaccharides, whereas the Δ*pilA::kan* mutant simply has less extracellular material overall. The dark red appearance of the Δ*pilA::kan* pelleted extracelular material (in

contrast to the white Δ*xapD::kan* pellet), indicates that cytochromes are in fact anchored in the matrix of the Δ*pilA::kan* mutant despite its decreased levels of extracellular polysaccharides.

The reduction of polysaccharide concentrations in the extracellular material of the Δ*pilA::kan* mutant appears to be the result of reduced retention of extracellular polysaccharides rather than decreased expression. The high concentration of loosely bound polysaccharides associated with the Δ*pilA::kan* extracellular material suggests that type IV pili may be involved in formation of a compact matrix and retention of polysaccharides within the extracellular matrix. Similarly, proper extracellular matrix formation has been linked to the presence of pili in *M. xanthus.* Exopolysaccharide production and type IV pili expression are tightly regulated in this organism, with a mutant lacking functional type IV pili also being deficient in extracellular polysaccharides (10, 143). *G. sulfurreducens* may also rely on interactions between type IV pili and extracellular polysaccharides to maintain its extracellular matrix.

This comparison shows that disruption of many extracelllar protiens can alter polysaccharide content, likely changing the charge at the outer surface of the cell, altering the tendency of cells to attach to a surface as well as to each other. An intact matrix facilitates contact with an insoluble electron acceptor, promoting efficient electron transfer. Studying proteins localized to the *Geobacter* extracellular matrix requires caution as disruption of one component can impact the overall matrix, with far reaching effects.

Chapter 5: Extracellular Matrix Protein Isolation and Identification

5.1 Overview

Biofilm formation and cell to cell attachment in *Geobacter sulfurreducens* is dependent on the presence and composition of the extracellular matrix. While the role of extracellular polysaccharides has been studied, little is known about the protein components. Proteomics was used to identify proteins associated with the *G. sulfurreducens* extracellular matrix, providing new targets for study. The majority of identified proteins were intracellular, highlighting the need for an isolation method that separates matrix material from cells with minimal lysis.

5.2 Introduction

Electron transfer to an insoluble acceptor by *Geobacter* requires tight contact between a cell's outer surface and the external acceptor (103). Surface contact is likely made through the extracellular material (rich in polysaccharides and *c*-type cytochromes) surrounding cells. The polysaccharides present in this matrix are essential for surface attachment as wells as cell to cell agglutination. In addition, polysaccharides help to anchor multiple *c*-type cytochromes in the extracellular matrix, facilitating electron transfer through this network (117). The importance of extracellular polysaccharides has been studied, but in general the roles and identities of the proteins found in the matrix are unclear.

With the goal of identifying proteins associated with the extracellular matrix of *G. sulfurreducens*, samples were prepared for mass spectrometry using two different methods. Both preparations contained high concentrations of intracellular proteins and

very few extracellular proteins were identified. Three cytochromes predicted to be extracellular were identified in matrix preparations, providing potential new targets of study; however, a matrix isolation with minimal intracellular contamination is needed for further identification of matrix associated proteins.

5.3 Methods

5.3.1 Bacterial strains and culture conditions

For isolation of extracellular matrix material, *G. sulfurreducens* PCA (ATCC 51573) was routinely cultured using mineral media (93) with 40 mM fumarate, 30 mM acetate in 1L volumes at 30°C.

5.3.2 Isolation of extracellular material

For proteomic analysis, extracellular material was isolated using either a "dirty" preparation or a "clean" preparation. For the dirty preparation, extracellular material was isolated using a previously described protocol (22). Briefly, cells were grown to OD_{600} = 0.6, pelleted and resuspended in 1/10 volume TNE (10 mM Tris-HCl pH 7.5, 100 mM NaCl, 5 mM EDTA) before shearing in a commercial blender (Waring Products, Inc., Torrington, CT) for 1 minute at low speed. Sheared cells were lysed by the addition of SDS (0.1% - 0.5% final concentration) with stirring for 5 minutes at room temperature. This lysate was centrifuged at 17,000 x g for 10 minutes then washed 5 times in Tris-HCl, pH 7.5.

For the clean matrix preparation, cells were again grown to OD_{600} = 0.6, resuspended in TNE, and sheared for 1 minute. At this point, samples were centrifuged (4,000 x g for 5 minutes) to pellet whole cells from sheared fraction. The sheared fraction

was then treated with 0.1 or 0.5% SDS, pelleted, and washed as described above. Protein concentration of the matrix material was determined using a bicinchonicic acid (BCA) protein assay (Thermo Scientific, Rockford, IL), and the total polysaccharide content was determined using the phenol sulfuric acid method, with glucose as a standard (95).

5.3.3 Detection of proteins

Sodium dodecyl sulfate-polyacrylamide gel electrophoresis (SDS-PAGE) using 15% Tris-HCl gels was used to analyze isolated proteins (64). Samples were boiled at 100ºC for 15 minutes in SDS loading buffer then electrophoresed until samples had just entered the resolving gel. Total protein was visualized as one thick band using the Colloidal Blue Staining Kit (Invitrogen Corp., Carlsbad, CA). To identify proteins in the extracellular matrix, bands were excised for in-gel trypsin digestion followed by liquid chromatography-mass spectrometry at the University of Minnesota Center for Mass Spectrometry and Proteomics. Protein localization was predicted by PSORTb v.3.0 (www.psort.org).

5.4 Results and Discussion

The quantity and color of extracellular material varied greatly between the two matrix isolation methods used in this study. A greater quantity of extracellular material was isolated using the dirty preparation compared to the clean preparation (Fig. 5.1). As the dirty preparation involved cell lysis before separation of matrix material, much of this volume may be due to contaminating intracellular proteins and cell debris. The pellet obtained from the clean isolation was less than 1/5 the size of the dirty pellet and was almost white in color, in contrast to the bright red (characteristic of cytochromes) of the

dirty preparation. In addition to decreased intracellular proteins in the clean preparation, reduced pellet size may be a result of incomplete separation of matrix from cells.

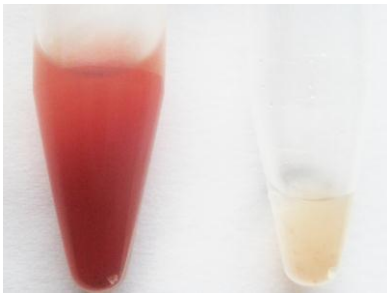

Fig. 5.1 Pelleted extracellular material from wild type, comparing dirty (left) and clean (right) preparations, both treated with 0.1% (wt/vol) SDS.

Mass spectrometry of isolated extracellular material identified many proteins predicted to be intracellular or with unknown localization, but very few extracellular proteins (Table 5.S1). Considering the number of proteins identified in each preparation (Table 5.1), the clean preparation (separation of cells and matrix material before SDS treatment) eliminated many intracellular proteins. Extracellular material was also treated with different concentrations of SDS. For both isolation methods, increasing SDS from 0.1% to 0.5% (wt/vol) decreased the total number of proteins identified by 40-50%.

Table 5.1 Number of proteins identified by LC-MS

Preparation Type	Total Proteins Identified[a]	Extracellular Proteins Identified[b]
Dirty, 0.1% SDS	106	3
Dirty, 0.5% SDS	63	2
Clean, 0.1% SDS	59	2
Clean, 0.5% SDS	30	1

[a]Minimum 95% protein identification probability, 3 peptides identified

[b] As designated by PSORTb v.3.0

Regardless of the method of extracellular matrix isolation, very few extracellular proteins were identified (Table 5.2). The highly abundant extracellular *c*-type cytochrome OmcZ was identified in all preparation types, while PgcA, a cytochrome thought to be periplasmic (132), was only identified in the dirty isolation treated with 0.1% (wt/vol) SDS (with a minimum of 3 peptides identified, 95% identification probability). For all the extracellular proteins identified, the number of identified peptides was very low, indicating very little protein present. In contrast, past studies have reported high concentrations of OmcZ in the extracellular matrix through western blot and immunogold-labelling (46, 117). The low abundance of peptides detected in this study may be a result of how the proteins were excised from the SDS-PAGE gels for digestion. Although successful in identification of *Myxococcus xanthus* matrix-associated proteins (27), isolating all protein in a single sample (one mixed-protein band rather than distinct bands) may not give representative information on what proteins are present in the *Geobacter* matrix. Many of the cytochromes predicted to be extracellular (Table 5.3) were not detected in isolated matrix material. In particular, the *c*-type cytochromes OmcS

and OmcE, easily visualized in heme stains of isolated matrix material (data not shown) were not detected through mass spectrometry.

Table 5.2 Extracellular[a] Proteins Identified

GSU Locus or Identity	Maximum # Peptides[b]
OmcZ	4
GSU2887, *c*-type cytochrome	4
PgcA, c-type cytochrome	3

[a] As designated by PSORTb v.3.0

[b] Minimum 95% protein identification probability

While PSORT (v. 3.0) predicts only 35 extracellular proteins (Table 5.3) in *G. sulfurreducens,* nearly 900 proteins are of unknown localization at this time. The extracellular proteins shown in Table 5.3 were computationally predicted, based on sequence features that correlate to specific localizations, such as motifs common to specific subcellular locations or signal peptides (147). Extracellular matrix proteins may have been identified through matrix isolations and mass spectrometry that are not currently listed as extracellular in this database. One notable protein with unknown localization according to PSORT is PilA, the protein subunit of type IV pili in *G. sulfurreducens*. While this protein was also not identified in any matrix preparation, pili are extracellular and likely a key component of the extracellular matrix. The insolubility of the pilin protein likely eliminated its isolation and detection in this study. Any extracellular proteins unable to enter the SDS-PAGE gel would, like the PilA protein, avoid detection.

Table 5.3 Predicted extracellular proteins[a]

GSU locus	Annotation
0019	pentapeptide repeat-containing protein
0045	Hypothetical
0310	Hypothetical
0417	flagellar hook assembly protein FlgD
0419	flagellar hook protein FlgE
0618	OmcE
0753	putative lipoprotein
1066	Hypothetical
1110	nucleoside diphosphate kinase
1251	BNR repeat-containing protein
1394	laccase family protein
1497	Hypothetical
1679	Hypothetical
1761	c-type cytochrome, PgcA
1770	Hypothetical
1865	putative DNA-binding/iron metalloprotein/AP endonuclease
1948	Hypothetical
2073	EF hand domain/PKD domain-containing protein
2076	OmcZ
2395	Hypothetical
2404	pentapeptide repeat-containing protein
2504	OmcS
2724	c-type cytochrome
2746	Hypothetical
2887	c-type cytochrome
2894	Hypothetical
2898	c-type cytochrome
2899	c-type cytochrome
3037	flagellar hook-associated protein 2
3042	flagellar hook-associated protein FlgL
3043	flagellar hook-associated protein FlgK
3051	flagellar basal body rod protein FlgG
3052	flagellar basal body rod protein FlgG
3174	hcp protein
3414	Hypothetical

[a] As predicted by PSORTb v.3.0

Overall, few extracellular proteins were successfully identified in this study for a number of possible reasons. First, there may truly be very few proteins associated with the extracellular matrix. Proteins previously reported to be extracellular, for instance OmcE and OmcS (71, 98), may only have a loose association with the extracellular material and are lost during isolation. As mentioned earlier, the technique of including all extracellular protein as a single sample for LC-MS may not be effective. High levels of intracellular proteins may block the detection of less abundant extracellular proteins, especially in the dirty preparation. With the clean preparation it is possible that not all matrix material was recovered, reducing the number of extracellular proteins detected. While the clean preparation appears to decrease the number of intracellular proteins, it does not increase the number of extracellular preparations. Shearing (without cell lysis) may not have been strong enough for complete separation of matrix from cells.

While mass spectrometry may not have successfully identified the complete set of proteins associated with the extracellular matrix of *G. sulfurreducens*, new targets were identified for study, including two cytochromes, PgcA and GSU2887. Deletion of these cytochromes and investigation of key matrix characteristics may reveal a potential role for these proteins in the extracellular network.

Table 5.S1 lists all proteins identified by LC-MS with a minimum of 95% protein identification probability and at least 3 peptides identified.

Table 5.S1 Proteins Identified by LC-MS

GSU locus	Protein identity
3304	LamB porin family protein
1629	glyceraldehyde 3-phosphate dehydrogenase 1
0974	phage tail sheath protein
1330	metal ion efflux outer membrane protein family protein
1331	RND family efflux transporter MFP subunit
3403	hypothetical protein
0714	hypothetical protein
0024	OmpA domain-containing protein
0785	nickel-dependent hydrogenase, large subunit
1468	2-oxoglutarate ferredoxin oxidoreductase subunit alpha
1332	CzcA family heavy metal efflux protein
0097	pyruvate ferredoxin/flavodoxin oxidoreductase
1177	succinate dehydrogenase flavoprotein subunit
1469	2-oxoglutarate ferredoxin oxidoreductase subunit beta
3401	branched-chain amino acid ABC transporter, periplasmic amino acid-binding protein
2636	alpha-amylase family protein
1470	keto/oxoacid ferredoxin oxidoreductase, gamma subunit
2739	hypothetical protein
2305	peptidoglycan-associated lipoprotein
1183	O-acetyl-L-homoserine sulfhydrylase
0810	OmpA domain-containing protein
0329	general secretion pathway protein D
0777	formate dehydrogenase, major subunit, selenocysteine-containing
0990	hypothetical protein
0332	Aminopeptidase
0344	NADH dehydrogenase I, G subunit
1932	hypothetical protein
0466	cytochrome c551 peroxidase
1466	Malate dehydrogenase
2196	Hydrolase
3132	DNA-binding protein HU
1835	glutamine synthetase, type I
1305	glutamate dehydrogenase
3423	transketolase
1124	phosphopantothenoylcysteine decarboxylase

2076	OmcZ
0510	Fe(III) reductase, beta subunit
3385	Phosphoenolpyruvate carboxykinase
1271	Aspartate carbamoyltransferase
0360	OmpA domain-containing protein
1660	bifunctional aconitate hydratase 2/2-methylisocitrate dehydratase
2675	hypothetical protein
1463	Aspartyl-tRNA synthetase
2863	DNA-directed RNA polymerase subunit beta
0988	hypothetical protein
0580	pyruvate phosphate dikinase
1593	Polyribonucleotide nucleotidyltransferase
1858	Cytochrome C Peroxidase
0987	hypothetical protein
2428	pyruvate carboxylase
0782	nickel-dependent hydrogenase, small subunit
2265	hydroxymyristoyl ACP dehydrase
2982	TonB dependent receptor
0496	RND family efflux transporter MFP subunit
1465	isocitrate dehydrogenase, NADP-dependent
2939	outer membrane porin FmdC
1161	RND family efflux transporter MFP subunit
1739	indolepyruvate ferredoxin oxidoreductase, alpha subunit
1106	type I citrate synthase
0357	cytochrome c family protein
1609	outer membrane efflux protein
3102	Enoylpyruvate transferase
3289	hypothetical protein
0973	hypothetical protein
1089	iron-sulfur cluster-binding protein
2940	lipoprotein, putative
1633	hypothetical protein
2887	cytochrome c family protein
0343	NADH dehydrogenase I, F subunit
2527	nitrite/sulfite reductase domain-containing protein
3300	biotin-requiring enzyme subunit
0989	NHL repeat-containing protein
3406	amino acid ABC transporter, periplasmic amino acid-binding protein
3277	lysM domain-containing protein
2726	hypothetical protein
3299	carboxyl transferase domain-containing protein
2859	Elongation factor Tu
0579	Glycyl-tRNA synthetase beta subunit

2055	extracellular solute-binding protein
0716	hypothetical protein
2446	2-oxoglutarate dehydrogenase
1899	Mce family protein
2618	preprotein translocase, YajC
0976	hypothetical protein
2316	mechanosensitive ion channel family protein
0509	Fe(III) reductase, alpha subunit
2286	Enolase
1761	PgcA, cytochrome c family protein
3246	thioredoxin peroxidase
3308	Adenylosuccinate synthetase
0814	outer membrane efflux protein
1272	Dihydroorotase
2271	lysyl-tRNA synthetase
2603	30S ribosomal protein S1
1912	Dihydroxy-acid dehydratase
3450	glutamate synthase-related protein
0910	aldehyde:ferredoxin oxidoreductase
3302	methylmalonyl-CoA mutase
2814	Rubrerythrin
0349	NADH dehydrogenase I, L subunit
0994	fumarate hydratase, class I
0921	ribonuclease, Rne/Rng family protein
2195	inosine-5'-monophosphate dehydrogenase
1460	Prolyl-tRNA synthetase
1482	outer membrane efflux protein
1936	nicotinate-nucleotide pyrophosphorylase
1520	Phenylalanyl-tRNA synthetase beta chain
1700	malic enzyme
2050	Protein translocase subunit secA
1718	elongation factor Tu GTP binding domain protein
3462	putative lipoprotein
2360	maltooligosyltrehalose synthase
2100	Catalase-peroxidase
1178	succinate dehydrogenase/fumarate reductase iron-sulfur subunit
2425	O-acetyl-L-homoserine sulfhydrylase
2876	50S ribosomal protein L13
2433	ATP-dependent protease
0270	Glucosamine--fructose-6-phosphate aminotransferase
1632	adenylosuccinate lyase
1282	hypothetical protein GSU1282
2731	polyheme membrane-associated cytochrome c

0004	DNA gyrase, A subunit
3136	Isoleucyl-tRNA synthetase
2028	type IV pilus biogenesis protein PilQ
0274	cytochrome c family protein
2038	hypothetical protein GSU2038
2737	polyheme membrane-associated cytochrome c

Chapter 6: Thesis conclusions and future work

6.1 Conclusions

The research described in this thesis explored components of a conductive *Geobacter* biofilm, highlighting the importance of extracellular polysaccharides in this functional network. Screening transposon mutants for surface attachment phenotypes resulted in the identification of a mutant (Δ*xapD::kan/* Δ1501) that was deficient in Fe(III) oxyhydroxide reduction, but showed high levels of attachment to negatively charged surfaces. As described in Chapter 2, the crystal violet attachment assays used in screening tested attachment to negatively charged surfaces. High attachment mutants identified in this screen showed poor attachment to positively charged electrodes and Fe(III) oxyhydroxide. In contrast, mutants that attached poorly in the crystal violet assays are predicted to show increased electrode attachment and possibly increased reduction of insoluble acceptors.

The presence of extracellular polysaccharides influences a cell's ability to attach to a surface, with the likely absence of negatively charged polysaccharides producing the attachment changes in the Δ*xapD::kan* mutant in comparison to wild type *G. sulfurreducens*. The extracellular matrix surrounding most bacterial cells is thought to be a hydrated network of secreted polysaccharides, proteins, nucleic acids, and lipids (35).When the matrix is dehydrated (as during SEM sample preparation), the polymeric network collapses, resulting in the appearance of filaments surrounding cells (33). In chapter 3, the absence of filaments surrounding cells in SEM images of the Δ*xapD::kan* (Δ1501) mutant suggested a diminished extracellular matrix. A cluster of genes

responsible for polysaccharide export was disrupted in this mutant resulting in a matrix with decreased levels of extracellular polysaccharides compared to wild type *G. sulfurreducens.* Investigation of a series of pili and cytochrome mutants, detailed in Chapter 4, demonstrated that extracellular polysaccharide content correlated with attachment. Fewer extracellular polysaccharides in a mutant's matrix resulted in increased attachment to negative surfaces.

AQDS reduction indicated that electron transfer to the outer surface of Δ*xapD::kan* mutant cells was not disrupted, however the mutant was unable to reduce an electrode (poised at a positive, electron accepting potential) or Fe(III) oxyhydroxide. An altered outer surface eliminated attachment to these positively charged surfaces in this mutant, thereby disrupting direct electron transfer. Along with the reduction of polysaccharides in the extracellular matrix of the Δ*xapD::kan* mutant, the concentration of extracellular *c*-type cytochromes was greatly reduced (Fig. 6.1). A gene cluster involved in polysaccharide export was interrupted in this mutant, but nothing clearly relating to cytochromes expression or biosynthesis was disrupted. Interruption of polysaccharide export nearly eliminated extracellular cytochromes, suggesting that a network of polysaccharides is needed to retain these important electron transfer proteins in the matrix. For this role, the disrupted polysaccharide export cluster was designated the *xap* (extracellular anchoring polysaccharides) gene cluster. The trend of decreased extracellular cytochrome content with decreased extracellular polysaccharide content was observed in additional matrix mutants, described in Chapter 4.

Disruption of extracellular appendages (type IV pili) and specific extracellular cytochromes also resulted in fewer extracellular polysaccharides and altered cytochrome content. Extracellular polysaccharide content was severely reduced in a Δ*pilA::kan* mutant in which the structural pilin subunit had been disrupted. Unlike the Δ*xapD::kan* mutant, polysaccharides in general seemed to be depleted rather than a specific subset of polysaccharides absent. Less overall extracellular material (proteins and polysaccharides) was recovered from this mutant, possibly indicating that pili may function in maintaining a compact matrix (Fig. 6.1). Interactions between type IV pili and polysaccharides could indicate a polysaccharide tethering role for pili, securing extracellular components distant from the cell surface. The restoration of key phenotypes (attachment, agglutination) through supplementation with extracellular polysaccharides alone (protein-free matrix material) suggests that polysaccharides play a key role in matrix integrity and mediate cell-surface and cell-cell interactions. In contrast, pili are not a requirement for 96-well plate attachment or cell to cell-cell agglutination.

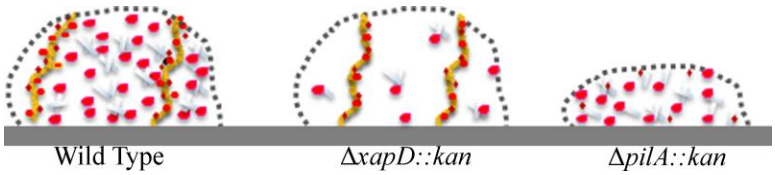

Fig. 6.1 Diagram comparing extracellular matrix material in wild type and mutants, showing an abundance of *c*-type cytochromes (red), pili (yellow), and polysaccharides (gray) that surround wild type *G. sulfurreducens* cells. Decreased polysaccharide and cytochrome content is depicted in the

Δ*xapD::kan* mutant extracellular material, while in addition to the absence of pili in the Δ*pilA::kan* mutant, there is also a general decrease in the quantity of extracellular material.

While cytochrome content decreased in the type IV pili mutant alongside the reduction of extracellular polysaccharides, the most severe reduction of extracellular *c*-type cytochromes was seen in the Δ*omcZ::kan* mutant. When this cytochrome was absent, extracellular polysaccharide content decreased to levels near that of the Δ*xapD::kan* mutant, the most drastic change however was the decrease in extracellular cytochromes. In addition to the absence of OmcZ, other *c*-type cytochromes (including OmcS and OmcE) appeared to be nearly absent in the matrix of this mutant. The presence of this important cytochrome may help to network together polysaccharides in the matrix, thereby retaining other cytochromes.

While the pathway of electron transfer from internal oxidative reactions to an extracellular acceptor in *G. sulfurreducens* is still unclear, the extracellular matrix plays an important role. The extracellular matrix bridges the gap between cell and external electron acceptor, facilitating both electron transfer and attachment (Fig. 6.2). Investigation of the Δ*xapD::kan* mutant as well as type IV pili and *c*-type cytochrome mutants revealed the complexity of the *Geobacter* extracellular matrix. The matrix is an intricate network of polysaccharides, type IV pili and cytochromes. Absence of any one of these components can disrupt the entire network. Deficiency in type IV pili results in less total matrix rather than less of a particular component, suggesting that pili may knit

together matrix components distant from the cell surface. Polysaccharides seem to play a specific role in the matrix with a lack of polysaccharides drastically reducing the levels of *c*-type cytochromes retained in the matrix as well as altering the characteristic outer surface charge and therefore changing a cell's surface attachment ability.

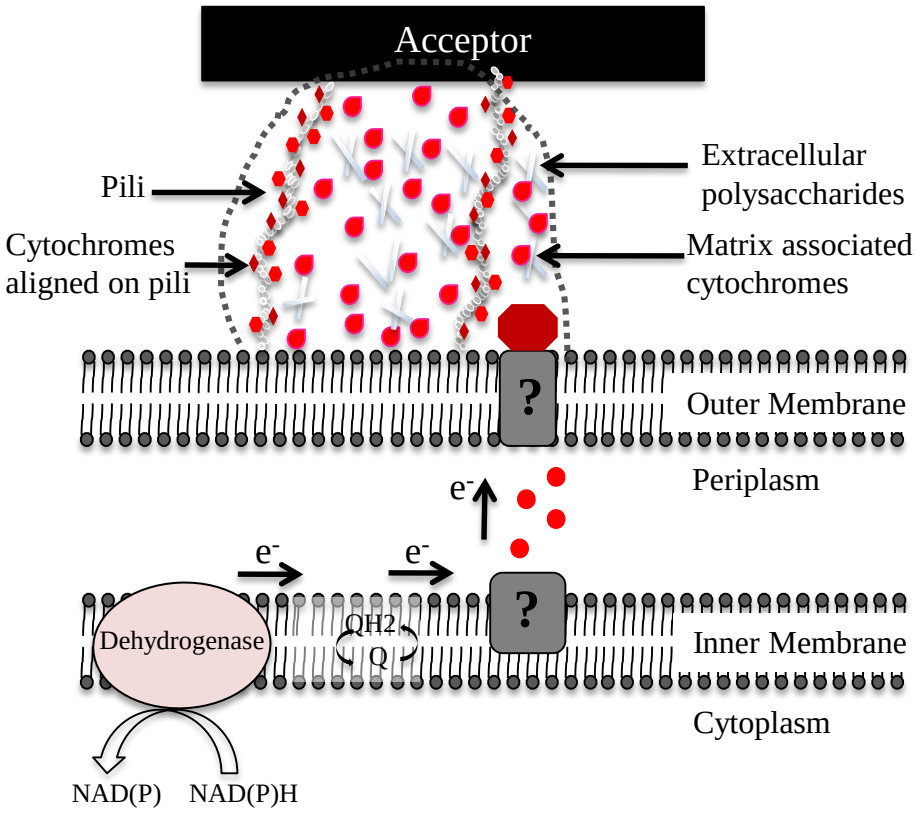

Fig. 6.2 Potential pathway for electrons out of *G. sulfurreducens* cells to an external electron acceptor. Electrons from the quinone pool are passed across the inner membrane, periplasm, and outer membrane via a series of redox-active proteins (putative cytochromes, shown in red). The extracellular matrix (which facilitates attachment to an external electron

acceptor) is a network of polysaccharides, pili, and associated-cytochromes that enable attachment and electron transport from outer membrane to terminal electron acceptor.

6.2 Future Work

6.2.1 Identification of extracellular polysaccharides

To identify the extracellular polysaccharides in the *Geobacter* matrix, samples will be sent to the University of Georgia Complex Carbohydrate Research Center. Here polysaccharides will be separated by size exclusion chromatography to determine size and number of polysaccharides present. This could be be followed by isolation of individual polysaccharides and glycosyl composition analysis to identify the polysaccharide subunits present in each.

Extracellular matrix should be sheared from cells (wild type *G. sulfurreducens* and Δ*xapD::kan* mutant) without lysis to limit contamination of any non-matrix polysaccharides, as described in Chapter 5. A comparison of wild type and Δ*xapD::kan* mutant polysaccharides will identify the polysaccharides absent from the mutant which are critical for surface attachment and retention of *c*-type cytochromes. Analysis of polysaccharides isolated from the Δ*pilA::kan* mutant and comparison to wild type would indicate if specific polysaccharides were absent or if the observed reduction in extracellular polysaccharides was indeed a result of less matrix overall as described in Chapter 4.

6.2.2 Identification of extracellular proteins

Depending on the method of isolation, the extracellular matrix of *G. sulfurreducens* has a protein: polysaccharide ratio approaching 1:1. Preliminary proteomics data indicated that the extracellular matrix preparations contained high concentrations of intracellular proteins. In order to identify the protein components of the extracellular matrix, a new isolation method is needed. This method should aim to limit contamination by intracellular proteins, while enriching for extracellular proteins. For example, mild sonication has been shown to successfully separate matrix material with minimal cell lysis (17, 121). The identification of the proteins in the extracellular matrix will provide new targets of study and the identification of components necessary for maintaining the structure and function of the *Geobacter* extracellular matrix.

REFERENCES

1. **Afkar, E., G. Reguera, M. Schiffer, and D. R. Lovley.** 2005. A novel *Geobacteraceae*-specific outer membrane protein J (OmpJ) is essential for electron transport to Fe(III) and Mn(IV) oxides in *Geobacter sulfurreducens*. BMC Microbiol. **5:**41.

2. **Appenzeller, B. M. R., Y. B. Duval, F. Thomas, and J. Block.** 2002. Influence of phosphate on bacterial adhesion onto iron oxyhydroxide in drinking water. Environ. Sci. Technol. **36:**646-652.

3. **Araujo, J. C., F. C. Teran, R. A. Oliveira, E. A. A. Nour, M. A. P. Montenegro, J. R. Campos, and R. E. Vazoller.** 2003. Comparison of hexamethyldisilazane and critical point drying treatments for SEM analysis of anaerobic biofilms and granular sludge. J. Electron. Microsc. **52:**429-433.

4. **Arnold, J. W., and L. J. Shimkets.** 1988. Cell surface properties correlated with cohesion in *Myxococcus xanthus*. J. Bacteriol. **170:**5771-5777.

5. **Arnold, J. W., and L. J. Shimkets.** 1988. Inhibition of cell-cell interactions in *Myxococcus xanthus* by Congo red. J. Bacteriol. **170:**5765-5770.

6. **Bardy, S. L., S. Y. M. Ng, and K. F. Jarrell.** 2003. Prokaryotic motility structures. Microbiology. **149:**295-304.

7. **Baron, D., E. LaBelle, D. Coursolle, J. A. Gralnick, and D. R. Bond.** 2009. Electrochemical measurements of electron transfer kinetics by *Shewanella oneidensis* MR-1. J. Biol. Chem. **284:**28865-28873.

8. **Behmlander, R. M., and M. Dworkin.** 1994. Biochemical and structural analyses of the extracellular matrix fibrils of *Myxococcus xanthus*. J. Bacteriol. **176:**6295-6303.

9. **Bendaoud, M., E. Vinogradov, N. V. Balashova, D. E. Kadouri, S. C. Kachlany, and J. B. Kaplan.** 2011. Broad-spectrum biofilm inhibition by *Kingsella kingae* exopolysaccharide. J. Bacteriol. **193:**3879-3886.

10. **Black, W. P., Q. Xu, and Z. Yang.** 2006. Type IV pili function upstream of the Dif chemotaxis pathway in *Myxococcus xanthus* EPS regulation. Mol. Microbiol. **61:**447-456.

11. **Black, W. P., and Z. Yang.** 2004. *Myxococcus xanthus* chemotaxis homologs DifD and DifG negatively regulate fibril polysaccharide production. J. Bacteriol. **186:**1001-1008.

12. **Bond, D. R., D. E. Holmes, L. M. Tender, and D. R. Lovley.** 2002. Electrode-reducing microorganisms that harvest energy from marine sediments. Science. **295:**483-485.

13. **Bond, D. R., and D. R. Lovley.** 2003. Electricity production by *Geobacter sulfurreducens* attached to electrodes. Appl. Environ. Microbiol. **69:**1548-1555.

14. **Bond, D. R., and D. R. Lovley.** 2005. Evidence for involvement of an electron shuttle in electricity generation by *Geothrix fermentans*. Appl. Environ. Microbiol. **71:**2186-2189.

15. **Bouhenni, R., A. Gehrke, and D. Saffarini.** 2005. Identification of genes involved in cytochrome *c* biogenesis in *Shewanella oneidensis*, using a modified *mariner t*ransposon. Appl. Environ. Microbiol. **71:**4935-4937.

16. **Bradford, M. M.** 1976. A rapid and sensitive method for the quantification of microgram quantities of protein utilizing the principle of protein-dye binding. Anal. Biochem. **72:**248-254.

17. **Branda, S. S., F. Chu, D. B. Kearns, R. Losick, and R. Kolter.** 2006. A major protein component of the *Bacillus subtilis* biofilm matrix. Mol. Microbiol. **59:**1229-1238.

18. **Butler, J. E., F. Kaufmann, M. V. Coppi, C. Nunez, and D. R. Lovley.** 2004. MacA, a diheme *c-t*ype cytochrome involved in Fe(III) reduction by *Geobacter sulfurreducens* . J. Bacteriol. **186:**4042-4045.

19. **Butler, J. E., N. D. Young, and D. R. Lovley.** 2010. Evolution of electron transfer out of the cell: comparative genomics of six *Geobacter* genomes. BMC Genomics. **11:**.

20. **Caccavo, F. J., D. J. Lonergan, D. R. Lovley, M. Davis, J. F. Stolz, and M. J. McInerney.** 1994. *Geobacter sulfurreducens* sp. nov., a hydrogen- and acetate- oxidizing dissimilatory metal-reducing microorganism. Appl. Environ. Microbiol. **60:**3752-3759.

21. **Cervantes, F. J., T. D. Dac, A. E. Ivanova, K. Roest, A. D. L. Akkermans, G. Lettinga, and J. A. Field.** 2003. Selective enrichment of *Geobacter sulfurreducens* from anaerobic granular sludge with quinones as terminal electron acceptors. Biotechnol. Lett. **25:**39-45.

22. **Chang, B., and M. Dworkin.** 1994. Isolated fibrils rescue cohesion and development in the Dsp mutant of *Myxococcus xanthus*. J. Bacteriol. **176:**7190-7196.

23. **Chen, X., and P. S. Stewart.** 2002. Role of electrostatic interactions in cohesion of bacterial biofilms. Appl. Microbiol. Biotechnol. **59:**718-720.

24. **Coppi, M. V., R. A. O'Neil, C. Leang, F. Kaufmann, B. A. Methe´, K. P. Nevin, T. L. Woodard, A. Liu, and D. R. Lovley.** 2007. Involvement of *Geobacter sulfurreducens* SfrAB in acetate metabolism rather than intracellular, respiration-linked Fe(III) citrate reduction. Microbiology. **153:**3572-3585.

25. **Coppi, M. V., C. Leang, S. J. Sandler, and D. R. Lovley.** 2001. Development of a genetic system for *Geobacter sulfurreducens*. Appl. Environ. Microbiol. **67:**3180-3187.

26. **Coppi, M. V., R. A. O'Neil, and D. R. Lovley.** 2004. Identification of an uptake hydrogenase required for hydrogen-dependent reduction of Fe(III) and other electron acceptors by *Geobacter sulfurreducens*. J. Bacteriol. **186:**3022-3028.

27. **Curtis, P. D., J. I. Atwood, R. Orlando, and L. J. Shimkets.** 2007. Proteins associated with the *Myxococcus xanthus* extracellular matrix. J. Bacteriol. **189:**7634-7642.

28. **Cuthbertson, L., V. Kos, and C. Whitfield.** 2010. ABC transporters involved in export of cell surface glycoconjugates. Microbiol. Mol. Bio. Rev. **74:**341-362.

29. **Dan, N.** 2003. The effect of charge regulation on cell adhesion to substrates: salt-induced repulsion. Colloids Surf. B. **27:**41-47.

30. **Danese, P. N., L. A. Pratt, and R. Kolter.** 2000. Exopolysaccharide production is required for development of *Escherichia coli* K-12 biofilm architecture. J. Bacteriol. **182:**3593-3596.

31. **Ding, Y. R., K. K. Hixson, M. A. Aklujkar, M. S. Lipton, R. D. Smith, D. R. Lovley, and T. Mester.** 2008. Proteome of *Geobacter sulfurreducens* grown with Fe(III) oxide or Fe(III) citrate as the electron acceptor. Biochim. Biophys. Acta. **1784:**1935-1941.

32. **Ding, Y. R., K. K. Hixson, C. S. Giometti, A. Stanley, A. Esteve-Nunez, T. Khare, S. L. Tollaksen, W. Zhu, J. N. Adkins, M. S. Lipton, R. D. Smith, T. Mester, and D. R. Lovley.** 2006. The proteome of the dissimilatory metal-reducing microorganism *Geobacter sulfurreducens* under various growth conditions. Biochim Biophys Acta. **1767:**1198-1206.

33. **Dohnalkova, A. C., M. J. Marshall, B. W. Arey, K. H. Williams, E. C. Buck, and J. K. Fredrickson.** 2011. Imaging hydrated microbial extracellular polymers: comparative analysis by electron microscopy. Appl. Environ. Microbiol. **77:**1254-1262.

34. **Erlandsen, S. L., C. J. Kristich, G. M. Dunny, and C. L. Wells.** 2004. High-resolution visualization of the microbial glycocalyx with low-voltage scanning electron microscopy: dependence on cationic dyes. J. Histochem. Cytochem. **52:**1427-1435.

35. **Flemming, H., and J. Wingender.** 2010. The biofilm matrix. Nat. Rev. Microbiol. **8**: 623-633.

36. **Franke, S., G. Grass, C. Rensing, and D. H. Nies.** 2003. Molecular analysis of the copper-transporting efflux system CusCFBA of *Escherichia coli*. J. Bacteriol. **185:**3804-3812.

37. **Franks, A. E., K. P. Nevin, R. H. Glaven, and D. R. Lovley.** 2010. Microtoming coupled to microarray analysis to evaluate the spatial metabolic status of *Geobacter sulfurreducens* biofilms. ISME J. **4:**509-519.

38. **Franks, A. E., K. P. Nevin, H. Jia, M. Izallalen, T. L. Woodard, and D. R. Lovley.** 2009. Novel strategy for three-dimensional real-time imaging of microbial fuel cell communities: monitoring the inhibitory effects of proton accumulation within the anode biofilm. Energy Environ. Sci. **2:**113-119.

39. **Fricke, K., F. Harnisch, and U. Schroder.** 2008. On the use of cyclic voltammetry for the study of anodic electron transfer in microbial fuel cells. Energy Environ. Sci. **1:**144-147.

40. **Gaspard, S., F. Vazquez, and C. Holliger.** 1998. Localization and solubilization of the iron(III) reductase of *Geobacter sulfurreducens*. Appl. Environ. Microbiol. **64:**3188-3194.

41. **Ghafoor, A., I. D. Hay, and B. H. A. Rehm.** 2011. Role of exopolysaccharides in *Pseudomonas aeruginosa* biofilm formation and architecture. Appl. Environ. Microbiol. **77:**5238-5246.

42. **Hoffmann, M., J. Seidel, and O. Einsle.** 2009. CcpA from *Geobacter sulfurreducens* is a basic di-heme cytochrome *c* peroxidase. J. Mol. Biol. **393:**951-965.

43. **Holmes, D. E., S. K. Chaudhuri, K. P. Nevin, T. Mehta, B. A. Methe, A. Liu, J. E. Ward, T. L. Woodard, J. Webster, and D. R. Lovley.** 2006. Microarray and genetic analysis of electron transfer to electrodes in *Geobacter sulfurreducens*. Environ. Microbiol. **8:**1805-1815.

44. **Holmes, D. E., K. T. Finneran, R. A. O'Neil, and D. R. Lovley.** 2002. Enrichment of members of the family *Geobacteraceae* associated with stimulation of dissimilatory metal reduction in uranium-contaminated aquifer sediments. Appl. Environ. Microbiol. **68:**2300-2306.

45. **Huang, T., E. B. Somers, and A. C. L. Wong.** 2006. Differential biofilm formation and motility associated with lipopolysaccharide/exopolysaccharide-coupled biosynthetic genes in *Stenotrophomonas maltophilia*. J. Bacteriol. **188:**3116-3120.

46. **Inoue, K., C. Leang, A. E. Franks, T. L. Woodard, K. P. Nevin, and D. R. Lovley.** 2010. Specific localization of the *c*-type cytochrome OmcZ at the anode surface in current-producing biofilms of *Geobacter sulfurreducens*. Environ. Microbiol. Rep. doi: 10.1111/j.1758-2229.2010.00210.x.

47. **Inoue, K., X. Qian, L. Morgado, B. Kim, T. Mester, M. Izallalen, C. A. Salgueiro, and D. R. Lovley.** 2010. Purification and characterization of OmcZ, an outer-surface, octaheme *c*-type cytochrome essential for optimal current production *by Geobacter sulfurreducens*. Appl. Environ. Microbiol. **76:**3999-4007.

48. **Johnson, J. M., and G. M. Church.** 1999. Alignment and structure prediction of divergent protein families: periplasmic and outer membrane proteins of bacterial efflux pumps. J. Mol. Biol. **287:**695-715.

49. **Kawai, Y., F. Wada, Y. Sugimura, M. Maki, and K. Hitomi.** 2008. Transglutaminase 2 activity promotes membrane resealing after mechanical damage in the lung cancer cell line A549. Cell Biol. Int. **32:**928-934.

50. **Keiski, C., M. Harwich, S. Jain, A. M. Neculai, P. Yip, H. Robinson, J. C. Whitney, L. Riley, L. L. Burrows, D. E. Ohman, and P. L. Howell.** 2010. AlgK is a TPR-containing protein and the periplasmic component of a novel exopolysaccharide secretin. Structure. **18:**265-273.

51. **Khare, T., A. Esteve-Nunez, K. P. Nevin, W. Zhu, J. R. I. Yates, D. R. Lovley, and C. S. Giometti.** 2006. Differential protein expression in the metal-reducing bacterium *Geobacter sulfurreducens* strain PCA grown with fumarate of ferric citrate. Proteomics. **6:**632-640.

52. **Kim, B. C., and D. R. Lovley.** 2008. Investigation of direct vs. indirect involvement of the *c* -type cytochrome MacA in Fe(III) reduction by *Geobacter sulfurreducens*. FEMS Microbiol. Lett. **286:**39-44.

53. **Kim, B. C., X. Qian, C. Leang, M. V. Coppi, and D. R. Lovley.** 2006. Two putative *c*-type multiheme cytochromes required for the expression of OmcB, an outer membrane protein essential for optimal Fe(III) reduction in *Geobacter sulfurreducens*. J. Bacteriol. **188:**3138-3142.

54. **Kim, B., C. Leang, Y. R. Ding, R. H. Glaven, M. V. Coppi, and D. R. Lovley.** 2005. OmcF, a putative *c*-type monoheme outer membrane cytochrome required for the expression of other outer membrane cytochromes in *Geobacter sulfurreducens*. J. Bacteriol. **187:**4505-4513.

55. **Kim, B., B. L. Postier, R. J. DiDonato, S. K. Chaudhuri, K. P. Nevin, and D. R. Lovley.** 2008. Insights into genes involved in electricity generation in *Geobacter*

sulfurreducens via whole genome microarray analysis of the OmcF-deficient mutant. Bioelectrochemistry. **73:**70-75.

56. **Klimes, A., A. E. Franks, R. H. Glaven, H. Tran, C. L. Barrett, Y. Qiu, K. Zengler, and D. R. Lovley.** 2010. Production of pilus-like filaments in *Geobacter sulfurreducens* in the absence of the type IV pilin protein PilA. FEMS Microbiol. Lett. 1-7.

57. **Korenevsky, A., and T. J. Beveridge.** 2007. The surface physicochemistry and adhesiveness of *Shewanella* are affected by their surface polysaccharides. Microbiology. **153:**1872-1883.

58. **Kouzuma, A., X. Meng, N. Kimura, K. Hashimoto, and K. Watanabe.** 2010. Disruption of the putative cell surface polysaccharide biosynthesis gene SO3177 in *Shewanella oneidensis* MR-1 enhances adhesion to electrodes and current generation in microbial fuel cells. Appl. Environ. Microbiol. **76:**4151-4157.

59. **Kovach, M. E., P. H. Elzer, D. S. Hill, G. T. Robertson, M. A. Farris, R. M. I. Roop, and K. M. Peterson.** 1995. Four new derivatives of the broad-host-range cloning vector pBBR1MCS, carrying different antibiotic-resistance cassettes. Gene. **166:**175-176.

60. **Kovach, M. E., R. W. Phillips, P. H. Elzer, R. M. I. Roop, and K. M. Peterson.** 1994. pBBR1MCS: a broad-host-range cloning vector. BioTechniques. **16:**800-802.

61. **Kristich, C. J., V. T. Nguyen, T. Le, A. M. T. Barnes, S. Grindle, and G. M. Dunny.** 2008. Development and use of an efficient system for random *mariner* transposon mutagenesis to identify novel genetic determinants of biofilm formation in the core *Enterococcus faecalis* genome. Appl. Environ. Microbiol. **74:**3377-3386.

62. **Krushkal, J., K. Juarez, J. F. Barbe, Y. Qu, A. Andrade, M. Puljic, R. M. Adkins, D. R. Lovley, and T. Ueki.** 2010. Genome-wide survey for PilR recognition sites of the metal-reducing prokaryote *Geobacter sulfurreducens*. Gene. doi: 10.1016/j.gene.2010.08.005.

63. **Kus, J. V., J. Kelly, L. Tessier, H. Harvey, D. G. Cvitkovitch, and L. L. Burrows.** 2008. Modification of *Pseudomonas aeruginosa* Pa5196 type IV pilins at multiple sites with D-Araf by a novel GT-C family arabinosyltransferase, TfpW. J. Bacteriol. **190:**7464-7478.

64. **Laemmli, U. K.** 1970. Cleavage of structural proteins during the assembly of the head of the bacteriophage T4. Nature. **227:**680-685.

65. **Lampe, D. J., M. E. Churchill, and H. M. Robertson.** 1996. A purified *mariner* transposase is sufficient to mediate transposition *in vitro*. EMBO. **15:**5470-5479.

66. **Lampe, D. J., T. E. Grant, and H. M. Robertson.** 1998. Factors affecting transposition of the *Himar1 mariner* transposon *in vitro*. Genetics. **149:**179-187.

67. **Lancero, H., N. B. Caberoy, S. Castaneda, Y. Li, A. Lu, D. Dutton, X. Duan, H. B. Kaplan, W. Shi, and A. G. Garza.** 2004. Characterization of a *Myxococcus xanthus* mutant that is defective for adventurous motility and social motility. Microbiology. **150:**4085-4093.

68. **Le Breton, Y., N. P. Mohapatra, and W. G. Haldenwang.** 2006. In vivo random mutagenesis of *Bacillus subtilis* by use of TnYLB-1, a *mariner*-based transposon. Appl. Environ. Microbiol. **72:**327-333.

69. **Leang, C., L. A. Adams, K. J. Chin, K. P. Nevin, B. A. Methe, J. Webster, M. L. Sharma, and D. R. Lovley.** 2005. Adaptation to disruption of the electron transfer pathway for Fe(III) reduction in *Geobacter sulfurreducens*. J. Bacteriol. **187:**5918-5926.

70. **Leang, C., M. V. Coppi, and D. R. Lovley.** 2003. OmcB, a *c*-type polyheme cytochrome, involved in Fe(III) reduction in *Geobacter sulfurreducens*. J. Bacteriol. **185:**2096-2103.

71. **Leang, C., X. Qian, T. Mester, and D. R. Lovley.** 2010. Alignment of the *c*-type cytochrome OmcS along pili of *Geobacter sulfurreducens*. Appl. Environ. Microbiol. **76:**4080-4084.

72. **Li, Y., H. Sun, X. Ma, A. Lu, R. Lux, D. Zusman, and W. Shi.** 2003. Extracellular polysaccharides mediate pilus retraction during social motility of *Myxococcus xanthus*. Proc. Natl. Acad. Sci. **100:**5443-5448.

73. **Lin, W. C., M. V. Coppi, and D. R. Lovley.** 2004. *Geobacter sulfurreducens* can grow with oxygen as a terminal electron acceptor. Appl. Environ. Microbiol. **70:**2525-2528.

74. **Lloyd, J. R.** 2003. Microbial reduction of metals and radionuclides. FEMS Microbiol. Rev. **27:**411-425.

75. **Lloyd, J. R., C. Leang, A. L. Hodges Myerson, M. V. Coppi, S. Cuifo, B. Methe, S. J. Sandler, and D. R. Lovley.** 2003. Biochemical and genetic characterization of PpcA, a periplasmic *c*-type cytochrome in *Geobacter sulfurreducens*. Biochem. J. **369:**153-161.

76. **Logan, B. E.** 2005. Simultaneous wastewater treatment and biological electricity generation. Water Sci. Technol. **52:**31-37.

77. **Logan, B. E., and J. M. Regan.** 2006. Microbial fuel cells-challenges and applications. Environ. Sci. Technol. **40:**5172-5180.

78. **Lovley, D. R., J. D. Coates, E. L. Blunt-Harris, E. J. P. Phillips, and J. C. Woodward.** 1996. Humic substances as electron acceptors for microbial respiration. Nature. **382:**445-448.

79. **Lovley, D. R., S. J. Giovannoni, D. C. White, J. E. Champine, J. P. Phillips, Y. A. Gorby, and S. Goodwin.** 1993.
Geobacter metallireducens gen. nov. sp. nov., a microorganism capable of coupling the complete oxidation of organic compounds to the reduction of iron and other metals. Arch. Microbiol. **159:**336-344.

80. **Lovley, D. R., E. J. P. Phillips, Y. A. Gorby, and E. R. Landa.** 1991. Microbial reduction of uranium. Nature. **350:**413-416.

81. **Lovley, D. R.** 2006. Bug juice: harvesting electricity with microorganisms. Nat. Rev. Microbiol. **4:**497-508.

82. **Lovley, D. R.** 2006. Microbial fuel cells: novel microbial physiologies and engineering approaches. Curr. Opin. Biotechnol. **17:**327-332.

83. **Lovley, D. R., and D. J. Lonergan.** 1990. Anaerobic oxidation of toluene, phenol, and p-cresol by the disssimilatory iron-reducing organism, GS-15. Appl. Environ. Microbiol. **56:**1858-1856.

84. **Lovley, D. R., and E. J. P. Phillips.** 1986. Organic matter mineralization with reduction of ferric iron in anaerobic sediments. Appl. Environ. Microbiol. **51:**683-689.

85. **Lovley, D. R., and E. J. P. Phillips.** 1987. Rapid assay for microbially reducible ferric iron in aquatic sediments. Appl. Environ. Microbiol. **53:**1536-1540.

86. **Lovley, D., R.** 1991. Dissimilatory Fe(III) and Mn(IV) reduction. Microbiol. Rev. **55:**259-287.

87. **Lower, B. H., R. Yongsunthon, L. Shi, L. Wildling, H. J. Gruber, N. S. Wigginton, C. L. Reardon, G. E. Pinchuk, T. C. Droubay, J. Boily, and S. K. Lower.** 2009. Antibody recognition force microscopy shows that outer membrane cytochromes OmcA and MtrC are expressed on the exterior surface of *Shewanella oneidensis* MR-1. Appl. Environ. Microbiol. **75:**2931-2935.

88. **Lowry, O. H., N. J. Rosebrough, A. L. Farr, and R. J. Randall.** 1951. Protein measurement with the Folin phenol reagent. J. Biol. Chem. **193:**265-275.

89. **Malvankar, N. S., M. Vargas, K. P. Nevin, A. E. Franks, C. Leang, B. C. Kim, K. Inoue, T. Mester, S. F. Covalla, J. P. Johnson, V. M. Rotello, M. T. Tuominen, and D. R. Lovley.** 2011. Tunable metallic-like conductivity in microbial nanowire networks. Nature Nanotech. doi: 10.1038/NNANO.2011.119.

90. **Marshall, K. C., and M. R. Stout.** 1971. Mechanisms of the initial events in the absorption of marine bacteria to surfaces. J. Gen. Microbiol. **68:**337-348.

91. **Marshall, M. J., A. S. Beliaev, A. C. Dohnalkova, D. W. Kennedy, L. Shi, Z. Wang, M. I. Boyanov, B. Lai, K. M. Kemner, J. S. McLean, S. B. Reed, D. E. Culley, V. L. Bailey, C. J. Simonson, D. A. Saffarini, M. F. Romine, J. M. Zachara, and J. K. Fredrickson.** 2006. *c*-type cytochrome-dependent formation of U(IV) nanoparticles by *Shewanella oneidensis*. PLoS Biol. **4:**e268. doi: 10.1371/journal.pbio.0040268.

92. **Marsili, E., D. B. Baron, I. D. Shikhare, D. Coursolle, J. A. Gralnick, and D. R. Bond.** 2008. *Shewanella* secretes flavins that mediate extracellular electron transfer. Proc. Natl. Acad. Sci. U. S. A. **105:**3968-3973.

93. **Marsili, E., J. B. Rollefson, D. B. Baron, R. M. Hozalski, and D. R. Bond.** 2008. Microbial biofilm voltammetry: direct electrochemical characterization of catalytic electrode-attached biofilms. Appl. Environ. Microbiol. **74:**7329-7337.

94. **Marsili, E., J. Sun, and D. R. Bond.** 2010. Voltammetry and growth physiology of *Geobacter sulfurreducens* biofilms as a function of growth stage and imposed electrode potential. Electronanal. **22:**865-874.

95. **Masuko, T., A. Minami, N. Iwasaki, T. Majima, S. Nishimura, and Y. C. Lee.** 2005. Carbohydrate analysis by a phenol-sulfuric acid method in microplate format. Anal. Biochem. **339:**69-72.

96. **Mayer, C., R. Moritz, C. Kirschner, W. Borchard, R. Maibaum, J. Wingender, and H. Flemming.** 1999. The role of intermolecular interactions: studies on model systems for bacterial biofilms. Int. J. Biol. Macromol. **26:**3-16.

97. **Mehta, T., S. E. Childers, R. Glaven, D. R. Lovley, and T. Mester.** 2006. A putative multicopper protein secreted by an atypical type II secretion system involved in the reduction of insoluble electron acceptors in *Geobacter sulfurreducens*. Microbiology. **152:**2257-2264.

98. **Mehta, T., M. V. Coppi, S. E. Childers, and D. R. Lovley.** 2005. Outer membrane *c*-type cytochromes required for Fe(III) and Mn(IV) oxide reduction in *Geobacter sulfurreducens*. Appl. Environ. Microbiol. **71:**8634-8641.

99. **Methe, B. A., K. E. Nelson, J. A. Eisen, I. T. Paulsen, W. Nelson, J. F. Heidelberg, D. Wu, N. Ward, M. J. Beanan, R. J. Dodson, R. Madupu, L. M. Brinkac, S. C. Daugherty, R. T. DeBoy, A. S. Durkin, M. Gwinn, J. F. Kolonay, S. A. Sullivan, D. H. Haft, J. Selengut, T. M. Davidsen, N. Zafar, O. White, B. Tran, C. Romero, H. A. Forberger, J. Weidman, H. Khouri, T. V. Feldbylum, T. R. Utterback, S. E. Van Aken, D. R. Lovley, and C. M. Fraser.** 2003. Genome of *Geobacter sulfurreducens*: metal reduction in subsurface environments. Science. **302:**1967-1969.

100. **Methe, B. A., J. Webster, K. Nevin, J. Bulter, and D. R. Lovley.** 2005. DNA microarray analysis of nitrogen fixation and Fe(III) reduction in *Geobacter sulfurreducens* . Appl. Environ. Microbiol. **71:**2530-2538.

101. **Nevin, K. P., D. E. Holmes, T. L. Woodard, E. S. Hinlein, D. W. Ostendorf, and D. R. Lovley.** 2005. *Geobacter bemidjiensi*s sp. nov. and *Geobacter psychrophilus* sp. nov., two novel Fe(III)-reducing subsurface isolates. Int. J. Syst. Evol. Microbiol. **55:**1667-1674.

102. **Nevin, K. P., B. Kim, R. H. Glaven, J. P. Johnson, T. L. Woodard, B. A. Methe, R. J. J. DiDonato, S. F. Covalla, A. E. Franks, A. Liu, and D. R. Lovley.** 2009. Anode biofilm transcriptomics reveals outer surface components essential for high density current production in *Geobacter sulfurreducens* Fuel Cells. PLoS One. **4:**e5628.

103. **Nevin, K. P., and D. R. Lovley.** 2000. Lack of production of electron-shuttling compounds or solubilization of Fe(III) during reduction of insoluble Fe(III) oxide by *Geobacter metallireducens*. Appl. Environ. Microbiol. **66:**2248-2251.

104. **O'Toole, G. A., L. A. Pratt, P. I. Watnick, D. K. Newman, V. B. Weaver, and R. Kolter.** 1999. Genetic approaches to study of biofilms. Methods Enzymol. **310:**91-109.

105. **Palmer, J., S. Flint, and J. Brooks.** 2007. Bacterial cell attachment, the beginning of a biofilm. J. Ind. Microbiol. Biotechnol. **34:**577-588.

106. **Pokkuluri, P. R., Y. Y. Londer, N. E. C. Duke, W. C. Long, and M. Schiffer.** 2004. Family of cytochrome c_7-type proteins from *Geobacter sulfurreducens*: structure of one cytochrome c_7 at 1.45 Å resolution. Biochemistry. **43:**849-859.

107. **Qian, X., G. Reguera, T. Mester, and D. R. Lovley.** 2007. Evidence that OmcB and OmpB of *Geobacter sulfurreducens* are outer membrane surface proteins. FEMS Microbiol. Lett. **277:**21-27.

108. **Qiu, Y., B. Cho, Y. S. Park, D. R. Lovley, B. Palsson, and K. Zengler.** 2010. Structural and operational complexity of the *Geobacter sulfurreducens* genome. Genome Res. **20:**1304-1311.geo

109. **Quentin, Y., G. Fichant, and F. Denizot.** 1999. Inventory, assembly and analysis of *Bacillus subtilis* ABC transport systems. J. Mol. Biol. **287:**467-484.

110. **Raven, K. P., A. Jain, and R. H. Loeppert.** 1998. Arsenite and arsenate adsorption on ferrihydrite: kinetics, equilibrium, and adsorption envelopes. Environ. Sci. Technol. **32:**344-349.

111. **Reguera, G., K. D. McCarthy, T. Mehta, J. S. Nicoll, M. T. Tuominen, and D. R. Lovley.** 2005. Extracellular electron transfer via microbial nanowires. Nature. **435:**1098-1101.

112. **Reguera, G., K. P. Nevin, J. S. Nicoll, S. F. Covalla, T. L. Woodard, and D. R. Lovley.** 2006. Biofilm and nanowire production leads to increased current in *Geobacter sulfurreducens* fuel cells. Appl. Environ. Microbiol. **72:**7345-7348.

113. **Reguera, G., R. B. Pollina, J. S. Nicoll, and D. R. Lovley.** 2007. Possible nonconductive role of *Geobacter sulfurreducens* pilus nanowires in biofilm formation. J. Bacteriol. **189:**2125-2127.

114. **Rholl, D. A., L. A. Trunck, and H. P. Schweizer.** 2008. In vivo *Himar1* transposon mutagenesis of *Burkholderia pseudomallei*. Appl. Environ. Microbiol. **74:**7529-7535.

115. **Richter, H., K. P. Nevin, H. Jia, D. A. Lowy, D. R. Lovley, and L. M. Tender.** 2009. Cyclic voltammetry of biofilms of wild type and mutant *Geobacter sulfurreducens* on fuel cell anodes indicates possible roles of OmcB, OmcZ, type IV pili, and protons in extracellular electron transfer. Energy Environ. Sci. **2:**506-516.

116. **Rollefson, J. B., C. E. Levar, and D. R. Bond.** 2009. Identification of genes involved in biofilm formation and respiration via Mini-*Himar* transposon mutagenesis of *Geobacter sulfurreducens*. J. Bacteriol. **191:**4207-4217.

117. **Rollefson, J. B., C. S. Stephen, M. Tien, and D. R. Bond.** 2011. Identification of an extracellular polysaccharide network essential for cytochrome anchoring and biofilm formation in *Geobacter sulfurreducens*. J. Bacteriol. **193:**1023-1033.

118. **Rooney-Varga, J. N., R. T. Anderson, J. L. Fraga, D. Ringelberg, and D. R. Lovley.** 1999. Microbial communities associated with anaerobic benzene degradation in a petroleum-contaminated aquifer. Appl. Environ. Microbiol. **65:**3056-3063.

119. **Rosenberg, L.** 1971. Chemical basis for the histological use of safranin O in the study of articular cartilage. J. Bone Joint Surg. Am. **53:**69-82.

120. **Rubin, E. J., B. J. Akerley, V. N. Novik, D. J. Lampe, R. N. Husson, and J. J. Mekalanos.** 1999. *In vivo* transposition of *mariner*-based elements in enteric bacteria and mycobacteria. Proc. Natl. Acad. Sci. **96:**1645-1650.

121. **Sadovskaya, I., E. Vinogradov, S. Flahaut, and G. Kogan.** 2005. Extracellular carbohydrate-containing polymers of a model biofilm-producing strain, *Staphylococcus epidermidis* RP62A. Infect. Immun. **73:**3007-3017.

122. **Saltikov, C. W., and D. K. Newman.** 2003. Genetic identification of a respiratory arsenate reductase. Proc. Natl. Acad. Sci. **100:**10983-10988.

123. **Shi, L., T. C. Squier, J. M. Zachara, and J. K. Fredrickson.** 2007. Respiration of metal (hydr)oxides by *Shewanella* and *Geobacter*: a key role for multihaem *c*-type cytochromes. Mol. Microbiol. **65:**12-20.

124. **Shimkets, L. J., and H. Rafiee.** 1990. CsgA, an extracellular protein essential for *Myxococcus xanthus* development. J. Bacteriol. **172:**5299-5306.

125. **Snoeyenbos-West, O. L., K. E. Nelson, R. T. Anderson, and D. R. Lovley.** 2000. Enrichment of *Geobacter* species in response to stimulation of Fe(III) reduction in sandy aquifer sediments. Microb. Ecol. **39:**153-167.

126. **Stewart, P. E., J. Hoff, E. Fischer, J. G. Krum, and P. A. Rosa.** 2004. Genome-wide transposon mutagenesis of *Borrelia burgdorferi* for identificaion of phenotypic mutants. Appl. Environ. Microbiol. **70:**5973-5979.

127. **Tender, L. M., S. A. Gray, E. Groveman, D. A. Lowy, P. Kauffman, J. Melhado, R. C. Tyce, D. Flynn, R. Petrecca, and J. Dobarro.** 2008. The first demonstration of a microbial fuel cell as a viable power supply: powering a meteorological buoy. J. Power Sources. **179:**571-575.

128. **Thamdrup, B.** 2000. Bacterial manganese and iron reduction in aquatic sediments, p. 41-84. *In* B. Schink (ed.), Advances in Microbial Ecologyvol. 16. Kluwer Academic/Plenum Publishers, New York.

129. **Thomas, P. E., D. Ryan, and W. Levin.** 1976. An improved staining procedure for the detection of the peroxidase activity of cytochrome *P*-450 on sodium dodecyl sulfate polyacrylamide gels. Anal. Biochem. **75:**168-176.

130. **Torres, C. I., M. A. Kato, and B. E. Rittmann.** 2008. Proton transport inside the biofilm limits electrical current generation by anode-respiring bacteria. Biotechnol. Bioeng. **100:**872-881.

131. **Tran, H. T., J. Krushkal, F. M. Antommattei, D. R. Lovley, and R. M. Weis.** 2008. Comparative genomics of *Geobacter* chemotaxis genes reveals diverse signaling function. BMC Genomics. **9:**471.

132. **Tremblay, P. L., Z. M. Summers, R. H. Glaven, K. P. Nevin, K. Zengler, C. L. Barrett, Y. Qiu, B. O. Palsson, and D. R. Lovley.** 2010. A *c*-type cytochrome and a transcriptional regulator responsible for enhanced extracellular electron transfer in *Geobacter sulfurreducens* revealed by adaptive evolution. Environ. Microbiol. doi: 10.1111/j.1462-2920.2010.02302.

133. **Vinogradov, E., A. Korenevsky, D. R. Lovley, and T. J. Beveridge.** 2004. The structure of the core region of the lipopolysaccharide from *Geobacter sulfurreducens*. Carbohydr. Res. **339:**2901-2904.

134. **Voisin, S., J. V. Kus, S. Houliston, F. St-Michael, D. Watson, D. G. Cvitkovitch, J. Kelly, J. Brisson, and L. L. Burrows.** 2007. Glycosylation of *Pseudomonas aeruginosa* strain Pa5196 type IV pilins with Mycobacterium-like alpha-1,5-linked D-Ara*f* oligosaccharides. J. Bacteriol. **189:**151-159.

135. **von Canstein, H., J. Ogawa, S. Shimizu, and J. R. Lloyd.** 2008. Secretion of flavins by *Shewanella* species and their role in extracellular electron transfer. Appl. Environ. Microbiol. **74:**615-623.

136. **Voordeckers, J. W., B. Kim, M. Izallalen, and D. R. Lovley.** 2010. Role of *Geobacter sulfurreducens* outer surface *c*-type cytochromes in reduction of soil humic acid and anthraquinone-2,6-disulfonate. Appl. Environ. Microbiol. **76:**2371-2375.

137. **Vu, B., M. Chen, R. J. Crawford, and E. P. Ivanova.** 2009. Bacterial extracellular polysaccharides involved in biofilm formation. Molecules. **14:**2535-2554.

138. **Waffenschmidt, S., T. Kusch, and J. P. Woessner.** 1999. A transglutaminase immunologically related to tissue transglutaminases catalyzes cross-linking of cell wall proteins in *Chlamydomonas reinhardtii*. Plant Physiol. **121:**1003-1015.

139. **Watnick, P. I., and R. Kolter.** 1999. Steps in the development of a *Vibrio cholerae* El Tor biofilm. Mol. Microbiol. **34:**586-595.

140. **Weber, K. A., L. A. Achenbach, and J. D. Coates.** 2006. Microorganisms pumping iron: anaerobic microbial iron oxidation and reduction. Nat. Rev. Microbiol. **4:**752-764.

141. **Wu, S. S., J. Wu, Y. L. Cheng, and D. Kaiser.** 1998. The *pilH* gene encodes an ABC transporter homologue required for type IV pilus biogenesis and social gliding motility in *Myxococcus xanthus*. Mol. Microbiol. **29:**1249-1261.

142. **Yang, Y., P. E. Stewart, X. Shi, and C. Li.** 2008. Development of a transposon mutagenesis system in the oral spirochete *Treponema denticola*. Appl. Environ. Microbiol. **74:**6461-6464.

143. **Yang, Z., R. Lux, W. Hu, C. Hu, and W. Shi.** 2010. PilA localization affects extracellular polysaccharide production and fruiting body formation in *Myxococcus xanthus*. Mol. Microbiol. **76:**1500-1513.

144. **Yi, H., K. P. Nevin, B. C. Kim, A. E. Franks, A. Klimes, L. M. Tender, and D. R. Lovley.** 2009. Selection of a variant of *Geobacter sulfurreducens* with enhanced capacity for current production in microbial fuel cells. Biosens. Bioelectron. **24:**3498-3503.

145. **Yokoyama, K., N. Nio, and Y. Kikuchi.** 2004. Properties and applications of microbial transglutaminases. Appl. Microbiol. Biotechnol. **64:**447-454.

146. **Youderian, P., N. Burke, D. J. White, and P. L. Hartzell.** 2003. Identification of genes required for adventurous gliding motility in *Myxococcus xanthus* with the transposable element *mariner*. Mol. Microbiol. **49:**555-570.

147. **Yu, N. Y., J. R. Wagner, M. R. Laird, G. Melli, S. Rey, R. Lo, P. Dao, S. C. Sahinalp, M. Ester, L. J. Foster, and F. S. L. Brinkman.** 2010. PSORTb 3.0: improved protein subcellular localization prediction with refined localization subcategories and predictive capabilities for all prokaryotes. Bioinformatics. **26:**1608-1615.

148. **Zhang, J. K., M. A. Pritchett, D. J. Lampe, H. M. Robertson, and W. W. Metcalf.** 2000. *In vivo* transposon mutagenesis of the methanogenic archaeon *Methanosarcina acetivorans* C2A using a modified version of the insect *mariner*-family transposable element *Himar1*. Proc. Natl. Acad. Sci. **97:**9665-9670.